Universidad Autónoma de Madrid

Bursty Behavioral Dynamics of Activity and Sleep

Amanda Sorribes

Doctoral Dissertation

Official Postgraduate Program of Biophysics
Universidad Autónoma de Madrid

November, 2015

Adviser: Dr. Gonzalo García de Polavieja Embid

Abstract

A characteristic feature of both human and animal life are the constant alternations between active periods dedicated to different behaviors, and periods of inactivity dedicated to rest and recuperation. The temporal pattern of active and inactive periods is rich with information on the processes that govern and regulate the transitions among behavioral states. Traditionally these temporal patterns had been believed to follow 'normal' statistics like so many other natural phenomena, but during the last two decades it has increasingly been discovered that many behaviors in both humans and other animals are instead governed by 'scale-free' bursty temporal dynamics. Bursty dynamics are characterized by having a temporal pattern where periods of many short and frequent events are separated by long periods of little or no activity. Bursty dynamics are thus more irregular than random dynamics and harder to predict. The aim of this doctoral thesis has been to study the bursty behavioral dynamics of spontaneous activity and sleep. The main theme has been to characterize the bursty dynamics in genetically tractable 'simpler' model organisms, to establish baseline results to build upon and to probe the underlying neuronal control of burstiness. The thesis consists of three main parts, in which we have studied activity dynamics in the fruit fly *Drosophila melanogaster*, sleep-wake dynamics in the zebrafish *Danio rerio* and in humans, and studied the properties of the neuronal I_h "pacemaker" current which controls spontaneous rhythmic activity and affects burstiness. In *Drosophila* we characterized the locomotor activity dynamics and found that it is bursty. Subsequently we experimentally tested a hypothesis on the origin of bursts, and found that decision-making circuits affect the bursty behavioral dynamics. We next characterized the sleep-wake

dynamics in the zebrafish at different ages across the lifespan and compared it to the development of sleep-wake dynamics in humans at different ages. We found that nightly wake increases as wake durations become longer and less fragmented with age in both zebrafish and humans. Wake dynamics were found to be highly bursty, while sleep dynamics were found to have a more complex temporal dynamics than predominantly described. The highly similar development of sleep-wake cycles in both species contributes to establishing zebrafish as a valuable model organism for further studies of sleep-wake dynamics and regulation. Finally, we studied the I_h current as the *DmIh* null mutation gives rise to alterations of the sleep-wake pattern in adult fruit flies. The mutation also produces a locomotor and decision-making phenotype in larvae, which have a much simpler nervous system and a well characterized neuromuscular junction suitable for electrophysiology. We found that the larval locomotor phenotype was due to the motoneurons, which exhibited a decreased excitability and reduced responsiveness to dynamic stimuli. Model organisms with sophisticated genetical tools like the fruit fly and the zebrafish have thus been shown to be highly valuable animal models for characterizing and probing the control and regulation of behavioral burstiness.

Resumen

Una distinguida característica de la vida humana y animal son las constantes alternancias entre periodos activos dedicados a diferentes comportamientos, y periodos de inactividad dedicados a descanso y recuperación. El patrón temporal de actividad e inactividad está lleno de información de los procesos que controlan y regulan las transiciones entre estados. Tradicionalmente se había considerado que estos patrones temporales seguirían una estadística 'normal' como tantos otros fenómenos naturales. Pero durante las dos últimas décadas se ha ido descubriendo que muchos comportamientos, tanto en humanos como en otros animales, siguen una dinámica temporal en ráfagas y 'sin escala'. La dinámica rafagosa se caracterizada por tener un patrón temporal donde periodos de muchos eventos cortos y frecuentes vienen separados por periodos largos de poca o ninguna actividad. La dinámica rafagosa es más irregular que la dinámica aleatoria, y es por lo tanto, más difícil de predecir. El objetivo de esta tesis doctoral ha sido estudiar la dinámica rafagosa del comportamiento espontáneo de actividad y sueño. La temática principal ha sido caracterizar la dinámica rafagosa en animales 'simples' y genéticamente maleables, para establecer resultados de base sobre los que construir y explorar el control neuronal subyacente de la dinámica rafagosa. La tesis consiste de tres partes principales, en las cuales hemos estudiado la dinámica de la actividad en la mosca de la fruta *Drosophila melanogaster*, la dinámica de sueño-vigilia en el pez cebra *Danio rerio* y en humanos, y estudiado las propiedades neuronales de la corriente "marcapasos" I_h que controla actividad espontánea rítmica y afecta a la rafagosidad. En *Drosophila* caracterizamos la dinámica locomotora y encontramos que es rafagosa. Después probamos experimentalmente una hipótesis sobre el

origen de ráfagas, y descubrimos que circuitos de toma de decisiones afectan a la dinámica del comportamiento en ráfagas. Posteriormente, caracterizamos la dinámica de sueño y vigilia en el pez cebra a diferentes edades a lo largo de su vida y lo comparamos con el desarrollo de la dinámica de sueño-vigilia en humanos a diferentes edades. Encontramos que la fragmentación de la vigilia disminuye, a medida que los episodios de vigilia y vigilia nocturna total aumentan con la edad tanto en el pez cebra como en humanos. La dinámica de vigilia mostró ser altamente rafagosa, mientras que la dinámica de sueño tenía una estructura temporal más compleja de lo que ha sido predominantemente descrito. El desarrollo de la dinámica de sueño-vigilia es muy similar en las dos especies; lo que contribuye a establecer al pez cebra como un organismo modelo valioso para futuros estudios de la dinámica y regulación del sueño y de la vigilia. Finalmente, estudiamos la corriente I_h en *Drosophila* dado que la mutación nula del *DmIh* da lugar a alteraciones en el patrón de sueño-vigilia en las moscas adultas. La mutación también produce un fenotipo locomotor y de toma de decisiones en larvas, las cuales tienen un sistema nervioso más simple y una unión neuromuscular altamente caracterizada e idónea para la electrofisiología. Hallamos que el fenotipo locomotor larvario se debía a la motoneurona, que tenía una excitabilidad disminuida y una respuesta reducida a estímulos dinámicos. Los animales modelo con herramientas genéticas sofisticadas como la mosca de la fruta y el pez cebra han, por lo tanto, sido mostrados como animales valiosos para caracterizar y explorar el control y la regulación del comportamiento en ráfagas.

Contents

List of Figures

1

Introduction

Animals are broadly defined as mobile multicellular organisms with a nervous system able to quickly respond to stimuli (Oxford Dictionaries, 2015). These nervous systems, brains in higher order animals, generate behavior in response to internal and external signals in order to survive and reproduce. A constant balance between active foraging behavior in search for food sources and other active behaviors, and inactive periods of rest and recuperation characterizes the overall structure of animal life.

The predominant view in neuroscience has been to consider brain function as a series of more or less complex stimulus-response systems, where the brain generates behavior as a consequence of perceived sensory events (Brembs, 2009). This approach has been very fruitful and has given rise to immense bodies of knowledge on visual processing, escape behavior, olfaction and many other areas of neuroscience (Allen et al., 2006; Silies et al., 2014; Wicher, 2015; Brembs, 2013).

Following the paradigm of stimulus-response interactions as the driving force of behavior, the temporal pattern of animal behavior would be highly contingent on the the timing of the perceived stimuli. Since many natural phenomena can be well approximated by a normal distribution by the central limit theorem, the simplest and most general case is to consider that most natural stimuli an animal encounters will be normally distributed. Consistent with this notion, animal movement was traditionally modeled as a normal diffusive process, where the durations of active locomotion are determined by a random process and are independent of the previous activity (Codling et al., 2008).

During the last two decades, however, it was discovered that the temporal dynamics of animal locomotor activity did not follow a random process but instead followed a fractal, or *bursty* temporal pattern (Wiens et al., 1995; Cole, 1995; Viswanathan et al., 1996; Sims et al., 2008; Humphries et al., 2012, 2013). Bursty dynamics are characterized by a temporal pattern comprising of periods where many short events succeed each other, followed by longer periods of little or no activity. In particular, in bursty dynamics the bursts of short activity are more frequently occurring than in random dynamics, as are the really long durations which separate bursts.

A few years later it was discovered that also wake periods in between sleep episodes followed bursty dynamics in humans and other mammals (Lo et al., 2002, 2004; Blumberg et al., 2005, 2007; Karlsson et al., 2011). Soon, other human activities like telephone and e-mail correspondence, library loans or entertainment consumption were also found to occur with a bursty temporal pattern (Barabási, 2005; Vázquez et al., 2006; Goh and Barabási, 2008). Apart from raising fundamental questions about the processes governing the timing of human behavior, the presence of bursty dynamics in humans also has important implications for how we model and design human services in our societies (Barabási, 2005).

Despite the advances in finding and characterizing bursty behavior in animals and humans, the origins of this temporal structure are not yet well understood. Following the classical view of animal behavior as a response to external stimuli, it has been suggested that the conditions of the natural environment might be responsible for the observed bursty foraging patterns (Viswanathan et al., 1996; Reynolds, 2014). Although an external influence cannot strictly be ruled out in empirical studies of animals moving through a natural environment, controlled studies in a laboratory setting have shown that also animals in featureless environments display bursty dynamics (Maye et al., 2007). If animal behavior was principally driven by reactions to external stimuli we would expect the temporal dynamics under such experimental conditions to resemble the random fluctuations of noise in the environment and sensory organs. Instead, the animal behavior showed an intrinsic spontaneous burstiness (Maye et al., 2007).

Since the bursty behavioral dynamics occur in spontaneously behaving animals, the question of the origin of this complex temporal organization remains. Theoretical work on human dynamics led to the novel proposition that the observed bursty behavioral dynamics occur as a consequence of an internal decision-making process, when tasks are primarily executed in the order of perceived priority (Barabási, 2005). The proposed model spurred further theoretical work on both the intrinsically based decision-making model (Oliveira and Barabási, 2005; Vázquez, 2005; Vázquez et al., 2006; Jo et al., 2012) and on alternative competing explanations based instead on the interaction of random

and recurring internal or external processes of different time scales (Stouffer et al., 2005, 2006; Hidalgo, 2006; Malmgren et al., 2008, 2009; Proekt et al., 2012).

In this doctoral thesis I have studied the bursty behavioral dynamics of activity and sleep, in spontaneously behaving animals under controlled conditions in a laboratory setting. The main motivating theme has been to characterize the bursty dynamics in genetically tractable 'simpler' model organisms, to establish these as baseline results to build upon and to probe the underlying neuronal control of burstiness. In light of the interdisciplinary nature of this biophysics dissertation, my aim has been to include a sufficient level of introduction and background throughout the chapters so as to satisfy interested readers coming from either biology or physics, or from other related fields.

The results presented in this dissertation have been obtained both through experimentation and analytical work. Many of the results would however not have been possible without the additional contribution of experimental data and inspiration by colleagues, to whom I am grateful for rewarding collaborations. Each result section will state clearly in the material and methods subsection when the experimental data were produced by a collaborator.

The dissertation work is divided into three main areas of study, presented in the result chapters 3–5. First, however, CHAPTER 2 *Studying Behavioral Dynamics in Drosophila melanogaster* will introduce the methodological motivation and background on the use of the fruit fly *Drosophila melanogaster* for behavioral studies, and introduce the conceptual and mathematical methodology used for studying bursts.

In CHAPTER 3 *Bursty Activity Dynamics in Drosophila melanogaster* we first characterized the bursty nature of spontaneous walking dynamics in *Drosophila*. By using powerful genetical tools available in the fruit fly, we were then able to experimentally test the hypothesized origin of bursty dynamics in decision-making processes by disrupting decision-making circuits in the fly brain and measuring the effect on behavioral burstiness.

In CHAPTER 4 *Sleep-Wake Dynamics in Model Organisms and Humans* we studied the dynamics of spontaneous sleep and wake cycles in the zebrafish

Danio rerio and in humans. A correct regulation of sleep is imperative to feeling well rested and sleep disorders are one of the most common reasons for seeking medical attention. Thus far the sleep-wake dynamics had only been studied in mammalian species, as sleep had predominately been considered a mammalian phenomenon. During the last ten–fifteen years genetically tractable simpler model organisms have however irrupted and revitalized the field of sleep research, as sleep became possible to measure by externally observable behavioral criteria. The zebrafish in particular has proven to be a valuable model as it possesses many of the experimental advantages of an invertebrate model, but with a vertebrate neuroanatomy and neurochemistry. We therefore studied the development of the sleep-wake dynamics across the lifespan in zebrafish, and compared it to human sleep-wake dynamics.

In CHAPTER 5 *Activity-Rest Dynamics and Neuronal Excitability of DmIh* we changed the experimental paradigm, and studied the neuronal ion current I_h in *Drosophila* as the *DmIh* null mutation affects the sleep-wake patterns in adult fruit flies. The I_h current is sometimes called the "pacemaker" current because of its fundamental role in the control of spontaneous rhythmic activity in a variety of excitable cells. The *DmIh* null mutation also produces a locomotor and decision-making phenotype in larvae, as well as pre- and postsynaptic morphological alterations in the neuromuscular junction. In this chapter we present the physiological effect of the *DmIh* null mutation on the larval locomotor system, with the use of electrophysiological experimentation in the neuromuscular junction.

2

Studying Behavioral Dynamics in *Drosophila melanogaster*

2.1 *Drosophila melanogaster* as a Model Organism

2.1.1 Introduction

The importance of the fruit fly *Drosophila melanogaster* in biological research can be traced back to the beginnings of the last century when Thomas Hunt Morgan, advised by colleagues, started using it in a laboratory setting for genetic analysis (Nobel Lectures, 1965). After a couple of years he identified his first mutant – a fly with white eyes instead of red, and he called the mutation *white*. In collaboration with three students, they formulated a revolutionary chromosome theory of heredity between the years 1910 – 1915, for which T. H. Morgan would later receive the Nobel Prize in Physiology or Medicine, in 1933 (Nobel Lectures, 1965; Rubin and Lewis, 2000).

Drosophila was among the first organisms used for genetic experimentation, and remains to this day one of the most frequently used and genetically best-known organisms (Pierce, 2004). In the early days of *Drosophila* research, millions of flies were bred and visually inspected under a microscope to find the spontaneous mutations that arise naturally over the generations (Nobel Lectures, 1965). To speed up the process, techniques such as exposing the flies to radiation or feeding them a chemical agent that creates point mutations in the DNA were introduced, and modern methods make use of transposable elements combined with a marker, which insert into the genome at random (St Johnston, 2002). Common to all these methods is the procedure known as *forward genetics*, whereby, after a mutation in the DNA produces (either naturally or induced) an observable phenotype, it is identified and isolated to try to find the genetic basis for the observed mutation. This methodology of (forward) genetic screening has produced many remarkable and influential results, in the beginning half of the last century mainly in the fields of genetics and developmental biology (St Johnston, 2002; Bellen et al., 2010).

The search for mutant phenotypes extended, however, from morphological and developmental alterations into the search for the genetic basis of behavior, pioneered by Seymour Benzer and his students during the late 1960s and early

1970s (Bellen et al., 2010; Jan and Jan, 2008). In the first study a simple and elegant assay to isolate single-gene mutants with defective phototaxis behavior was described, and a few years later they published a seminal work describing single-gene mutations affecting the circadian rhythm of the activity-rest cycle. Over the following three decades it has been shown that these mutations affect the components of a cellular biochemical clock which is found in a wide range of cells, although the main time-keeping is controlled by only a few dozen neurons in the fly brain. Homologues to these biochemical clock genes have been found in mice and humans as well, evidencing the conserved mechanism of biological time-keeping (Bellen et al., 2010). Further advances on the genetic basis of behavior were made in Benzer's lab, including learning and memory mutants, stress-sensitivity, mating behavior and vision (Jan and Jan, 2008; Bonini, 2008). *Drosophila* has continued to be very important in the field of behavioral genetics and neuroethology, showing e.g. how a polymorphism in the single gene *foraging* can give rise to different foraging behavior (Sokolowski, 2001), probing the neural and genetic basis for visual attention and decision-making processes (van Swinderen, 2011), and lately, using *Drosophila* to unravel the biological mysteries of sleep (Hendricks et al., 2000; Shaw et al., 2000; Cirelli and Bushey, 2008) – which we shall see more of in chapter 4, *Sleep-Wake Dynamics in Model Organisms and Humans*.

While knowing as much as possible about *Drosophila* is interesting from an ethological point of view, it has also proven itself immensely useful for discovering conserved mechanisms across species, in particular, also for human function and disease. Since the whole genome sequencing of *Drosophila melanogaster* in the year 2000 (Adams et al., 2000), 77% of known human disease genes have a recognizable counterpart in the *Drosophila* genome (Reiter et al., 2001), even though the fly genome is about 20 times smaller than the human genome, counted in base pairs, and comprises about half of the number of genes as the human genome (Adams et al., 2000; IHGSC, 2004). The smaller size of the *Drosophila* genome is indeed an advantage when sequencing and performing *reverse genetics*, where the function of a given gene is the target of study, because the fly genome contains less duplicate genes than mammalian

model organisms, making a "break it and see what happens"-approach much more feasible (Gu et al., 2002). Since the early years of the new millennium, as sequencing became less expensive and less time-consuming, several other model organisms have had their genomes sequenced, from nematode worms to mice, mosquitoes and fish, including the zebrafish, which we will see more of in the chapter of Sleep Dynamics.

2.1.2 Fly Life Cycle, Rearing and Breeding

Another aspect which has helped establish *Drosophila melanogaster* as a model organism in experimental research from the very beginnings (Nobel Lectures, 1965), is that it is small and easy to grow in the laboratory, it requires little space to culture and care for, the females lay many eggs and it has a short generation time, along with being inexpensive to maintain. Working with *Drosophila* is further helped by the strong collaborative tradition of the *Drosophila* community, dating back to the days of T. H. Morgan (Rubin and Lewis, 2000). In this line, the FlyBase Consortium (The FlyBase Consortium, Web) runs a centralized database of genetic and genomic data (Crosby et al., 2007), the Drosophila Genomics Resource Center (The Drosophila Genomics Resource Center) collects and distributes DNA clones, vectors and cell lines, and whole live fly stocks can be ordered from several stock centers around the world, with the Bloomington Drosophila Stock Center at Indiana University (Bloomington Drosophila Stock Center, Web) being the largest and oldest, established in the original Morgan laboratory (Bloomington Drosophila Stock Center, b).

Drosophila melanogaster is an insect of the order Diptera and as such, it goes through a complete 4-stage metamorphosis during its early life. The development rate is temperature dependent and under standard laboratory conditions (25 °C) the whole process takes about 9–10 days (Stocker and Gallant, 2008). The first developmental stage begins when an egg becomes fertilized and the female deposits the eggs on a suitable food medium. After about 24 hours the embryo has matured into a first instar larva that hatches and starts feeding on the surrounding food. As the larva eats and grows it molts

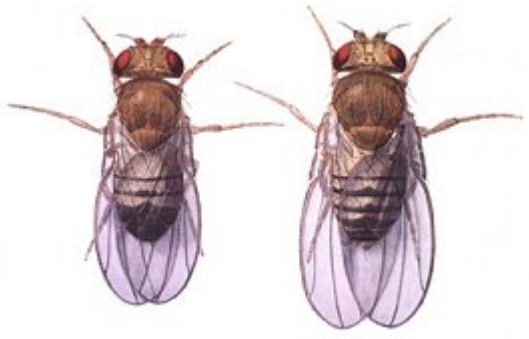

Figure 2.1: Illustration of male and female *Drosophila melanogaster*. Drawing depicting two fruit flies: male on the left, female on the right. Note the slight difference in size, and the darker hind tip of the male fly compared to the female. The drawing is not to scale, the actual body length (excluding wings) is about 3 mm. *Source*: (NASA, 2004).

twice into second and third instar developmental stages, denominated L1, L2, L3. The larval stage takes approximately four days and towards the end of the third instar it starts the "wandering stage", where it leaves the food in search for a dry place to pupate (Stocker and Gallant, 2008; Chippindale et al., 1999). Extensive metamorphosis takes place during the pupation stage which will last for another four days, whereupon the adult fly eccloses (emerges) from its pupal case. During the first 8–10 hours post-ecclosion the flies remain sexually immature, which is experimentally important for securing virgin females for later genetic crosses. The first few days of adulthood are sometimes known as the "juvenile stage" as extensive neuronal plasticity and maturation occur during this time (Ganguly-Fitzgerald et al., 2006). The adult females can lay 100–200 eggs per day, and have a fecundity peak between the ages of 4–12 days (Stocker and Gallant, 2008). The life expectancy of *Drosophila* varies considerably with genetic background and experimental conditions, but lies typically in the range of 30–60 days (Chippindale et al., 1999).

When rearing and breeding *Drosophila* in the laboratory for behavioral experimental purposes, the flies are kept in an incubator with a set temperature and a light that switches on and off on a controlled schedule, usually on a

12 hour light/12 hour dark (LD 12:12) cycle, to entrain the flies' circadian rhythms (Rosato and Kyriacou, 2006). When preparing for genetic crosses or experimental studies the flies are kept at 23–25 °C, while flies in stock and for longer keeping can be kept at 18 °C, since the development is slowed down at lower temperatures. Flies are grown in vials or bottles with a standard fly food (Bloomington Drosophila Stock Center, a) in the bottom, where bottles are larger and better suited for fly stock keeping, while vials are more suitable for keeping flies for crosses and in preparation for experimentation. Stocks need to be transferred to new vials or bottles every two weeks approximately, although the exact intervals are usually worked out depending on the stocks' viability, density and the temperature of keeping. Vials on the other hand, if used for breeding can be flipped over to a fresh tube after 2–3 days to increase the speed and production of offspring (Stocker and Gallant, 2008).

When the flies are reared and bred to be used in genetic crosses or for experiments, it is important to separate the females from the males before they have become sexually mature. This should be done within 8 hours post-ecclosion to be sure and on the safe side that a female was not fecundated by an incorrect male genotype, as several hours can pass by before a female deposits the eggs on food, and because female flies have been shown to perform sperm selection between mates after copulation (Snook and Hosken, 2004). For the kind of experiments we have performed, described further in section 2.2.2, it is also important to use virgin females because otherwise the female will lay fecundated eggs that will grow into larvae, which risk disturbing the experiment and the measuring procedure. The newly ecclosed flies are luckily quite easy to tell apart, as the males are slightly smaller than the females and with a darker and rounder abdomen, while the females have a lighter color and if very recently ecclosed, have a slightly bloated abdomen with a greenish spot which further eases the classification (see Figure 2.1). This separation of sexes is usually done at a "fly pushing station" (Stocker and Gallant, 2008), comprising of (in our laboratory) a dissecting microscope, a CO_2-pad with foot pedal for brief anesthetization of flies (both from Tritech Research Inc., CA USA) and a fine and soft paintbrush for gentle manipulation. An additional invaluable

tool is the (personal) aspirator, which allows gentle individual manipulation of awake flies. The aspirator can be made from standard laboratory equipment by taking a Pasteur pipette and severing its long tapered tip so that the resulting diameter coincides quite closely with the size of the flies (measure with a female as they are slightly larger), covering the large end of the pipette with a fine meshed cloth and connecting it to a flexible plastic tube of a length to your liking. Finally, construct a rechangeable mouth piece by using e.g. a cut-off large micropipettor tip, and connect it to the rubber tube with an additional layer of fine meshed cloth (it makes it easier to change the tip). The aspirator allows one to manipulate single flies, even from within populated vials, and in case of need the task of sexing and dividing the newly ecclosed flies into single-sex vials can be done with just an aspirator and a trained eye. The fly pushing station is also used for fly husbandry, as obtaining the desired genotype often requires performing several genetical crosses that require sex separation and may include trait selection of genetic markers.

2.1.3 Targeted Gene Expression: The GAL4/UAS Method

A big advancement for the *Drosophila* researcher came with the introduction of the GAL4/UAS tool for targeted gene expression, in 1993 (Duffy, 2002). The system allows the selective activation of any cloned gene in a wide variety of tissue- and cell-specific patterns (Brand and Perrimon, 1993). This is achieved by a bipartite approach, exploiting the diploid nature of *Drosophila* (meaning it has two full sets of chromosomes), designed such that the Gal4 driver will be inherited from one parent and the UAS element from the other (see Figure 2.2).

The Gal4 and UAS DNA sequences do not usually reside in the *Drosophila* genome, but stem from the yeast *Saccharomyces cerevisiae*. There, the GAL4 enzyme is a transcriptional activator that binds to a DNA region known as the Upstream Activating Sequence (UAS), and when bound, will activate transcription of the nearest downstream gene. A few years prior to Brand and Perrimon (1993) seminal paper it had been shown that the GAL4/UAS element was capable of stimulating transcription in both *Drosophila*, as well as in a wide

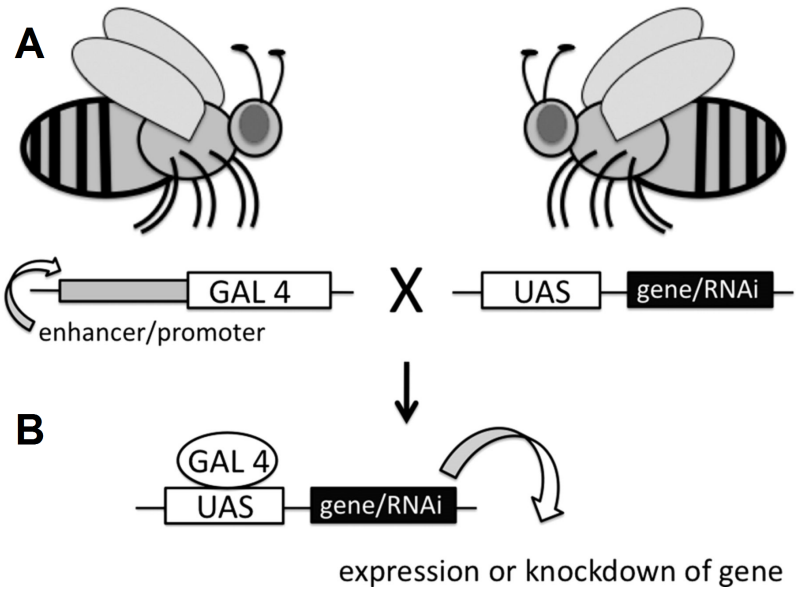

Figure 2.2: The bipartite Gal4/UAS transgenic system for targeted gene expression. **(A)** Flies with the yeast transcription activator protein Gal4 inserted into the genome (left) are crossed ("mated") with other flies carrying the UAS Upstream Activation Sequence (right). **(B)** In their offspring the Gal4 protein will specifically bind to the UAS DNA sequence and activate gene transcription downstream. The promoter or enhancer sequences upstream of the Gal4 element will control the temporal and spatial expression, while the placement of the UAS sequence will determine which gene is transcribed. *Source*: Modified from (Neckameyer and Argue, 2013).

variety of other systems. Importantly, it was also shown that the expression of GAL4 in *Drosophila* showed no apparent or harmful effects on the phenotype (Duffy, 2002).

The insertion of the Gal4 element into the *Drosophila* genome happens at random, so *a priori* it is not possible to control where it will be expressed. Combined with a UAS region coupled with a reported gene, like for example the green fluorescent protein (GFP), however, the expression patterns can be

mapped and the interesting lines are kept. Extensive libraries of GAL4-drivers exist today, where over 7000 lines with detailed mapping of target cells have been made available (Jenett et al., 2012), which can be ordered from one of the fly stock centers. An important strength of this bipartite system is that parent lines can be kept homozygote even with detrimental or lethal target genes, as the activation of the system only occurs in their crossed offspring, when both the GAL4 and the UAS elements are present in the genome concurrently.

Another important addition to the spacial and specific gene expression control is the temporal ability to control when the gene expression will be active, by using temperature sensitive components. In one of the studies of this thesis we introduced the temperature sensitive blocker of neuronal activity *shibire*^{ts} (Kitamoto, 2001), but more generally, there also exists a temperature sensitive GAL4 repressor (Gal80^{ts}) which allows for on/off-protocols, where flies are allowed to grow at the permissive or prohibiting temperature and are then switched over by changing the temperature (McGuire et al., 2003). A great advantage of these protocols is that the target gene can be inactive and thus not interfere during the development of the flies, but can then be activated in a controlled manner during the study, by simply raising/lowering the temperature.

With this method it is not only possible to express genes that create a gain-of-function, but also to create loss-of-function by expressing a Dominant Negative (DN) of the gene under study. The dominant negative is a protein that is very similar to the one that is desired to block, but with little or no physiological function. This can be achieved by creating a point mutation in the gene's DNA or by truncating parts of the coding sequence. While the DN is being expressed by the GAL4/UAS system, the gene producing the natural protein still remains intact and continues to function so the DN must thus compete with the natural copy inside the expressing cells. The GAL4/UAS driver system, however, is very powerful and produces many more DN copies than the cell produces the natural copy, so the effect is a blockage of activity. This system of producing a Dominant Negative to study gene function was used in chapter 5, *Activity-Rest Dynamics and Neuronal Excitability of DmIh*.

2.2 Measuring *Drosophila*'s Innate Activity Patterns

2.2.1 Environmental Conditions

Even though fruit flies are quite easy to handle and breed, it is important to know about and to take into consideration that they can also be quite sensitive to environmental factors, especially when planning behavioral studies. As mentioned in the previous section, the *Drosophila* development and physiology is temperature dependent as the flies cannot regulate their own body temperature beyond behaviorally seeking an adequate thermal environment. In studies of thermosensation and hygrosensation, it was found that wild type flies prefer a temperature of $\sim 24\,^{\circ}$C and a relative humidity of the air below 77% but not dry (Sayeed and Benzer, 1996). Thus, the recommended conditions for *Drosophila* research are at 23–25 °C with $\sim$ 60–70% relative humidity, allowing complex behavioral experiments to be done at room temperature. Depending on other factors, however, such as experiments designed with heat shock protocols, lower or higher temperatures can also be required.

To control for these environmental factors and to try to keep them as constant across experiments as possible, all the behavioral experiments were performed inside an incubator with controlled temperature, set at 23 °C unless otherwise noted. As the fruit flies' activity levels are also strongly influenced by the circadian day-night light cycle (Rosato and Kyriacou, 2006; Sokolowski, 2001), the incubator also had a programmable light cycle (Tritech Research Inc., CA USA: `DT2-MP-680` DigiTherm™ Heating/Cooling Incubator Standard w/ Opaque Door with `-CIRC-TL` Built in Circadian Temperature Ramping and Lighting System). To avoid data loss in case of power blackouts, both the incubator and the activity measuring set-up, described in the next section, were connected to a battery backup power with a capacity of several hours of run-time.

Apart from the external environmental conditions affecting the life and behavior of *Drosophila*, its immediate social environment has also been shown to affect development and maturation. Exposure to socially enriched environments within the first week as adult flies affect the number of synapses and the size

of information-processing regions, although the fly brain shows plasticity also after this time period (Heisenberg et al., 1995; Ganguly-Fitzgerald et al., 2006). Ganguly-Fitzgerald et al. (2006) showed that social exposure directly affect activity levels, where flies that have been socially isolated sleep less during the day than flies exposed to social interactions before the experiments. The increased daytime sleep need was in addition proportional to the size (4, 10, 20, 60, and 100 individuals) of the social group. For my experiments I therefore always took extra care to keep the social environment constant, at 20 flies per vial before the experiments. In addition to the social environment it is also advisable to leave the flies to mature during the first three days of post-ecclosion, when many complex behaviors develop (Hirsch and Tompkins, 1994). Therefore, flies were usually selected for experiments at day 3 post-ecclosion so that the first day of recording would coincide with day 4, when activity and sleep patterns have consolidated to adult levels (Shaw et al., 2000).

2.2.2 *Drosophila* Activity Monitor System

To study the spontaneous activity of *Drosophila* we used the *Drosophila Activity Monitor System* (second generation, DAM2) (TriKinetics Inc., 2005) to record the spontaneous locomotion behavior of flies. The DAMS monitoring and recording system was initially developed for circadian rhythms and chronobiology studies (Rosato and Kyriacou, 2006; TriKinetics Inc., 2005), but it has also been adopted by the sleep community (Hendricks et al., 2000), and lends itself well for our studies of the fine-scale dynamics of behavior as well. The DAM System is an automated monitoring system that consists of one or several connected monitors with 32 channels each arranged in a 8 by 4 grid (see Figure 2.3), with accompanying small glass tubes of 65 mm length and 5 mm inner diameter that fit in the channels, as well as wires and software to record the activity on a PC. Each channel on a monitor has an infrared detector system around it such that it detects every time something passes through the channel, whereby the monitor records the occurrence as a beam-break event. These beam-break events are then collected by the PC software, summed and recorded as 'counts'

per unit time. The investigator controls this time unit, or binning, as a setting in the software prior to the initiation of the experiment.

To measure the activity of flies, each fly is individually placed in a glass tube which has previously been filled with enough food for the duration of the experiment in one end, while the open end is closed behind the fly with a small cotton ball which allows air to get through. The side with food has previously been sealed with a black rubber cap, so the food doesn't dry out during the course of the experiment. The flies are at this point gently handled with an aspirator and are not anesthetized, so their natural rhythms won't get disturbed more than absolutely necessary. Thereafter, each glass tube is introduced into a channel on the monitor, such that the free space between the food surface and the cotton ball is centered around the infrared detector on the monitor. When all the tubes have been mounted, two elastic rubber bands are stretched around the tubes in 8-shapes, to keep the tubes from sliding when handling

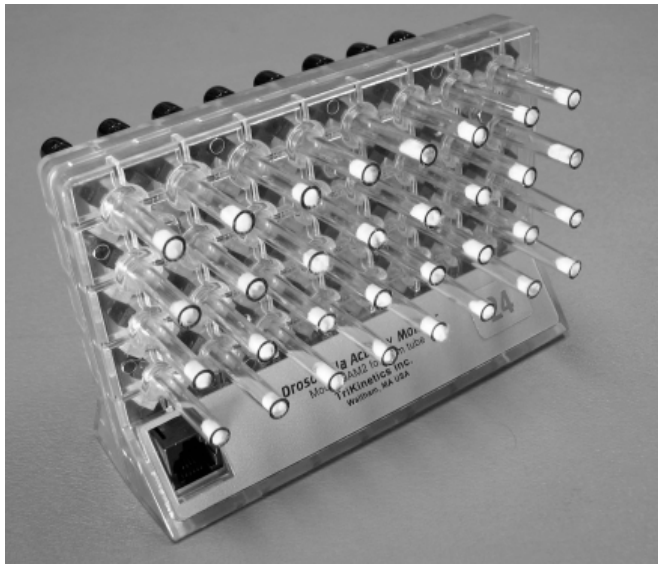

Figure 2.3: *Drosophila* Activty Monitor. A DAM2 monitor loaded with 32 tubes for long-term individualized monitoring of fly activity. *Source*: (TriKinetics Inc., 2005)

the monitors. Once the monitors have been placed in the incubator and the doors have been shut, effectively sealing it all off from external stimuli, the flies are usually left for at least 24 hours to settle into the new environment before recordings are started.

This procedure has been used successfully since the start of our experiments, but over the years I also started taking into account the placement of the monitors in the incubator as a possible environmental factor, thus ideally spreading the genotypes in such ways that this effect is minimized (see Figure 2.4 [p. 20]). I also experimented with mixing and intertwining genotypes on a per-channel-basis throughout all the monitors and while this would indeed minimize the environmental effects, it is very laborious and also prone to human error – and a mistaken interchange of genotypes would definitely be a larger source of error than the minor environmental effects of placement of monitors within the incubator. When measuring sexual differences I did change from a placement of one sex in channels 1–16 (top half) vs. the other sex in channels 17–32 (bottom half of monitor) to an odd-even placement of sexes across the channels, which does not require a noticeable increase of effort in comparison to the concentration and effort it takes to load the flies gently and successfully into the monitors anyway.

As a last note on this section about measuring the spontaneous activity of *Drosophila*, it is worth mentioning that there exist other methods to measure the activity, in particular video recording. Since video recording allows for a much finer spacial detail and time-scale than DAMS – where typically the measurements are set to collect data in 1-minute bins – studies using video recording of flies inside DAMS monitors showed that the data obtained with DAMS showed a good level of correspondence with the data obtained by detailed video analysis, especially during the nights (Hendricks et al., 2000; Zimmerman et al., 2008; Martin et al., 1998). While other more natural and 'free-ranging' set-ups than flies inside one-dimensional DAMS tubes could be achieved with video tracking systems, like in (Martin et al., 1998; Hendricks et al., 2000; Zimmerman et al., 2008), at the time of experimentation these systems had the draw-back that they did not scale well with population-size or allowed for several days of

recording. In addition, these video recordings typically require(d) some human intervention to validate the data, as well as computer processing power, while DAMS data require very little processing power and human oversight. Thus, since the DAM System has been shown to give relatively good measurements of activity levels during the night, the data are smaller and less error prone, and since several DAMS monitors can be placed in an incubator concurrently, which minimizes the environmental effects when comparing effects between genotypes as all the flies have been subjected to the exact same environment, we have used the DAM System as the chosen experimental system for the behavioral activity and sleep experiments presented in this thesis.

Figure 2.4: Experimental set-up of DAMS in incubator. A close up photo of six DAM2 monitors placed inside the incubator in preparation of an experiment (open door not shown), spread across three shelves. The incubator has a programmable daily lights on and off schedule to keep the circadian rhythm entrained; here seen with the lights on. Please note that these six DAM2 monitors have not been connected with cables to the PC yet.

2.3 Analyzing the Fine-Scale Dynamics of Spontaneous Activity

To begin with, we should start by defining what we mean by "fine-scale dynamics" of spontaneous behavior. When referring to behavioral studies, *dynamics* refers to the temporal structure of the behavior under study. The specification of *fine-scale* implies that we will take into account all the details of the temporal relationships between the episodes of the behavior, as opposed to circadian studies for instance, that are mainly occupied with large trends and phase shifts over several days.

To understand the dynamics of a behavior, we thus need to analyze the timings of the changes in that behavior. In our case, to study the spontaneous walking activity of *Drosophila* we need to study the timings of said locomotion, as opposed to the other state, in which the fly is not walking. By doing this we can treat the transitions between walking and not walking as a stochastic process, for which there exists an extensive mathematical framework to draw from. Hence, by studying *when* activity occurs, we can try to learn about the processes that govern that activity.

Depending on the question in mind, we can study the initiation of a behavior by looking at when it occurs with respect to its previous episode, that is, study the times between events of the behavior – the inter-event intervals (IEIs). Complementary, by studying the duration of the episodes we can learn something about the processes that govern the maintenance of the behavior. On the other hand, if our concern is to study the dynamics of the resting periods, we need to analyze the times between episodes of rest, and similarly, the maintenance dynamics of rest is given by the durations of the resting episodes.

2.3.1 Processing Raw Data into Bouts

To analyze the fine-scale dynamics of locomotor behavior, the first step is thus to process the raw recordings into active and non-active episodes, or *bouts*.

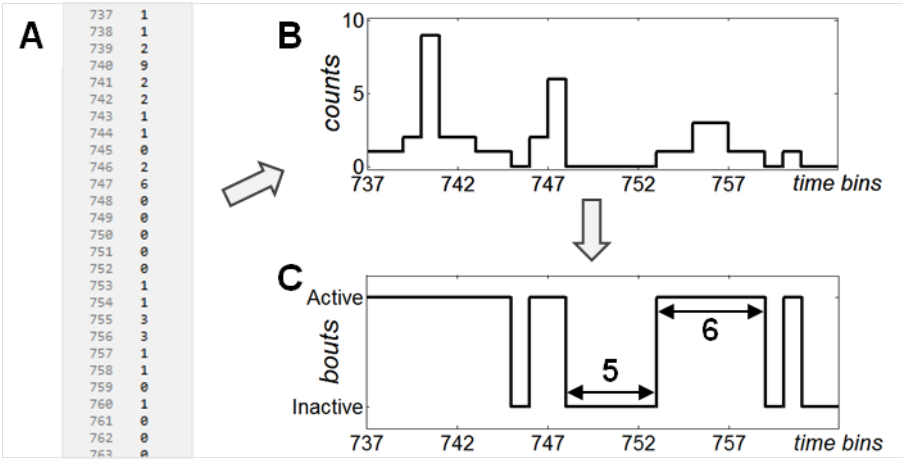

Figure 2.5: Turning raw locomotor activity counts into activity and inactivity bouts. (A) An extract from a data file from the DAM System for one fly. The right hand column shows the number of beam breaks during each time unit and the left hand column indicates the row number (the time bin since the start of the recording). **(B)** Plot of the count of beam breaks vs time. For this experiment the DAM System was set to record in 1-minute bins, so this extract from minutes 737–763 shows us the activity of one fly during almost half an hour. **(C)** The number of consecutive active or inactive minutes is summed to construct each bout. In the figure are indicated one inactivity bout of 5 minutes (lower arrow) and one activity bout of 6 minutes (upper arrow).

The recordings from the DAM System monitors come as long successions of numbers, where each number represents the cumulative count of times each fly crossed the infrared beam during each time unit (Figure 2.5 A). A count of 0 (zero) thus means that the fly did not show any locomotion during that time bin. While it is still possible that the fly is awake, eating or clawing at the cotton stopper, it is unlikely that it is active in locomotion without crossing the midpoint of the tube, as it has been shown that when the flies show active locomotion they tend to utilize the full extension of tube, walking back and

forth (Hendricks et al., 2000; Zimmerman et al., 2008). An active bout is constructed by summing the consecutive time units with non-zero beam-breaks, and an inactive bout is constructed, respectively, by summing the number of consecutive time-units without any locomotor activity (Figures 2.5 B and C). The raw recordings are thus dichotomized into non-overlapping alternating bouts of activity and inactivity. This data processing step is summarized in Figure 2.5.

2.3.2 Randomness, Burstiness and Memory

To learn about the underlying processes that produce the observed behavior, we need to take into account both the inter-relation between the timing of the events, and the distribution of these inter-event intervals as a whole (Goh and Barabási, 2006, 2008). If we consider a generalized temporal pattern, we can identify three distinct possibilities: A regular pattern, like the ticking of a clock; a random pattern, like radioactive decay; and a bursty pattern – where several events occur in short succession, followed by long periods of low activity or quiescence – like the firing activity of cortical neurons. What distinguishes these patterns is how predictable they are: the regular pattern is highly repetitive and predictable, a truly random, Poisson process pattern is characterized by its mean inter-event interval, while a bursty pattern is highly irregular and more unpredictable. Examples of these patterns are shown in Figure 2.6 a–c, where 2.6 a is a random pattern created by a Poisson process, 2.6 b is a bursty pattern generated by a power law and 2.6 c a is highly regular pattern.

The temporal pattern generated by the (homogeneous) Poisson process is an important benchmark when studying animal behavior, or complex systems in general, because it is a truly *random* pattern. The probability of an event occurring at any given time is completely independent of what has happened before, and only depends on a characteristic event rate, which is constant for each process. The distribution of inter-event intervals follows an exponential distribution with the probability density function (pdf): $f(t) = \Pr(t) = \lambda \cdot e^{-\lambda t}$, where λ is the global rate of the events per unit time. The cumulative probability density

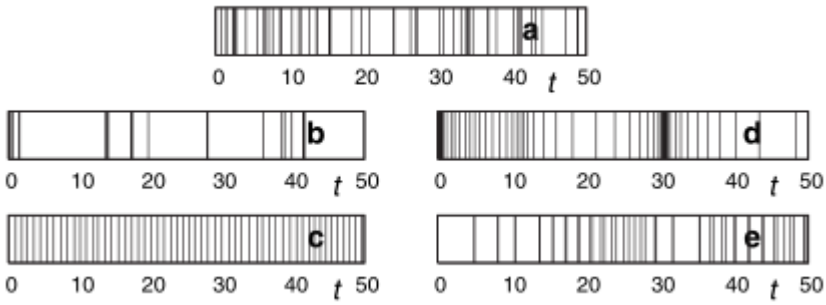

Figure 2.6: Examples of random, bursty and regular event patterns, with and without memory effects. The black vertical stripes represent events occurring and the white spaces between them the inter-event intervals, within the time frame of 50 time units. **(a)** A random pattern, generated by a Poisson process with $\lambda = 1$. **(b)** A bursty signal generated by the power law inter-event time distribution $P(\tau) \sim \tau^{-1}$. **(c)** A regular ("anti-bursty") pattern generated by the Gaussian inter-event time distribution with $m = 1$ and $\sigma = 0.1$. **(d)** and **(e)** Memory effects are introduced to the inter-event interval distribution from (a) to create seemingly more bursty (d) and regular (e) patterns, just by shuffling the event orders. *Source*: Figure from (Goh and Barabási, 2008).

function (cdf) is obtained by integrating the pdf over all values smaller than t, and is thus given by $F(t) = \Pr(\tau < t) = 1 - e^{-\lambda t}$, where τ is a non-negative random variable representing the time until some event of interest. Finally, the complementary cumulative probability density function (ccdf), or "survival function" of the inter-event intervals, that is, the probability that an event has not yet occurred by time t, is defined as

$$S(t) = 1 - F(t) = 1 - \Pr(\tau < t) = \Pr(\tau \geq t) \tag{2.1}$$

such that $S(t) = e^{-t/\beta}$ where $\beta = \lambda^{-1}$ is the characteristic time between events, for the Poisson process. The independence of previous events, or

memorylessness, is what is especially characteristic of the Poisson process.

When considering bursty inter-event interval patterns on the other hand, these can differ from the Poisson process pattern in two main ways: A bursty pattern can either be due to a change in the distribution of inter-event intervals (Figures 2.6 b and c), or be due to the presence of memory effects between events (Figures 2.6 d and e) (Goh and Barabási, 2006, 2008). An appearance of burstiness can occur if the duration of the previous inter-event intervals affects the probability of the timing of the next event, even if the distribution of IEIs at large has a random structure. To distinguish between these two generating mechanisms of bursty patterns, Goh and Barabási (2008) introduced the burstiness parameter B and the memory parameter M to quantify these separate effects.

Burstiness

To measure the burstiness due to the distribution of inter-event intervals, the burstiness parameter B is defined as:

$$B = \frac{\sigma - \mu}{\sigma + \mu} \quad , \tag{2.2}$$

where μ is the mean and σ is the standard deviation of the inter-event interval distribution. With this definition, B will take values in the range $(-1, 1)$, with a magnitude that correlates with the distributions burstiness. For highly regular (periodic) patterns, the standard deviation of the inter-event intervals will be close to zero, so the burstiness parameter will be dominated by the fraction $-\mu/\mu$ leaving $B \to -1$. For the neutral, random case, the mean and the standard deviation of a Poisson process are both equal to the characteristic rate λ, such that $B_{\mathrm{Poisson}} = (\lambda - \lambda)/(\lambda + \lambda) = 0$. On the opposite end, a highly bursty pattern will be composed of many very short intervals as well as fairly long ones, and therefore will be dominated by the standard deviation of the inter-event intervals σ, and thus $B \to 1$.

Memory

To characterize the memory effects in a bursty signal, the memory parameter M was chosen to be defined as the first step of the autocorrelation function, namely, the correlation coefficient of consecutive inter-event intervals. If τ_i and τ_{i+1} are two consecutive inter-event intervals, the memory parameter is defined as:

$$M = \frac{1}{N-1} \sum_{i=1}^{N-1} \frac{(\tau_i - \mu_1)(\tau_{i+1} - \mu_2)}{\sigma_1 \sigma_2} \tag{2.3}$$

where N is the total number of inter-event intervals in the signal, μ_1 (μ_2) are the sample mean and σ_1 (σ_2) are the sample standard deviation of the τ_i (τ_{i+1}), $i = 1, \ldots, N-1$ inter-event intervals. This memory parameter will be bound in the range $(-1, 1)$, where high degrees of memory will be observed in signals where similar intervals succeed (short–short or long–long) leaving $M \to 1$, and anti-memory patterns will be observed when the interval lengths alternate (short–long or long–short), yielding $M \to -1$. Since the memory parameter M only considers the correlation between adjacent intervals, it is important to note that this is a measurement only of short term memory effects.

Detrended Fluctuation Analysis

To measure long term memory effects of the inter-event intervals of behavior, we have used detrended fluctuation analysis (DFA) algorithm, which detects long-range correlations embedded in non-stationary signals (Peng et al., 1994, 1995). The DFA algorithm consists, briefly, of integrating the time series and dividing it into smaller evenly sized subsets, or "boxes". For each subset the trend is found by fitting a straight line to the integrated signal in the box, and the full detrended signal is obtained by subtracting the local trends in each box. The root mean-square fluctuation $F(n)$ is then calculated on the full integrated and detrended signal. The process is repeated for all the possible sizes of boxes, such that we obtain a relationship between $F(n)$ and the box size n. This relationship is typically increasing with box size and linear on a double logarithmic scale. The last step is thus to characterize this relationship

by considering the scaling exponent α of the straight line fit between $\log(F(n))$ and $\log(n)$. For random, memoryless signals like from a Poisson process the scaling exponent is $\alpha = 0.5$, while an $0 < \alpha < 0.5$ indicates that short and long inter-event intervals tend to alternate, and an $0.5 < \alpha < 1$ that short (long) intervals tend to follow short (long) intervals. For $\alpha \geq 1$ the power law relation breaks down, with special cases of α equal to 1 and 1.5 corresponding to $1/f$ noise and Brown noise, respectively.

2.3.3 Finding Simple Functional Forms

While calculating the burstiness parameter and the memory effects is important for finding out about the source of the observed burstiness, we also need to study the distribution of inter-event intervals to learn more about the dynamics and hopefully about the underlying generating mechanism. This is done by trying to find the most simple mathematical functional forms or standard basic distributions to describe and compare the inter-event distributions to. While more complicated functional forms pose no technical problem, the difficulties arise at the time of interpretation. Complex functional forms increase the number of parameters, and clear cut interpretations of the parameters and how they relate to the biological system are usually difficult. In addition, complex functional forms are prone to over-fitting, whereby the function adapts to all the small turns and curves, when in fact these could be due to noise in the signal.

There are four main classes of simple functional forms that have known or interpretable generating mechanisms behind, and that are commonly used in the study of complex systems. These are the exponential function, the power law, the stretched exponential and the log-normal distribution (Newman, 2004; Goh and Barabási, 2008). The latter three of these are all able to fit bursty distributions which are known for having a “fat” or “heavy” tail – meaning that the probability of finding really long inter-event intervals is higher than for the exponential function. Briefly, the exponential function is observed when the inter-event intervals stem from a memoryless process with a constant rate, which

we saw corresponds to the Poisson process. In contrast, a power law is indicative of fractal, or scale-free dynamics, whereby there exists no characteristic rate. Distributions that follow a power law are often called self-similar, because they are invariant to scaling factors and thus retain the relationship between "large" and "small" – regardless of the scale, or *zoom* used to observe them. Next, the stretched exponential function and the corresponding Weibull distribution is a generalization of the exponential function where a shape parameter is introduced as a power of time, so that the probability of observing an event depends on how much time has transcurred since the previous event. Lastly, the log-normal distribution is observed when a large number of independent components' interactions create a multiplicative effect, which also gives rise to a heavy-tailed distribution.

We say that an empirical inter-event interval distribution follows a functional form, when by a fitting method the function is found to have a good fit to the data. There exist two main methods for estimating the parameters of the function to the data: goodness-of-fit measures, like least squares, and maximum likelihood estimation. The exact fitting procedures and choices among the methods will be presented in each chapter as they are used.

3

Bursty Activity Dynamics in *Drosophila melanogaster*

3.1 Introduction & Background

Bursty phenomena have been observed across the fields, throughout both the physical and biological realms, as well as in man-made systems (Barabási, 2005; Goh and Barabási, 2008). Relating to animal behavior, bursty phenomena or "scale-free" behavior has predominantly been studied in free ranging animals and the observations have been linked to foraging behavior, mate encounters and predator evasion (Viswanathan et al., 2011). Although the experimental studies and results presented in this chapter mainly take a neurobiological approach to the dynamics of spontaneous behavior, we will start with a short overview of the modeling approaches and empirical evidence from the fields relating to spatial ecology and Lévy statistics, to not forgo this vast body of literature which is relevant and related to our work, even though its framework has not been the main focus of our studies. Thereafter we will briefly be introduced to the neuroscientific approach to studying animal behavior and the "discovery" of spontaneous behavior in invertebrates.

3.1.1 Modeling Animal Movement Patterns

Traditionally in the field of spatial ecology, the non-oriented movement of animals had predominantly been assumed and modeled as a normal diffusion process based on Brownian motion (Viswanathan et al., 2011; Reynolds and Rhodes, 2009). In the long-term limit, normal diffusion assumes that animal movements can be modeled as uncorrelated random walks (Codling et al., 2008; Viswanathan et al., 2011). In an uncorrelated random walk, an animal's path is modeled as a succession of randomly oriented straight lines with step-lengths drawn from a distribution with finite variance, e.g. from the exponential distribution (Codling et al., 2008). After a sufficiently long time, by the central limit theorem, the spatial distribution will converge on a Gaussian distribution, with the mean squared displacement of the diffusive process linearly dependent on time. In this model, *uncorrelated* specifies that

the direction of movement of each new step is completely independent of the directions previously taken (Codling et al., 2008). This model has been useful in many cases for describing experimentally observed movement and dispersal of animals and micro-organisms (Skellam, 1951; Broadbent and Kendall, 1953; Fenchel, 2004).

It was however noted that animal motion seldom is uncorrelated but tends to progress in approximately the same direction as the previous steps, a quality coined as "persistence" (Patlak, 1953). This gave rise to the correlated random walk (CRW) models, where memory effects are introduced through correlations between the orientation of steps to create persistence, and has been used to model animal motion in various contexts (e.g. Siniff and Jessen, 1969; Kareiva and Shigesada, 1983; Bovet and Benhamou, 1988, and for overview see Codling et al., 2008; Viswanathan et al., 2011; Turchin, 1998). Important to note about CRWs is that while these models effectively create persistence on the local scale, the memory effect diminishes over time leaving the step orientations uniformly distributed overall. Thus, on large spatial and temporal scales CRWs also become uncorrelated random walks (Viswanathan et al., 2011).

In the 1980s, however, work on fractals and anomalous diffusion from fields such as critical phenomena, non-linear and complex systems in physics reached the field of spatial ecology, through the work by Shlesinger and Klafter, who suggested that the movement pattern of some animals could be described by a Lévy flight (Shlesinger and Klafter, 1986), a term coined by Mandelbrot in his highly influential book "The Fractal Geometry of Nature" (Mandelbrot, 1982). A Lévy flight is a random walk in which the distribution of jump sizes is drawn from a power law and thus has infinite variance, creating fractal trajectories that have no characteristic scale. Lévy flight patterns are characterized by clusters of many short jumps interspersed by longer jumps between them, which in turn is repeated at all scales, leading to a self-similar and scale-invariant pattern (Klafter et al., 1996; Codling et al., 2008), Figure 3.1. The distribution of jump sizes ℓ has an inverse power law tail with $p(\ell) \sim \ell^{-\mu}$, with $1 < \mu < 3$ being the power-law (Lévy) exponent (Reynolds, 2012; Viswanathan et al., 2011). A defining characteristic of the Lévy flight is that the jumps are instantaneous

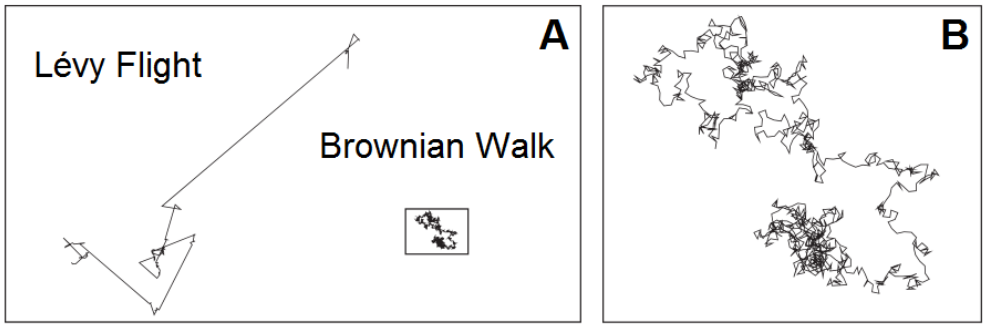

Figure 3.1: Examples of Lévy flight and Brownian walk. (A) The Lévy flight and the Brownian walk have the same trajectory length, but the Lévy flight visits much larger areas. The trajectories are to scale. **(B)** An enhancement of the Brownian walk trajectory of panel A. Notice how the Brownian walk trajectory returns many times to the same place, and thus explores a much smaller area than does the Lévy flight trajectory. *Source*: Modified from (Viswanathan et al., 2011, p. 55).

between points and that the mean squared displacement between them is infinite. Since instantaneous jumps are not compatible with physical and biological systems, this can be overcome by defining the Lévy walk, where movement between points is given a finite velocity (usually constant), so that the spatial probability density converges to a Lévy stable distribution with Lévy index $\alpha = \mu - 1$, with $0 < \alpha < 2$. Lévy walks give rise to superdiffusion, meaning that the mean square displacement grows faster than linear with time, and thus in contrast to the correlated random walks above, Lévy walks can be used to model phenomena with long-range dispersals (Klafter et al., 1996; Viswanathan et al., 2011).

The first experimental findings of non-Brownian motion of animals were made in the swimming behavior of micro-organisms (Levandowsky et al., 1988a,b), and the fractal structure of insect movement trajectories which were presented some years later (Wiens et al., 1995; Cole, 1995), Figure 3.2. In 1996, an influential study by Viswanathan, H.E. Stanley and collaborators on

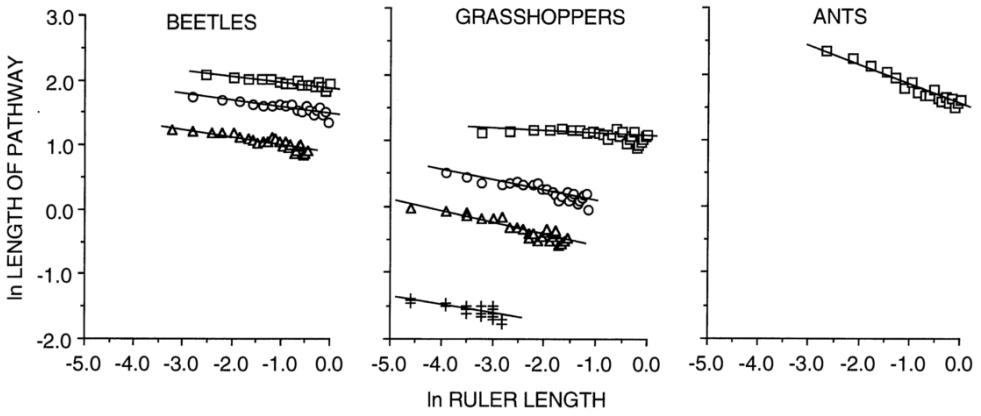

Figure 3.2: Fractal patterns of insect movement. Regression line fits between the logarithm of the insect movement pathway lengths (y-axes) and the logarithm of the measurement scale for three beetles species (left), four grasshopper species (center) and one ant species (right). The linear regression yielded fractal dimensions D of 1.17–1.19 (beetles), 1.09–1.21 (grasshoppers) and 1.31 (ants). *Source*: (Wiens et al., 1995).

the foraging paths of free-ranging wandering albatrosses (*Diomedea exulans*) looking for prey on the ocean surface found that the flight times t followed a power-law distribution $t^{-\mu}$ with $\mu \approx 2$, and suggested several possible explanations, such that the albatrosses foraged in fractally structured environments or that the pattern might have occurred due to the turbulent atmosphere and oceans (Viswanathan et al., 1996), Figure 3.3 A. Three years later, Viswanathan and colleagues published similar findings in bumblebees and deer, and showed that truncated Lévy walks with $\mu \approx 2$ can outperform Brownian walks when searching for resources that are sparsely and randomly distributed (Viswanathan et al., 1999). In the truncated Lévy walk model a step ends when the animal finds food and thus truncates some search steps, leading to a power law distribution with an exponential (Gaussian) tail. This led them to propose the *Lévy flight*[1] *foraging hypothesis* which states that "since (truncated) Lévy flights

[1]Although Lévy flights strictly speaking are defined as instantaneous (discrete) jumps and Lévy walks represent continuous movement with a velocity, and thus corresponds better to

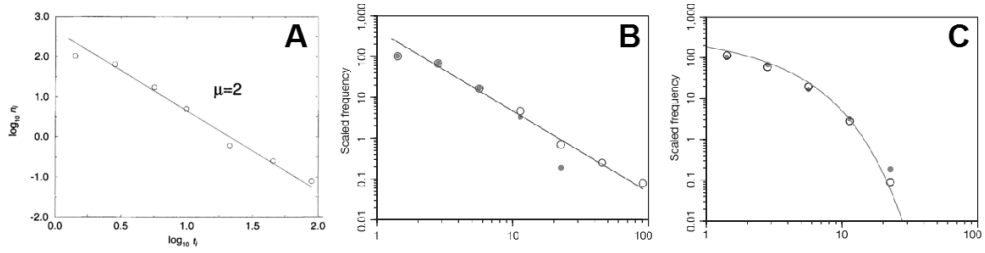

Figure 3.3: Flight duration distribution of albatrosses, original and revisited. (A) Log-binned distribution of the number of intervals n_i vs the flight time intervals t_i. A linear regression finds μ=2, and thus that the flight-time intervals are power-law distributed. **(B)** The original data (open circles) and power-law fit (solid line) from panel A, plotted together with the corrected data (solid dots) for comparison. **(C)** The corrected data (solid dots) no longer follow a power law, and is instead well fitted by a gamma distribution (solid line and open circles). The albatross data are thus better fit by an exponential tail. *Source*: Panel A from (Viswanathan et al., 1996) and panels B and C from (Edwards et al., 2007).

optimize random searches, biological organisms must have therefore evolved to exploit Lévy flights" (Viswanathan et al., 1999, 2008). Several studies followed, where support for Lévy walks were found in the movement patterns of for example reindeer (Maarell et al., 2002), jackals (Atkinson et al., 2002), gray seals (Austin et al., 2004) and spider monkeys (Ramos-Fernández et al., 2004).

A reanalysis of the original wandering albatross data in 2007 by Edwards and colleagues (including the original authors), found however that there had been experimental errors included in the longest flight times, and when reanalyzed and compared to newly acquired high-resolution data, no evidence for Lévy flight was found, but instead exponentially distributed flight times for the longest flights (Edwards et al., 2007), Figure 3.3 B–C. A reanalysis of the deer and bumblebee data with modern statistical techniques found that neither

biological systems, in the literature on random searching the terms "flight" and "walk" have come to be interchangeable (Reynolds and Rhodes, 2009).

exhibited Lévy flight behavior, and that more rigorous statistical methods had to be used to determine the existence of power laws and to determine their scaling exponents, putting in question the strength of the empirical evidence for biological Lévy walks. Shortly after, in a survey of 24 studies of foraging movements and dispersals, including some mentioned above, only six were found to have correctly estimated the power law exponent, and for some, an exponential distribution provided a better fit (James and Plank, 2007). Concurrently, composite correlated random walk (CCRW) models, inspired by empirical evidence of intermittent search behavior in patchy environments where local search and relocation phases alternate, were shown to also optimize the search time and proposed as alternatives to the Lévy flight mechanism. CCRWs can be generated by mixing classical random walks of different time scales, and can easily be confounded with Lévy walks because they also display move-length distributions with heavy tails and superdiffusivity (Bénichou et al., 2006; Benhamou, 2007).

Only a year later, Sims and colleagues published a large-scale study of several marine predators which were found to show Lévy-walk-like behavior (Sims et al., 2008), which was again criticized a few years later for incorrectly estimating the scaling exponents (Edwards et al., 2012) (but rebutted (Sims and Humphries, 2012)). It was also suggested that the observed pattern might be due to oceanic turbulence (Reynolds, 2014). Many more experimental, theoretical and modeling efforts have been made, where empirical evidence both in favor of the Lévy flight hypothesis has been presented (e.g. Raichlen et al., 2014; Sims and Humphries, 2012; Sims et al., 2014), as well as reanalyses of previously published findings showing little support for Lévy flights (Edwards, 2011). In addition, there have been studies finding more complex behaviors which are not easily explained solely by the Lévy walk model (Bazazi et al., 2012; Humphries et al., 2010). These findings are more consistent with mixed models, where animals are thought to perform Lévy walks between patches of food, and switching over to Brownian motion when in abundant areas of food (Lomholt et al., 2007; Humphries et al., 2010; Sims and Humphries, 2012), a characteristic encompassed by and in evidence for the Lévy flight

foraging hypothesis by its proponents. Yet others have found that individual variability created the impression of a Lévy flight (Petrovskii et al., 2011) or that it was due to intraspecific interactions (Breed et al., 2014). Remarkably, a new study with new data on wandering albatrosses, as well as a reanalysis of the previous data, showed wandering albatrosses exhibiting Lévy and Brownian movement patterns and thus again support the Lévy flight foraging hypothesis (Humphries et al., 2012, 2013). The effect of data acquisition and sampling were shown through simulations to give rise to misidentification of power laws (Plank and Codling, 2009; Codling and Plank, 2011; Gautestad, 2013), and theoretical advances have investigated the conditions under which the Lévy flight optimizes the search and found that it only does so under certain, non-universal, conditions (Reynolds, 2010; James et al., 2011; Palyulin et al., 2014), or investigated the hypothesis that Lévy walks emerge as adaptations to the statistical patterns of the landscape (Benhamou, 2007; Sims et al., 2008; Reynolds, 2009), just to mention a few.

Nevertheless, it is important to point out that there is growing evidence of heavy tailed distributions in animal foraging patterns (be it from Lévy walks, CCRWs or other underlying mechanisms), and that the technical issues about correct parameter extraction have been mainly settled during the last few years' discussions about usage of correct statistical methods (Clauset et al., 2009; Virkar and Clauset, 2012). There does however remain active debate about under what conditions the optimal search occurs, as well as notably, about whether the underlying generating mechanism i) is a Lévy walk at all, and if so, ii) if it was evolutionary selected for or not. A growing number of mechanisms able to generate power laws and other heavy tailed distributions have been published (Mitzenmacher, 2001; Newman, 2004; Barabási, 2005; Proekt et al., 2012), which suggest that the patterns we see in animal behavior could have arisen freely as by-products of other processes. A recent addition to the debate by A.M. Reynolds (2015) suggesting "that the Lévy flight foraging hypothesis should be amended, or even replaced, by a simpler and more general hypothesis" (Reynolds, 2015) prompted 9 published comments and a reply (see URL of Reynolds, 2015), and is a good indicator of the state of the field as of today.

3.1.2 Movement Patterns and Spontaneous Behavior

A very different approach is that of neuroscience, where one of the main goals is to unravel circuitry and neuronal function that give rise to and control behavior, in this case, animal movement. For over a century, insect movement has been studied in a wide variety of species, as insects have provided the perfect 'simpler' model systems to understand behavior and the components of which it is constituted. One of the most important functional systems for flying insects is the visual system, which in *Drosophila* accounts for about two-thirds of the fly's nervous system (Strausfeld, 1976). Flying insects have evolutionarily had an enormous success, with tens of millions of species occupying almost every habitable land mass on the planet (Dudley, 2000).

Important early advances on component-based modeling of insect vision were made by Reichardt and Hassenstein during the 1950s, when they developed the correlation model – now known as the elementary motion detector (EMD), which they tested and corroborated by studying the walking behavior of tethered beetles (*Cholorphanus*) clasping onto and walking on a light-weight "Y-maze globe", in response to visual stimuli (Hassenstein and Reichardt, 1956), Figure 3.4 A. The EMD is a simple and elegant theoretical model that explains the minimal computations that are needed in order to perceive motion from two elemental units of photoreceptors, by introducing a time delay between the signals and a non-linear multiplication when these are correlated (Borst and Egelhaaf, 1989). Reichardt later moved on to study the visual system of fruit flies in collaboration with Götz, who had designed a torque compensator for an experimental set-up known as the torque meter, in which a tethered fly is attached to a torque compensator in the center of a cylindrical rotatable drum, so that the visual field of a fly can be controlled (Götz, 1964; Reichardt and Wenking, 1969). The fly is attached by the head and thorax, such that the abdomen, legs and wings can be moved freely and used to produce movements which are registered by the torque compensator, Figure 3.4 B. When in this setting the flies tend to fly (for about 20 minutes), and the intended flight maneuvers can be measured as a response to different visual stimuli (Brembs,

2008). Two general modes of operation are used at the torque meter: open-loop, where the fly is presented with visual stimuli and the yaw torque is measured in response; and closed-loop, where a feedback loop is established between the yaw torque and the cylinder rotation, so that the fly controls its own visual environment, creating in effect a "flight simulator". With this torque meter they, and many others, studied for example the principles of optomotor reactions (Götz, 1972), fixation, tracking and chasing behavior (Virsik and Reichardt, 1976), and stabilization of the panorama (Heisenberg and Wolf, 1979). Since then extensive research on the fly visual system has continued, making it probably the best understood sensory and control system for which we have an understanding on all levels of complexity: from the systems/components level down through single cells and recently even to the molecular level (reviewed in e.g. Silies et al., 2014; Behnia and Desplan, 2015).

The dominating paradigm for behavioral neuroscience for most of the past century had been to consider the brain as a set of simple input-output systems (more or less complex) and thus treat each system as a black-box problem, where the goal is to find the internal components or circuitry that provide the observed behavior in response to a stimulus. Many of the early advances on the visual system of *Drosophila* were achieved by applying control theory tools from electronics and physics to visual stimulus-response relationships, in order to construct a control model of the expected motor output for tested and novel input stimuli (Reichardt and Poggio, 1976; Brembs, 2009). The experiments at the torque meter had initially been performed in open-loop mode, where the flies' behavioral responses had no effect over the visual stimuli received, but also closed-loop experiments showed interesting effects of complex visual processing. In 1975 Collete and Land observed how flies during free flight would switch from one behavioral pattern to another without any apparent external cues, and found the only plausible explanation to be "free will" of the flies (Collett and Land, 1975), unfortunately without any experimental proofs. In 1979, however, Heisenberg and Wolf presented the novel observation at the torque meter that even in the absence of visual stimuli in featureless visual arenas the flies would produce spontaneous variable motor outputs. These "actions" were generated

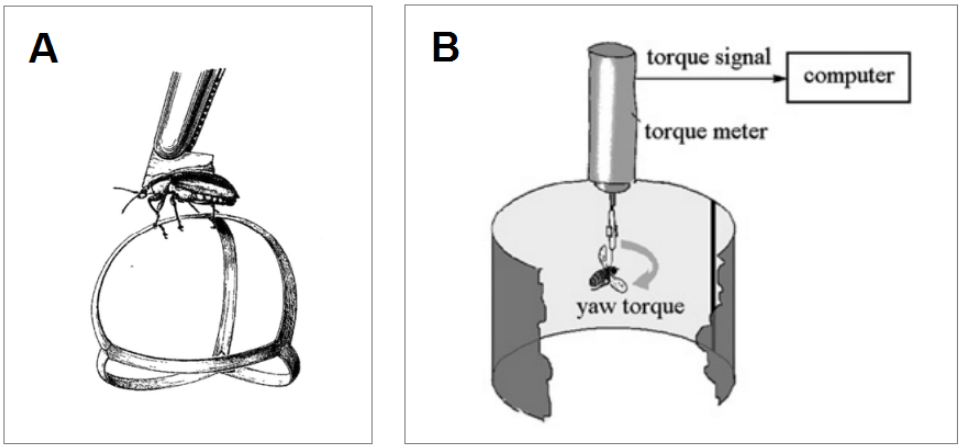

Figure 3.4: Tethered walk and flight assays in insects. (A) The response to visual stimuli is measured in a tethered beetle by its behavioral choices of selecting the right or the left direction at a bifurcation, when walking on a light-weight "Y-maze globe". **(B)** The response to visual stimuli is measured in a tethered fruit fly by the torque meter, which measures the yaw-torque (turning force) exerted by the fly when trying to turn left or right. The yaw torque signal is sent to a computer that records the activity and that can control the visual panorama of the fly by rotating the drum, if the set-up is operated under closed-loop. by the torque meter, which then sends the signal to a computer. *Source*: Panel A from (Poggio, 2011) and panel B from (Sareen et al., 2011).

actively by the flies independently of any input and were not "responses", showing a variability in the behavior which did not appear to originate in a noisy input-output system and was thus concluded to be voluntary, in stark contrast to the prevailing control theory paradigm of the stimulus-response, input-output function of the brain (Heisenberg and Wolf, 1979). In a more recent study Maye and colleagues confirmed the spontaneous nature of the behavior, and studied the yaw torque behavior under closed-loop conditions as well, where they found the same kind of variability in the behavioral patterns (Maye et al., 2007).

The discovery led to further progress on the "initiation activity" (Heisenberg, 1983), as well as to the next and extraordinary discovery: even when flies were placed in an "inverted flight simulator", where left and right turns were flipped to have the opposite effect on the visual surrounding to what they do in natural conditions, the flies were able to learn to control it and continue to fly straight after a few minutes of trial and error (Heisenberg and Wolf, 1984; Wolf et al., 1992). This directly challenged the prevailing notion that insects and 'simple' organisms were thought to have a hard-wired neuronal "autopilot" that assured straight flight (Rowell, 1988). Plasticity to "inversion goggles" of the visual field had been shown in primates in famous experiments during the 1950s and 60s. The inverted flight simulator experiments provided evidence of a remarkably plastic nervous system also in invertebrates, where spontaneous activity and flexible adaptation were the prominent features, and led to the proposal of the operant loop in flies (Wolf and Heisenberg, 1991; Wolf et al., 1992). In operant behavior, animals actively generate actions and evaluate the sensory feedback in order to find the motor output that controls the environment as desired (Brembs, 2009). This idea of animal brains as output-input systems which generate behavior and assess the consequences, sometimes known as *forward models*, is increasingly recognized as an important explanatory concept for vertebrate motor control, and are now also being found in invertebrates such as *Drosophila* (Webb, 2004; Brembs, 2013; Heisenberg, 2015). While the control theory based approach to animal behavior both gave, and continues to give us new and fascinating insights into how the nervous system produces everything from stereotypical responses to stimuli; to learning and memory formation; to visual attention and decision-making processes, there also exists this other parallel paradigm of animal behavior in which the animals rely on endogenous, voluntary behavior to adapt to the external world.

3.1.3 Concluding Remarks

In this *Introduction & Background* section we have seen a statistical modeling approach and a neuroscientific approach to animal locomotor behavior, the latter focused mainly on invertebrate research. The work presented in this chapter has drawn inspiration from both of these fields, using tools and methodology from the statistical approach to measure the burstiness in spontaneous behavior, while using the neuroscientific tradition of controlled experiments in the lab and genetic manipulation to further dissect the neural basis of behavioral variability.

3.2 Dynamics of Spontaneous Walking Activity

3.2.1 Introduction

Drosophila melanogaster has been used extensively to study biologically intrinsic patterns for almost half a century, starting with the mutational studies of circadian rhythm components (Konopka and Benzer, 1971) (see also 2.1.1 *Introduction*). The fine-scale dynamics of walking activity were first investigated during the "discovery" of Lévy statistics across physical and biological systems during the 1990s, discussed in the introduction to this chapter. The first account was given by Cole (1995), where *Drosophila* was reported to move in fractal time, with a self-similar activity pattern on all scales (Cole, 1995). Following, Martin et al. (1999a) studied the walking activity under various environmental conditions and also found a fractal dimension, although only for flies walking in complete darkness and without any food. If either of these were present, the activity dynamics were described to "resemble [what] would be obtained from a random distribution" (Martin et al., 1999a, p. 79). In the next study, Martin et al. (2001) found that the fractal property of the temporal pattern was lost when selectively blocking neuronal activity in the ellipsoid-body, a subpart of the brain region known as the central complex and known to control locomotor behavior (reviewed in Strauss, 2002).

These studies thoroughly examined the fractal properties of walking flies, however, as we just saw, these are only present under specific conditions. Since the optimal foraging hypothesis is built on Lévy statistics and Lévy statistics is based on power laws, the previous studies have centered on finding the power-law nature of fly walking activity, and merely noted when this was lost, without much further investigation. Much of fly life does however take place in daylight and in presence of food, leaving ecologically relevant behavioral conditions open for closer examination.

We used the *Drosophila* Activity Monitor (DAM2) System, described in section 2.2.2 [p. 17], to measure the walking activity of flies. In the DAM2 monitor each fly is housed individually in a small glass tube, sealed with a softly

packed cotton stopper which allows for air to pass on one side and enough food for the duration of the experiment on the other. Unlike the previous studies, which measured the activity of flies without access to food and were thus limited in time, we studied the walking activity for several consecutive days and nights, to obtain long-running data. We found that the activity dynamics of *Drosophila* can be described by a stretched exponential function (Weibull distribution), and that *Drosophila* has markedly bursty dynamics also under these conditions.

The work presented in this section has been published previously, as a part of: Amanda Sorribes, Beatriz G. Armendariz, Diego Lopez-Pigozzi, Cristina Murga, Gonzalo G. de Polavieja (2011) *The Origin of Behavioral Bursts in Decision-Making Circuitry*. PLoS Computational Biology 7(6):e1002075. doi:10.1371/journal.pcbi.1002075

3.2.2 Results & Discussion

Fitting to Empirical Distributions, Approach and Considerations

To study the dynamics of walking activity in the DAM2 System, we need to study the fine-scale structure of the timing of events (as described in section 2.3 *Analyzing the Fine-Scale Dynamics of Spontaneous Activity*). To find a simple functional form that fits the data of inter-event intervals, the first inclination might be to plot the histogram of the data to obtain the empirical probability (relative frequency), and fit a theoretical probability density function (pdf) to this empirical distribution. This approach works well for distributions that are mostly centered around a mean value, but for bursty processes which are characterized by many short inter-event intervals interspersed by a few long and very long ones, the empirical histogram becomes very noisy for large and rare values, as only a few bins will be represented while the majority of bins will be zero in the tail. Incidentally, for bursty distributions which are right-skewed and heavy-tailed, the right tail region is where much of the information about the burstiness resides, as the degree of burstiness is mainly characterized by the relative occurrence of these very long inter-event intervals in relation to medium and short ones.

An approach to mitigating the sampling error in the tail is to use bin sizes of increasing widths, so that each bin now gets a larger sample size and the sampling error is reduced. If this method is used, each sample count has to be normalized by the bin width, so that the sample counts become independent of the choice of bin widths. A commonly used choice of bin widths is logarithmic binning, where each bin is a fixed multiple wider than the one before it (Newman, 2004). This has the added benefit of creating equidistant bin spaces on logarithmically scaled axes.

Another approach is to use the complementary empirical distribution function, defined as the complementary cumulative distribution function (ccdf) for the empirical data (van der Vaart, 2000). The complementary cdf, or "survival function", describes the probability of finding an inter-event interval greater than or equal to t for each t, and is a monotonically decreasing function starting at $\Pr(0) = 1$, as all time intervals are greater or equal to $t = 0$ for a non-empty distribution (see also Equation 2.1 [p. 24]). Using the ccdf is thus more powerful than using logarithmic binning as the empirical ccdf has information (non-zero values) for every t up until and including the largest value in the data set, without losing some of the detailed positional information otherwise lost by aggregating large values into wide bins in the tails.

Before we dive into analyzing the fine-scale dynamics of *Drosophila* walking behavior, however, there are some important considerations that need to be addressed. The first consideration is to collect sufficient data from each animal to be able to perform meaningful model fits for each individual. In older studies it used to be quite common to pool data from several or many individuals together and then perform model fits on the pooled data, a strategy used in all the previously mentioned studies on *Drosophila* walking dynamics cited above in the introduction (section 3.2.1 [p. 44]). Performing model fits to pooled data has however been shown to give rise to spurious results, especially when encountering power laws, since by a version of the central limit theorem the power-law distribution acts as the limiting distribution for the sum of independent random variables drawn from heavy-tailed distributions (Stumpf and Porter, 2012) and is therefore expected to be found often even if the

underlying distributions are not power-law distributed. It has also been shown that power laws can be obtained when fitting to collective pooled data of Poisson individuals acting randomly but at different rates (Hidalgo, 2006).

Another important consideration, especially when working with spontaneous animal locomotion, is to take into account the naturally occurring circadian rhythm of activity and rest, which modulates the probability of being active according to the time of day. In the case of seasonal or circadian variations it has been shown that if an individual acts randomly according to a Poisson process, but at a dynamically variable rate, it also gives rise to apparent power-laws of the inter-activity distribution (Hidalgo, 2006; Malmgren et al., 2009).

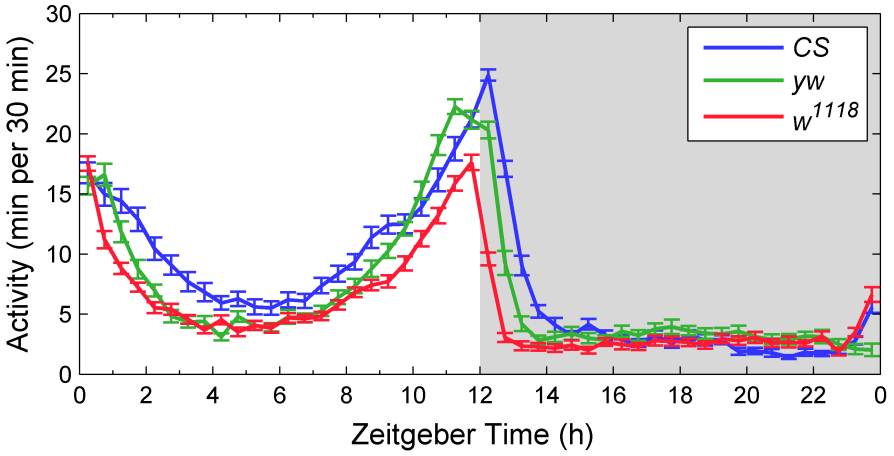

Figure 3.5: Circadian activity pattern for three standard genetic background lines. Plot of population mean daily activity pattern, for 3-day-old *Canton-S* (*CS*, blue), *yellow-white* (*yw*, green) and *white*^{1118} (w^{1118}, red). Zeitgeber Time (ZT) denotes the subjective time of day, where ZT=0 denotes the start of the day (lights on, white background) and ZT=12 the start of the night (lights off, gray background). After an initial day of adaptation, the walking activity was measured for 3 consecutive days, and for each fly a daily average pattern was calculated as the number of active minutes per half an hour. The population mean is calculated as the mean of the individual average daily patterns. Number of flies n=28—32, error bars represent s.e.m. *Source*: Modified from (Sorribes et al., 2011).

If we recall from section 3.1.1 *Modeling Animal Movement Patterns*, this is the basis for the composite correlated random walk (CCRW) models, which as we saw, also gave rise to power-laws of the intermittent animal foraging behavior. In *Drosophila* this consideration is of particular importance given that the activity pattern is highly dependent on the subjective time of day, with more activity during the day-time (lights on) with peaks of activity occurring after the subjective sunrise and before the subjective sunset (Figure 3.5).

Finally, a very important consideration is that of validating the method used for model fitting or parameter estimation. As we saw in the Introduction & Background section 3.1.1 *Modeling Animal Movement Patterns*, much controversy arose over the presence or not of power laws, $\Pr(t) \sim t^{-\alpha}$, in animal movement data, and over whether the exponent α had been correctly estimated in many studies. As it turns out, power laws are particularly tricky to estimate, as a power law cannot hold over the entire empirical probability distribution because a pure power law cannot be normalized. This leads to the necessity of only finding a power-law relationship over some region of the data, with the added arbitrariness of deciding these limits. An additional complication resides in that, traditionally, the presence of power laws used to be established by a linear regression (sometimes even visually) of the data on a log-log plot (Stumpf and Porter, 2012). For an empirical distribution to be considered to follow a power law, an often used criteria was that the power law hold over at least one order of magnitude with a linear regression coefficient $r^2 > 0.99$ (Coughlin et al., 1992; Martin et al., 1999a). This approach has however been shown to be problematic for two main reasons. First, it has been shown that linearity on a log-log plot is a consequence, but not a predictor, of an underlying power-law relationship, as many other heavy-tailed distributions can "look straight" on a log-log plot, as well as previously mentioned, other generating mechanisms (like mixed exponentials) can give rise to power-law-like distributions (Newman, 2004; Hidalgo, 2006; Clauset et al., 2009). Secondly, it has been shown that even if the distribution *is* in fact a power law (created explicitly by drawing from a power law with known exponent), the linear regression method still does not estimate the scaling exponent α correctly (Clauset et al., 2009). The first

objection deals primarily with the problem of model selection (which we will not see in this chapter, but will be presented and employed in section 4.2 *Ontogeny of Sleep-Wake Dynamics in Zebrafish and Humans*), while the second stresses the importance of verifying the parameter estimation technique (which we will see in section 3.2.2 *Validating the Parameter Estimation Method*).

Intrinsic Burstiness of Walking Activity

To study the fine-scale dynamics of *Drosophila* we used the DAM2 System which allowed us to record for several consecutive days from each individual fly, to obtain sufficient data (Figure 3.6). Moreover, with the DAM2 System we were able to collect data from up to 32 individual flies concurrently in each monitor. We measured the walking dynamics in the wild-type (WT) strain *Canton-S* (*CS*) and in the genetic background strains *yellow-white* (*yw*) and *white*^{1118} (w^{1118}),

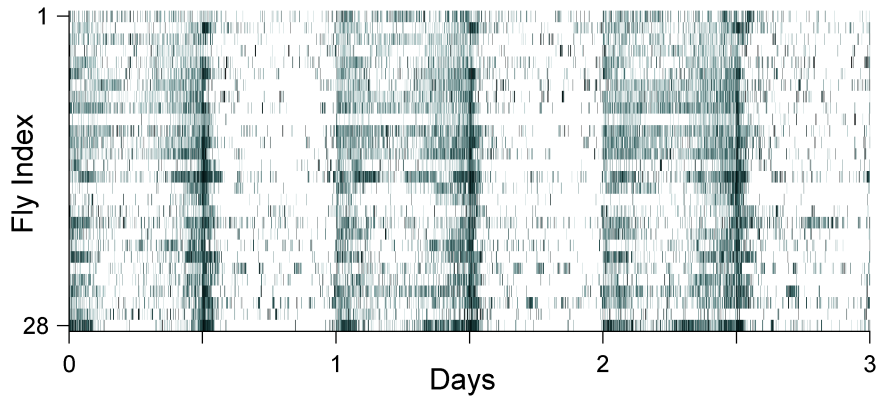

Figure 3.6: Raster plot of *Drosophila* walking activity. After an initial day of adaptation, the walking activity of 28 *Canton-S* flies (y-axis) was measured for 3 consecutive days in 1-minute bins (x-axis). The color of the bins represent the number of beam-breaks, where white denotes no activity and darker gray-scale colors indicate more intense walking activity. The flies were kept on a 12:12 light:dark schedule, which is clearly visible in the flies' activity patterns, with more activity during the light hours (the first half of the day).

commonly used as backgrounds for genetic mutations and transgenic crosses and thus frequently also serving as control lines. Additionally, we measured the dynamics in young (3 days) and adult (4 weeks) flies. To avoid a circadian influence on the walking dynamics we only used data from the night (lights off) period which has a largely stationary activity profile, in contrast to the day-time period (lights on) which shows a non-stationary activity dynamics with a mid-day *siesta*, Figures 3.5 and 3.6.

After an initial day of adaptation (24 h or more) the flies' walking activity was recorded for 3 days. From the recordings we constructed the inter-activity intervals (IAIs) and activity bouts (ABs) for each fly, as described in section 2.3.1 *Processing Raw Data into Bouts* [p. 21]. When plotting the empirical complementary cumulative distribution function (ccdf) of the IAIs from the night (Figure 3.7 A, black error bars) there is a clear deviation from random behavior as the empirical IAI distribution has a heavier tail than the exponential function which corresponds to Poissonian behavior (Figure 3.7 A, dotted line for Poisson distribution with the same mean IAI as the empirical data). A heavy tail is indicative of bursty dynamics, where short and very long inter-activity intervals are found more often than in random (Poisson) dynamics.

We found that the stretched exponential function (which when normalized is also called the Weibull distribution) gives an excellent fit to the full range of IAIs (Figure 3.7 A, gray line), and thus avoids the problem of the power law which can only fit a portion of the data. The ccdf of the Weibull distribution is given by

$$\Pr(\tau \geq t) = \exp(-(t/\lambda)^k) \tag{3.1}$$

where τ represents the inter-activity intervals, λ is the scale parameter and k is the shape parameter of the Weibull distribution. As we see by the presence of λ the Weibull distribution has a natural scale, in contrast to the power law which is scale free. It must be stressed however, that we are measuring IAIs during a complete night-cycle, and thus there must exist a cut-off at the high end because an IAI cannot last longer than a full night (12 h) by external constraints. This is true of finite systems that exhibit power-law dynamics as well, which is why power laws with exponential cut-offs are sometimes used (Clauset et al., 2009).

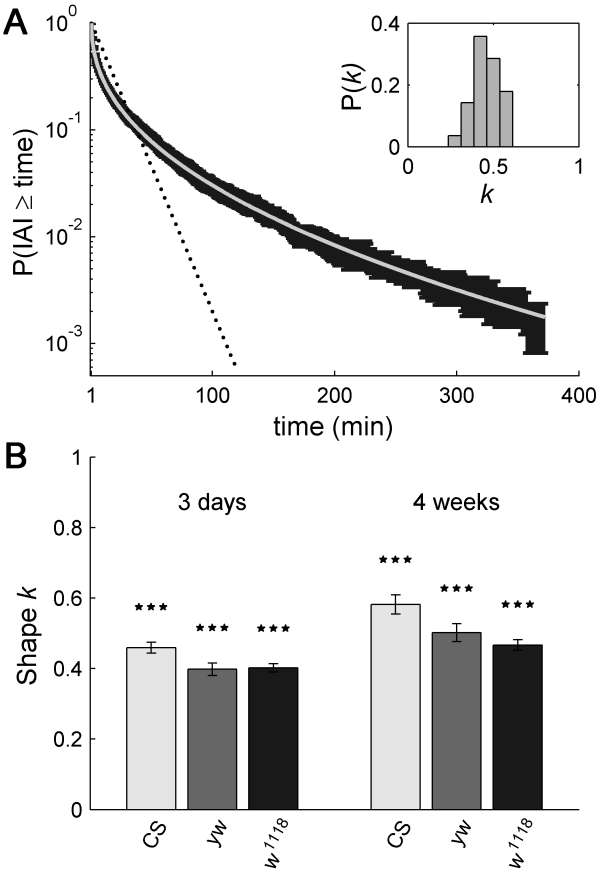

Figure 3.7: The Weibull distribution fits the empirical IAIs well. **(A)** Mean IAI ccdf (black) of *CS* flies has a heavier tail than the exponential distribution with the same mean IAI (dotted line). The Weibull distribution (gray) with k=0.45, λ=6.0 fits the data accurately (r^2=0.998). **(A-Inset)** Individual fits to the same flies reveal that each fly has bursty dynamics with k=0.46±0.08 and r^2=0.92±0.07 s.e.m. **(B)** Shape parameter k for young (left) and adult (right) flies all show bursty dynamics with k<1 and significantly differs from k=1 (Poisson) with p<10^{-7}. Number of flies n=28—32, error bars represent s.e.m. *Source*: 0.1371/journal.pcbi.1002075.g001 (Sorribes et al., 2011).

The most important parameter from the Weibull fit, however, is the shape parameter k which allows for a parametrization of the degree of burstiness. When k=1 the stretched exponential function takes on the form of a (normal) exponential function, and therefore describes a Poisson process, while when k<1 the shape parameter describes bursty behavior – the lower the k the burstier the dynamics. The shape parameter k from the Weibull distribution fit can thus describe both random and bursty behavior in a continuous and flexible manner.

While we have shown the excellent Weibull fit to the mean IAI distribution from the 3-day-old *CS* flies in Figure 3.7 A, it is important to perform the fits on the individual level and not on pooled data, as discussed in the previous section. We find that every fly shows bursty dynamics with k=0.46 (mean) $\pm$ 0.08 (s.d.) and that all flies are fit well by the Weibull distribution, with r^2=0.97 $\pm$ 0.02, Figure 3.7 A–Inset. The other two common genetic backgrounds were also well fit by the Weibull distribution and found to have similar burstiness values with k=0.40 $\pm$ 0.10 (*yw*) and k=0.40 $\pm$ 0.07 (w^{1118}) for the 3-day-old flies. The older flies also showed bursty behavior with k=0.58 $\pm$ 0.14 (*CS*), k=0.50 $\pm$ 0.14 (*yw*) and k=0.47 $\pm$ 0.09 (w^{1118}), Figure 3.7 B. The older flies were on average found to have a 22.2% mean increase of the shape parameter k, meaning that there is a general decrease of burstiness with age. Please note that parameter values in the text are reported as mean $\pm$ standard deviation, while the error bars in the figure show standard error of the mean.

As a comparison we also plotted the empirical cumulative distribution on double-logarithmic axes, where a straight line raises the possibility of finding power-law dynamics, Figure 3.8. While it could be possible to squint and find "straight" regions in this plot, the Weibull distribution provides a good fit for the complete range of inter-activity intervals.

We conclude that *Drosophila* walking activity as measured by the DAM2 monitors does not show power-law scaling, but that it nonetheless is heavy-tailed and bursty. This is an important finding because previous results (Martin et al., 1999a) had suggested that under conditions where the walking dynamics had lost its power-law scaling the dynamics instead followed an exponential

distribution, meaning that the dynamics were random when not power law. We instead found that the walking dynamics retain a high degree of structure and are not random, as is evident from the heavy tail of the inter-activity interval distribution (Figure 3.7).

In addition these results are interesting when considering the Lévy flight foraging hypothesis, which states that animals´ search strategies naturally evolved in such a way that they exploit optimal Levy patterns. In over a dozen marine animals it was found that the search strategy of some animals is highly dependent on environmental variation of food density (Humphries et al., 2010). In areas where the prey were sparse the animals would use Lévy

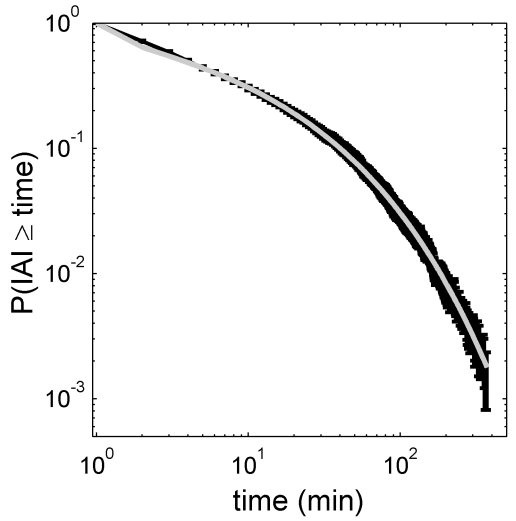

Figure 3.8: Double-logarithmic plot of inter-activity intervals (IAIs). This figure presents the the same empirical IAI survival distribution from *Canton-S* flies as in Figure 3.7 (black error bars) and the Weibull fit (gray line). There is no pronounced straight region which can be a sign of the presence of power-law scaling in the IAIs. Instead the Weibull distribution shows a good fit to the entire range of inter-activity intervals with k=0.45, λ=6.0. Since k<1 the IAIs are markedly bursty, although less so than with power-law dynamics. Error bars represent s.e.m. *Source*: Modified from (Sorribes et al., 2011).

flight search patterns, while in abundant areas the animals would switch over to Brownian (random) search motions. In *Drosophila* it was shown that the activity dynamics of flies walking in an arena without food for several hours showed power-law scaling (Cole, 1995; Martin et al., 1999a), a finding compatible with the Lévy flight foraging hypothesis. We found in this study, however, that the "opposite" is not true in fruit flies – the *Drosophila* walking activity inside DAM2 monitor tubes with *ad libitum* access to food does not default to a random behavior but still displays a strong burstiness, presumably not related to food searching behavior but generated by other intrinsic processes driving spontaneous behavior.

Validating the Parameter Estimation Method

To validate our results and conclusions, we tested the fitting method to make sure that the parameters were estimated correctly. For this, we evaluated two different techniques for fitting the Weibull distribution to data: "linear" and "non-linear". The Weibull survival distribution is given by $y = \exp(-(t/\lambda)^k)$ (Equation 3.1). The linear fit was obtained by calculating the least-squares regression between $y' = k \cdot x' + C$, where $y' = log(-log(y))$, $x' = log(x)$ and $C = -k \cdot log(\lambda)$. For the non-linear fit we used Matlab's Curve Fitting Toolbox™ ("NonlinearLeastSquares" method) to fit $log(y) = -(x/\lambda)^k$ with Matlab R2007b.

To examine the quality of the fitting methods to the type of empirical data we obtain with the *Drosophila* Activity Monitor System, we created synthetic data sets drawn from the Weibull distribution with known k and λ. To imitate the experimental data we discretized the randomly drawn data into bins of 1 (1-"minute" bins). An important detail that should not be overlooked when fitting to binned data (artificial or empirical) is that the x-vales must represent the midpoint of the bin, not the beginning (or end part) of the bin – otherwise, the fits will not estimate the parameters correctly (*pers. obs.*). To simulate the experimental data we created data sets of sizes similar to the number of IAIs for the lights-off period we encounter in our empirical data: 50 (red), 100 (orange), 150 (green), 200 (light blue) or 250 (dark blue), drawn from the

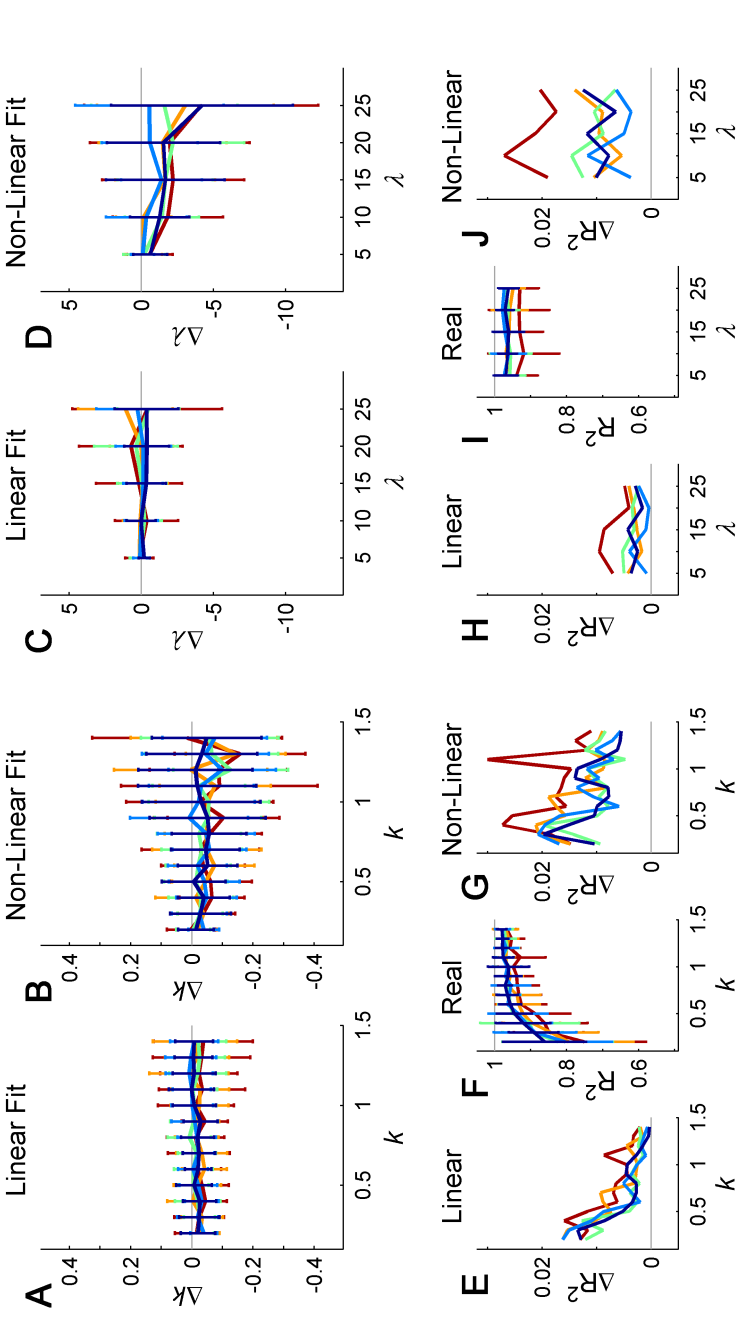

Figure 3.9: The linear fit correctly estimates the parameters. (A-D) Difference between the estimated and true parameters of the Weibull distribution. **(E-J)** Comparison of the coefficient of determination R^2 between the fits and the true fit. **(A, B, E–G)** k is varied over the interval k=[0.2:0.1:1.4] with λ=15. **(C, D, H–J)** λ is varied over the interval λ=[5:5:25], with k=0.8. Error bars denote the standard deviation (s.d.) over 30 independent runs. *Source:* (Sorribes et al., 2011).

Weibull distribution with parameters varying in the empirically found ranges: k=0.2—1.4 and λ=5-–25. To replicate the typical number of flies we have for each genotype, we drew 30 random data sets for each set of parameter values (k, λ), Figure 3.9 (error bars represent standard deviation).

To estimate the accuracy of the fitting methods we compared the estimated parameters to the true parameters (the parameters of the Weibull distribution from which the data were drawn) by calculating the differences Δk and $\Delta\lambda$, Figure 3.9 A–D. We see that the linear fit is better than the non-linear fit at estimating the parameter values since it has less bias in both parameters and smaller standard deviations for all sample sizes. In addition, the linear fit correctly estimates the parameters over the full range of parameter values that we might encounter in our experimental data.

To test the fits we compared the coefficient of determination R^2 for the regressions of the two fitting methods against the value obtained by calculating the R^2 between the synthetic data and the "regression" line constructed with the true parameters used in the Weibull distribution from which the synthetic data were drawn. The ΔR^2 between the best fit of the fitting methods and the "real" fit shows that the non-linear fitting method tends to over-fit more than the linear fit (Figure 3.9 E, G H J). This is an important point because it shows that the fitting method should not be determined by the highest R^2, but by the method that most accurately reproduces the true, underlying, parameter values. In addition we see in Figures 3.9 F, I that the survival distributions are quite noisy for small k's (k<0.5) and small sample sizes, with coefficients of determination quite low (R^2<0.9), but that the parameter estimations of both k and λ are accurately obtained with the linear fitting technique. All the parameter values from fits with the Weibull distribution presented in this thesis have been estimated using this linear fitting method.

We have thus validated the fitting method and conclude that we can accurately estimate the parameters of the Weibull distribution with the linear fitting method, and corroborate our previous finding that *Drosophila*'s spontaneous walking activity is heavy-tailed and bursty.

Burstiness and Memory in the Fly Activity Dynamics

Whilst the Weibull distribution has proven useful for characterizing the intrinsic bursty nature of *Drosophila*'s walking activity inside the DAM2 System, the characterization and parameterization is still dependent on finding a good fit between the model distribution and the empirical distribution. As the exact statistical model chosen to describe heavy-tailed distributions has been contended on multiple occasions (especially regarding power laws, see e.g. Clauset et al., 2009 for examples, and section 3.1.1 *Modeling Animal Movement Patterns* for a discussion and further references), we have also employed the distribution-agnostic burstiness parameter B and memory parameter M to distinguish the source and magnitude of burstiness in the inter-activity intervals.

The burstiness parameter B was introduced in section 2.3.2 [p. 25] and measures the relative importance of the mean and the variance (standard deviation) in the IAI distribution. When $B \to -1$ the IAI distribution shows a regular (anti-bursty) pattern and when $B \to 1$ the IAI distribution is highly bursty, while if $B = 0$ the IAI distribution shows random (Poisson) dynamics. To examine the relationship between the burstiness parameter and the Weibull distribution, we can substitute the mean μ and the standard deviation σ of the Weibull distribution into Equation 2.2 to obtain the analytical relationship between the burstiness parameter B and the Weibull parameters k and λ. The n'th moment of the Weibull distribution is given by $\lambda^n \Gamma(1 + 1 \cdot k^{-1})$, such that

$$\begin{aligned} \mu &= \lambda \cdot \Gamma(1 + k^{-1}) \,, \\ \sigma &= \lambda \cdot \sqrt{\Gamma(1 + 2k^{-1}) - \Gamma^2(1 + k^{-1})} \end{aligned} \tag{3.2}$$

which when introduced into the burstiness parameter $B = (\sigma - \mu)/(\sigma + \mu)$ yields

$$B = \frac{(\Gamma(1 + 2k^{-1}) - \Gamma^2(1 + k^{-1}))^{1/2} - \Gamma(1 + k^{-1})}{(\Gamma(1 + 2k^{-1}) - \Gamma^2(1 + k^{-1}))^{1/2} + \Gamma(1 + k^{-1})} \,. \tag{3.3}$$

From this last Equation 3.3 we see that the burstiness parameter B only depends on the shape parameter k of the Weibull distribution, and that it thus is independent of the scale λ. The relationship between B and k is negatively dependent due to the negative exponent of k in the gamma function. In addition,

we see from Equation 3.2 that the mean inter-activity interval ($\hat{\mu}$) is directly proportional to the scale parameter λ.

We thus set out to measure the burstiness B in 3-day-old and 4-week-old common wild-type and genetic background strains. For the young flies we found (mean $\pm$ s.d. for all values) B=0.37 $\pm$ 0.09 (*CS*), B=0.42 $\pm$ 0.11 (*yw*) and B=0.40 $\pm$ 0.08 (w^{1118}), and for adult flies B=0.24 $\pm$ 0.14 (*CS*), B=0.28 $\pm$ 0.16 (*yw*) and B=0.31 $\pm$ 0.13 (w^{1118}), Figure 3.10 C and Figure 3.11 A. In Figure 3.10 B we plot the shape parameter k again, for comparison. Generally we find that the two measures of burstiness strongly agree, but for experimental (finite) data the Weibull parameter k has shown to be more sensitive to data in the right tail (large values) of the interval distribution whereas the burstiness parameter B is more dominated than k by the short time events.

In addition to measuring burstiness in the inter-activity intervals (IAIs), Figure 3.10 A–C, we also examined the dynamics of the Activity Bouts (ABs), Figure 3.10 D–F. The dynamics of the activity bouts measure the intervals of active time and thus characterize the dynamics of sustained activity. Figure 3.10 D shows the total time active during the 12h night (averaged over the three days) while Figures 3.10 E F shows the shape k and burstiness B of the ABs. For young flies we found the burstiness parameters to be in the range of k=0.47–0.66 and B=0.21–0.38, while in the adult flies the range was k=0.53–0.64 and B=0.24–0.32. We see that the maintenance of activity bouts is also bursty, albeit just slightly less so than the dynamics of activity initiation (IAIs). Generally we observe that there are some differences between the commonly used background strains in both the overall activity levels and in the burstiness parameters. It is thus imperative to measure burstiness in strains with genetic mutations or transgenic flies together with their controls, to assess the effect on burstiness.

We have shown that the IAI distribution has bursty dynamics, but as we saw in section 2.3.2 *Randomness, Burstiness and Memory* [p. 23] burstiness can also arise from memory effects in the time-series of events. Systems with the same inter-event interval distribution can nevertheless show differences in perceived burstiness due to memory effects, where systems with a stronger memory component are burstier. We measured the memory effects with the memory

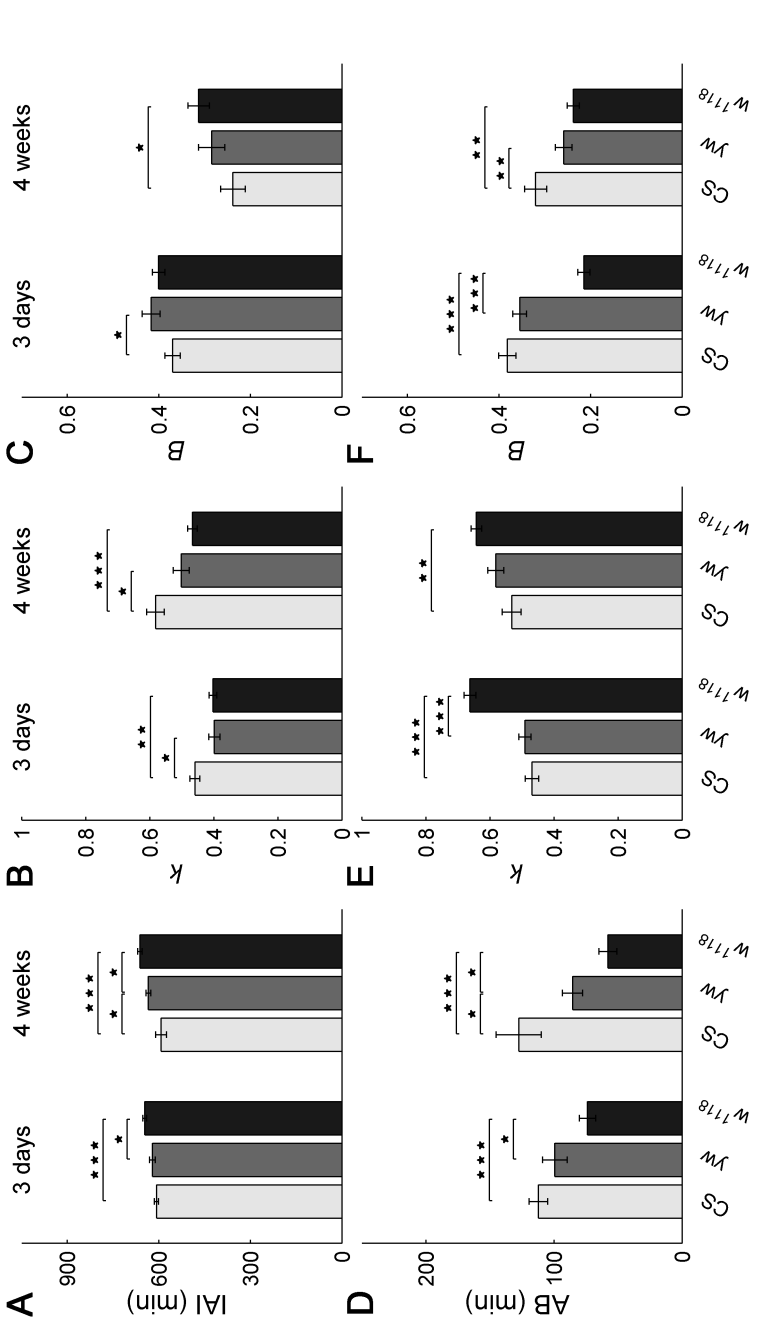

Figure 3.10: Burstiness of activity initiation (IAIs) and activity maintenance (ABs) in common fly strains at two different ages. Total times (per 12-hour night) and burstiness of Inter-Activity Intervals **(A-C)** and Activity Bouts **(C-F)** for the commonly used strains *Canton-S* (*CS*), *yellow-white* (*yw*) and *white*^{1118} (w^{1118}). All strains at young and adult ages are found to display bursty dynamics of both activity initiation **(B,C)** and maintenance **(E,F)**. Error bars denote s.e.m. *Source:* (Sorribes et al., 2011).

parameter M, defined as the correlation coefficient of consecutive inter-event intervals (Equation 2.3 [p. 26]). The memory parameter M measures short-term memory (between adjacent intervals), and a strong memory component, $M \to 1$, will be observed in systems where similar intervals succeed each other, while a strong "anti-memory", $M \to -1$, when the lengths of the intervals alternate. The antithesis to both of these is $M = 0$, which describes a memoryless sequence of intervals and thus describes a Poisson process.

We calculated the memory parameter M for the inter-activity intervals for all the fly strains and both age groups. When comparing to see if there was a memory effect present in the time series it would not however be entirely accurate to compare it to $M = 0$, as a zero memory is only possible to achieve in very large (infinite) time series. When time series are finite – and especially when small – there will almost always be a "residual" memory effect due to limited sampling. To mitigate this sampling effect we created 1000 randomly shuffled versions of each of the original empirical data sequences, to create the memoryless control distributions to compare against. The memory parameters were found to be in the range M=[-0.05 0.07] for young flies and M=[-0.05 0.01] for adult flies. *Canton-S* and *yellow-white* showed small but significant deviations from the shuffled versions at both ages, while *white*^{1118} did not have any memory component contributing to the bursty dynamics at either age (p>0.5), Figure 3.11 B (white bars show the shuffled versions), making it ideal as a control strain when testing for burstiness.

To summarize the contributions of burstiness and memory to the walking dynamics of *Drosophila*, we have plotted these values on a B-M plot, Figure 3.11 C. This enables us to characterize the dynamics in a more complete way since we are dealing with two separate and different mechanisms for creating bursty dynamics, namely the IAI distribution (as measured by the burstiness B) and memory (as measured by the memory coefficient M). The 2-dimensional B-M plot allows us further to compare the bursty dynamics of *Drosophila* walking activity with human behavioral dynamics and other bursty phenomena published previously by Goh and Barabási (2008). The region where *Drosophila* IAI dynamics are located coincides with that of human dynamics, which both

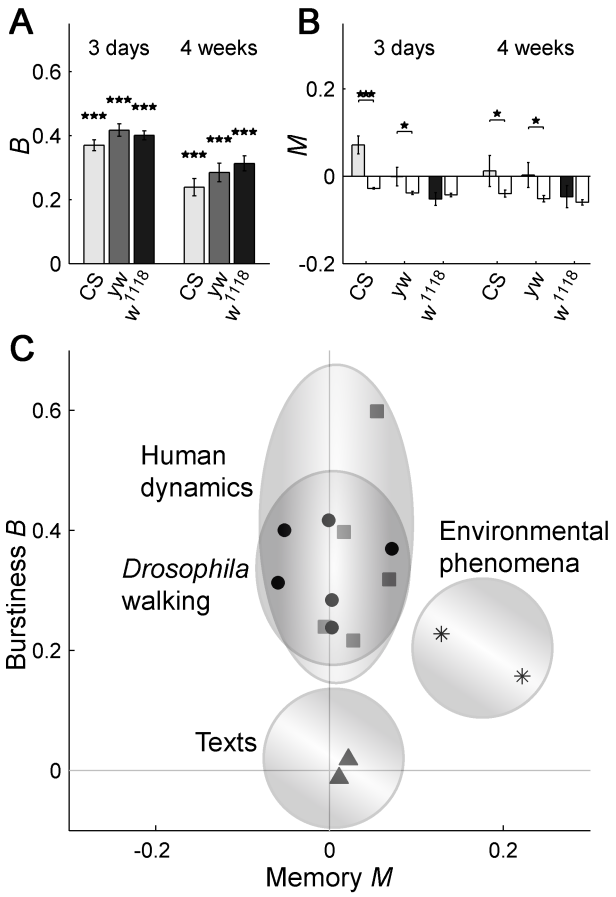

Figure 3.11: Walking dynamics is dominated by burstiness of the distribution and not by memory effects. (A) Burstiness parameter B shows bursty dynamics with $B>0$ for all genotypes and ages ($p<10^{-7}$). **(B)** Memory parameter M shows a weak effect of memory in *CS* and *yw* but not in w^{1118}, as compared to shuffled data (white bars). **(C)** *Drosophila* dynamics compared to other bursty data in the B-M plane. *Drosophila* and humans have similar dynamics, clearly differentiated from environmental phenomena and texts. *Source*: doi:10.1371/journal.pcbi.1002075.g002 (Sorribes et al., 2011).

are dominated by the burstiness of the inter-event distribution and only weakly affected by memory effects in the time series, Figure 3.11 C. Meteorological and earthquake bursty dynamics on the other hand have stronger memory effects, while the distances between consecutive occurrences of a given letter in a text have both low burstiness and low memory (Goh and Barabási, 2008). As a result, the possibility of predicting the dynamics of *Drosophila* is similar to that of human dynamics in that it is even more difficult to predict than earthquakes or meteorological phenomena.

3.2.3 Conclusions

We studied the walking activity dynamics of *Drosophila melanogaster* in three frequently used strains: the wild-type strain *Canton-S* (*CS*) and the commonly used background strains *yellow-white* (*yw*) and *white*^{1118} (w^{1118}). Additionally we studied the activity dynamics at two different ages: 3 days old (young) and 4 weeks old (adults). We measured the walking activity with the *Drosophila* Activity Monitor (DAM2) System, where each fly is housed individually in a small tube with *ad libitum* access to food for the entire duration of the experiment. The DAM2 System records each time the fly crosses the midpoint of the tube, and experimentally it has been verified that when the flies are active in locomotion they generally walk back and forth along the whole tube and thus generate an activity count when crossing the midpoint. Up to 32 flies can be recorded individually but simultaneously in each monitor and the experiments usually run for several days to obtain sufficient data for each fly. Fly activity is strongly influenced by the circadian rhythm, with a midday 'siesta' and activity peaks after sunrise and before sunset while the nightly activity is predominantly stationary (Figures 3.5 and 3.6). Since non-stationarity in time series can give rise to erroneously high variances due to changing dynamics throughout the measuring period, we centered on studying only the activity dynamics during the night, which show a stable pattern.

We found that the *Drosophila* walking activity dynamics are bursty with heavy-tailed distributions for all flies, genotypes and age groups (Figure 3.7). Both the initiation of activity (described by the inter-activity intervals) and the maintenance of activity (described by the activity bout durations) showed bursty dynamics (Figure 3.10). We further found that *Drosophila* walking dynamics could be well described by the stretched exponential function (Weibull distribution), and validated the fitting method with synthetic data (Figure 3.9). Finally, to determine the source of burstiness we measured the relative importance of the mean and the standard deviation of the distribution, as well as memory effects between consecutive intervals in the time series. We found that burstiness mainly stems from the interval lengths distribution and not from memory effects, and that the spontaneous activity dynamics of *Drosophila* are very similar to human dynamics (Figure 3.11).

3.2.4 Material and Methods

Fly Strains and Rearing

The wild type strain *Canton-S* and the common genetic background strains *white*^{1118} and *yellow-white* were kindly provided by I. Canal and J.F. Celis (Universidad Autónoma de Madrid and Centro de Biología Molecular, Spain).

Fly stocks were maintained on a standard cornmeal food in incubators at 18 °C before commencing the experiment, and at 23 °C for at least one full generation before the experiment. Both the stocks and the experimental flies were housed in incubators on a 12 h light/12 h dark cycle starting at 8:00 AM.

Locomotor Activity Assay

Locomotor activity data were obtained with the DAM2 System, as described in section 2.2 *Measuring Drosophila's Innate Activity Patterns* [p. 16]. The data were collected in 1-minute bins. One complete 32-channel monitor was used

for each genotype. The experiments were performed inside incubators at 23 °C, with no external stimuli, apart from the light cycle. Both male and virgin female flies were used for the experiments, and were around 3 days old at the start of the experiment. The fly rearing and experiments for this assay were performed by Beatriz G. Armendariz, a fellow student in the de Polavieja lab at the time.

Data Analysis

Data analysis was performed with Matlab R2007b (The MathWorks Inc., MA USA) by writing my own custom built code. The fitting technique and other analyses have been described more in detail in the preceding results section. Much of the analysis has been streamlined into the custom built software *FlySiesta*, which can be found at `http://www.neural-circuits.org/flysiesta`.

Statistical Analysis

Statistical analysis was performed by using the two-tailed Student's t-test with the Bonferroni correction when conducting multiple comparisons between groups. The data were first tested for normality with a Lillie-test; in case of a pass (failure to reject the null hypothesis) the parametric t-test was used, while if the requirements to pass the normality test were not met by one or more groups the hypothesis testing was performed by bootstrapping the t-statistic (sampling with replacement and computing the t-statistic), using 10.000–100.000 sampling iterations. The p-value of the statistical test is represented in all figures as either one star ($p<0.05$), two stars ($p<0.01$) or three stars ($p<0.001$).

3.3 Behavioral Bursts and Decision-Making Circuits

3.3.1 Introduction

Bursty and scale-free behavior has been observed in many animal species, as we have seen in the Introduction & Background to this chapter, but also human activities have been observed to show bursty, non-Poissonian behavioral dynamics. Activities such as communications and letter writing, as well as entertainment and work patterns, have been shown to occur with bursty dynamics (Barabási, 2005; Oliveira and Barabási, 2005). From the field that studies animal foraging trajectories a prominent hypothesis is that animals have evolved to make use of scale-free patterns because these have been shown to optimize the search (under some conditions) (Viswanathan et al., 1999) – it does not however consider the underlying mechanisms of *how* these patterns would emerge. From work on human dynamics though, Barabási (2005) proposed a model with an underlying mechanism that can generate the observed behavioral bursts, known as the priority-list model (Barabási, 2005; Vázquez, 2005; Vázquez et al., 2006). In this model tasks are executed according to perceived priority, in combination with an additional random component. It is the interplay between this random component and the decision-making process which assigns and executes tasks according to priority which gives rise to behavioral bursts.

While the data modeling in Barabási (2005) received the usual scrutiny regarding whether the distribution is truly a power law or a lognormal (Stouffer et al., 2005), and whether a cascading non-homogeneous Poisson process (Malmgren et al., 2008, 2009) or a sum of Poisson processes with different mean rates (Hidalgo, 2006) might explain the communications pattern better (and yet another study refuted the critiquing studies (Jo et al., 2012)), the important fundamental idea in the model is that cognitive functions like decision-making processes can be the underlying generating mechanism for bursty behavior. This connection between decision-making processes and bursty behavior is a novel proposition, as the other proposed alternative explanatory models are based

on Poisson processes and are thus inherently random models. These proposed generating mechanisms are therefore fundamentally different and would need empirical validation, so we decided to experimentally test whether neuronal circuitry implicated in decision-making also controls behavioral burstiness.

As we have seen in the previous section 3.2 *Dynamics of Spontaneous Walking Activity*, *Drosophila* shows markedly heavy-tailed activity distributions and bursty behavior. As we saw in the introductory section 3.1.2 *Movement Patterns and Spontaneous Behavior*, fruit flies are not merely hard-wired input-output systems but capable of initiating behavior (Wolf et al., 1992; Maye et al., 2007), probabilistically activate actions and behave in operant loop to learn which actions obtain the desired result (Wolf et al., 1992; Heisenberg, 2001; Brembs, 2009). Importantly, *Drosophila* is also capable of complex decision-making when presented with options of contradicting cues (Tang and Guo, 2001; Tang and Juusola, 2010). Neuroanatomical identification and characterization of choice behavior in flies have found that dopaminergic neurons and the neuroanatomical substructure (neuropil) known as the mushroom body (MB) are necessary for decision-making processes (Tang and Guo, 2001; Zhang et al., 2007; Yin et al., 2009; Brembs, 2009; Claridge-Chang et al., 2009; Riemensperger et al., 2011). In particular, dopaminergic neurons have been found to be necessary for decision-making in olfactory-driven (Claridge-Chang et al., 2009) and visually-driven choices of walking flies (Riemensperger et al., 2011) and in tethered flight (Zhang et al., 2007), while the mushroom body was also found to be necessary for decision-making in tethered flight (Tang and Guo, 2001; Zhang et al., 2007) and involved in visual attention-like behavior (Xi et al., 2008). The mushroom body is perhaps best known as the neuropil responsible for olfactory memory formation and retrieval (reviewed in e.g. Gerber et al., 2004), but it has also been implicated in behavioral variability and habit formation, and has been suggested to be responsible for establishing the appropriate level of behavioral flexibility (Brembs, 2009). The dopaminergic neurons, in turn, have been found to form a reinforcement circuit in which the choice of appropriate actions is established (Claridge-Chang et al., 2009). The complex behavioral repertoire of decision making in *Drosophila* thus already

shows components compatible with the proposed priority-list model, as it has circuitry capable of reinforcing some actions, that is, to give them higher priority.

To experimentally test the proposed link between decision-making processes and behavioral burstiness we studied the walking activity dynamics of flies with disrupted choice behavior with the same method as described in section 3.2. We found that in flies with enhanced dopaminergic signaling or impaired mushroom body function, components previously found to disrupt normal decision making, the degree of burstiness was also affected. This is consistent with the fundamental idea of the decision-based generating model where when individuals execute tasks based on some perceived priority, the timing of tasks becomes heavy tailed and thus bursty.

The work presented in this section has been published previously, as part of: Amanda Sorribes, Beatriz G. Armendariz, Diego Lopez-Pigozzi, Cristina Murga, Gonzalo G. de Polavieja (2011) *The Origin of Behavioral Bursts in Decision-Making Circuitry*. PLoS Computational Biology 7(6):e1002075. doi:10.1371/journal.pcbi.1002075

3.3.2 Results & Discussion

To explore the possible implication of decision-making circuitry on behavioral burstiness, we employed the analysis methods previously described in section 3.2 *Dynamics of Spontaneous Walking Activity*. Briefly, behavioral burstiness was assessed by evaluating the shape parameter k obtained by fitting a Weibull distribution to the complementary cumulative distribution function of the inter-activity intervals (IAIs) for each fly and then calculating the mean for each genotype, as described in section 3.2 *Dynamics of Spontaneous Walking Activity*. Burstiness was also measured with the burstiness parameter B (section 2.3.2 [p. 25]) to obtain a distribution-agnostic comparative measure, and with the memory parameter M (section 2.3.2 [p. 26]) to assess and determine the source of burstiness.

Dopamine Levels and Burstiness

We began by studying the implication of dopamine (DA) on burstiness in *Drosophila*, as it has been found to disrupt normal decision-making (Zhang et al., 2007; Claridge-Chang et al., 2009; Riemensperger et al., 2011). In *Drosophila* it is possible to both enhance and silence dopamine signaling by using mutants and transgenic crosses.

Enhancement of dopamine is accomplished by using the mutant line *fumin* (*fmn*), which has a higher level of dopamine in the synaptic cleft due to a genetic lesion in the dopamine transporter gene (Kume et al., 2005). High levels of dopamine led to a 38.0% increase of the shape parameter k ($p<0.0001$, Figure 3.12 A) as well as a decrease of the burstiness parameter B by 22.6% ($p<0.0001$, Figure 3.12 B). As to the memory coefficient M we could not detect any effect ($p=0.136$, Figure 3.12 C). The summary of these results can be seen in the B-M plot (Figure 3.12 D), which shows the control strain to be further from Poissonian behavior than the mutant strain, that is, increased dopamine makes the flies act more randomly than normal.

We also examined the effect of reducing dopaminergic signaling, by using the bipartite GAL4/UAS system, described in more detail in section 2.1.3 *Targeted Gene Expression: The GAL4/UAS Method*. By using the GAL4/UAS system, we can selectively express *shibire*^{ts1} (*shi*^{ts1}), a temperature-sensitive mutation of the enzyme dynamin which is necessary for a correct synaptic function. The temperature sensitive property allows it to act as an on/off switch for neuronal activity. At temperatures below 29 °C – known as the permissive temperature (PT) – the synapses work as normal, but at temperatures above 29 °C – known as the restrictive temperature (RT) – the synaptic functioning ceases to work within minutes (Grigliatti et al., 1973; Kitamoto, 2001). After an initial day of adaptation to the experimental set-up, the fly walking activity was recorded for three days at 23 °C (permissive temperature) to obtain baseline values, whereupon the temperature was switched to 31 °C (restrictive temperature) for three additional days (although often only the first day of RT was used for analysis as many flies could not survive for several consecutive days at

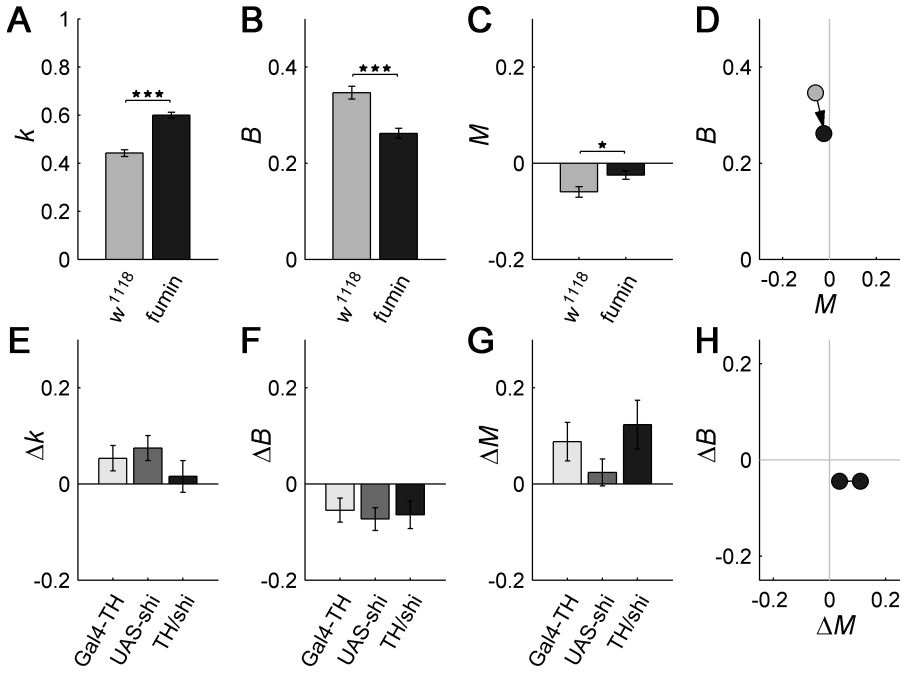

Figure 3.12: Behavior becomes more random with increased dopaminergic signaling. **(A–D)** Effect of increased dopamine levels. *fumin* shows an increase of k **(A)** and a decrease of B **(B)** compared to its control w^{1118}, denoting a reduction of burstiness. **(C)** Both groups show only low levels of memory, indicating that the observed burstiness stems from the distribution of IAIs and not from their internal order. **(D)** B-M-plot for control (gray) and *fumin* (black). **(E–H)** Disruption of dopaminergic signaling does not change IAI burstiness **(E,F)** or memory **(G)**, compared with controls. Δ denotes values at RT$-$PT. **(H)** Approximation of net effect of silencing dopamine, without the heat effect. Here "Δ=Gal4/*shi* – mean(Controls)" at PT (right dot) and RT (left dot). Number of flies n=29—64, bars indicate mean $\pm$ s.e.m. *Source*: doi:10.1371/journal.pcbi.1002075.g004 (Sorribes et al., 2011).

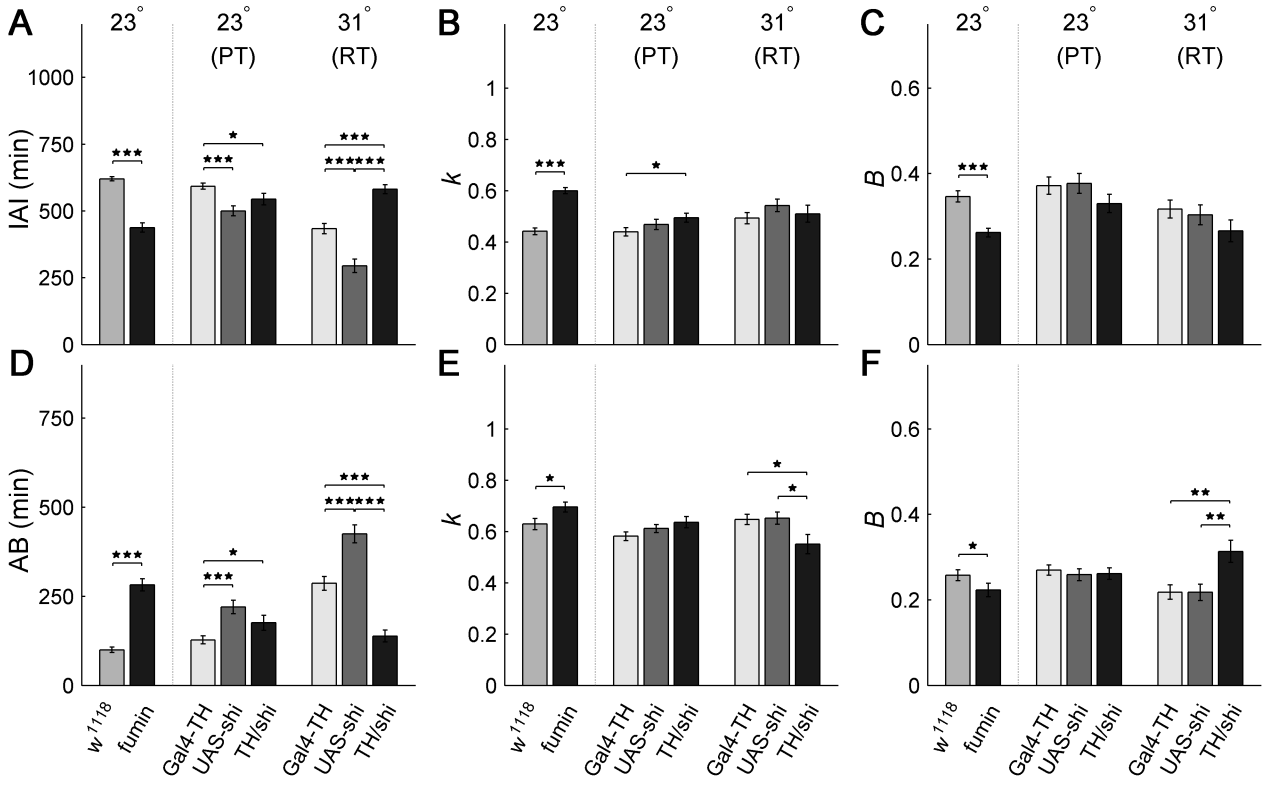

Figure 3.13: Activity levels and burstiness do not correlate with dopamine (DA) levels. (A,D) Average total time spent in IAI **(A)** and AB **(B)** during the dark period. High DA (*fumin*) produces hyperactivity, while low DA (TH/shi^{ts1}) causes inactivity, with respect to their controls. **(B,C)** High DA leads to decreased burstiness while low DA has no effect. **(E,F)** High and low DA levels have opposing effect on AB burstiness. Same data as in Figure 3.12, bars indicate mean $\pm$ s.e.m. *Source*: (Sorribes et al., 2011).

the higher temperature). Parameters were then calculated as the difference between the values at RT minus the values at PT for each fly, to obtain the effect of selective neuronal silencing.

To silence dopaminergic neurons we expressed *shibire*^{ts1} with the tyrosine hydroxylase (TH) GAL4 driver, since TH is an enzyme necessary for the proper synthesis of dopamine and present in most dopaminergic neurons (Friggi-Grelin et al., 2003). No change of shape, burstiness or memory parameters were however found when dopaminergic signaling was silenced ($p>0.168$, Figure 3.12 E–G). To approximately separate the effects of the heat treatment from the targeted silencing of the dopaminergic system, we calculated the net effect of neuronal silencing by subtracting the mean of the B and the M of the two control lines at the permitted and restricted temperatures from the transgenic's B and M at the corresponding permitted and restricted temperatures. The B-M plot in Figure 3.12 H thus shows a summary of the net change of the controls subtracted from the TH-GAL4/UAS-*shi*^{ts1}at each temperature.

Although reduced dopamine levels did not affect the IAI burstiness, that is, the initiation of activity, the burstiness B of activity bout durations increased by 10.6–9.3% ($p<0.03$, Figure 3.13 E,F). Neither shape parameters (Figure 3.13 B,E) nor burstiness parameters (Figure 3.13 C,F) nor memory parameters (Figure 3.13 A,C,G) could be found to have any clear correlation with total activity (Figure 3.13 A,C). We have shown that animal behavior becomes more random with increasing dopamine levels, while the dynamics of activity bout maintenance are affected when the levels of dopamine are decreased.

Mushroom Bodies and Central Complex Circuitry

We next explored the possible implication of mushroom body (MB) circuitry on burstiness, by expressing *shibire*^{ts1} with several MB GAL4 drivers, using the same permissive/restrictive temperature protocol as for the transgenic TH line which disrupted dopamine signaling. Line 247-GAL4/UAS-*shi*^{ts1}('247') was selected for assessing changes in burstiness due to decision-making processes, as these flies were shown to have disrupted choice behavior in a visual

salience-based assay where they were exposed to contradictory cues (Zhang et al., 2007). In addition, four more MB lines were tested: c309-GAL4/UAS-*shi*^{ts1}('c309'), 201Y-GAL4/UAS-*shi*^{ts1}('201Y'), 17d-GAL4/UAS-*shi*^{ts1}('17d') and H24-GAL4/UAS-*shi*^{ts1}('H24'). Both general activity levels and burstiness were assessed, to make sure that the possible changes in burstiness were not due solely to an overall change in activity level.

Differences emerged between the lines when comparing the level of active time, where line c309 was more active, 201Y and H 24 less active, while 247 and 17d showed no significant change, Figure 3.15. The burstiness level of transgenic 247 flies showed a mean increase of 16.9% (k) and 17.1% (B) at the restricted temperature ($p<0.004$, Figure 3.14 A and $p<0.013$ Figure 3.14 B) as compared to controls. There was however no accompanying change in mean activity ($p>0.08$, Figure 3.15 A,D). The burstiness shown by lines c309, 17d and H24 was not significantly different from controls whereas line 201Y's decrease in the burstiness parameter B (10.9—14.8%) was statistically significant ($p<0.005$), Figure 3.14 B. The memory parameter M remained unchanged in all the MB *shibire*^{ts1} lines, Figure 3.14 C. The approximate net effect of silencing MB circuitry without the conditional heat-effect was obtained like before, by subtracting the mean B and M of the two control lines from the transgenic's B and M at PT and RT. This is summarized in the B-M plot, Figure 3.14 D. Finally, an analysis of the burstiness of the activity bouts (ABs) maintenance was made in order to complete the study of behavioral timings dependent on the MB, Figure 3.15 D–F. The increase in the burstiness parameter B applied to ABs displayed by line H24 was significant ($p<0.01$) as was the decrease of the shape parameter k applied to ABs ($p<0.05$). The other MB lines, however, showed no significant changes in the k and B parameters applied to ABs ($p>0.05$ in Figure 3.15 F). Thus, we found that no correlation exists between changes in burstiness and time spent in activity/inter-activity, Figure 3.15 A–C and D–F.

While all of these lines express in the mushroom bodies, the MBs are composed of five distinct substructures known as lobes. The five lobes are further neuroanatomically, biochemically and functionally divided into three lobe sets, known as the α/β lobes, the α'/β' lobes, and the γ lobe (Crittenden et al., 1998).

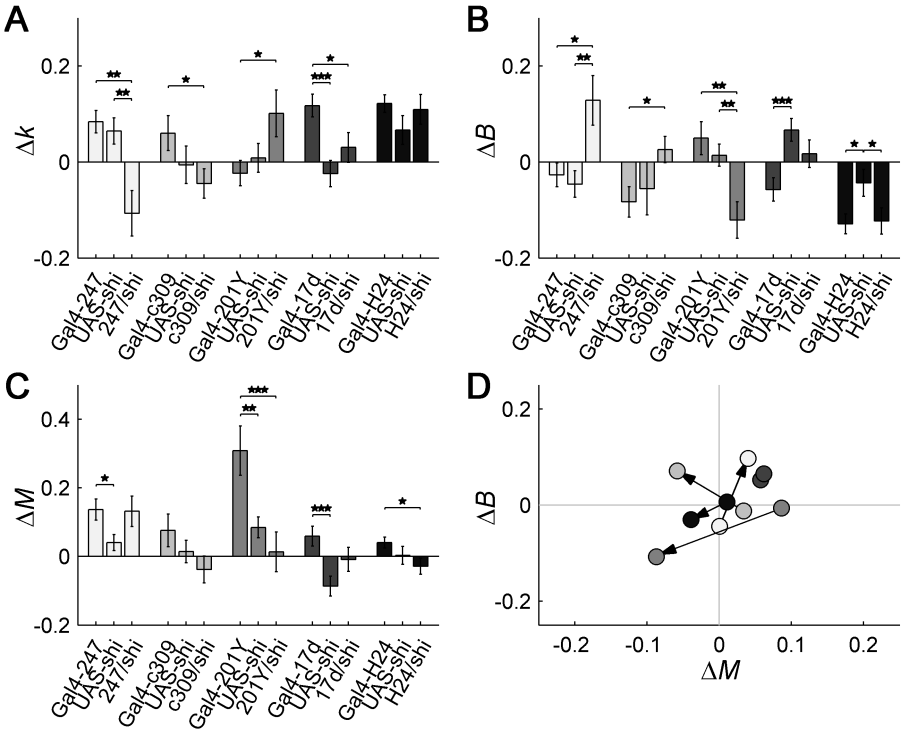

Figure 3.14: Silencing mushroom body (MB) neurons affects burstiness. **(A–C)** Change (Δ) in parameters between permissive and restrictive temperatures (RT−PT). Silencing MB with line 247/shi^{ts1}increased burstiness **(A,B)** while silencing with line 201Y/shi^{ts1}decreased burstiness **(B)**. The other MB lines had no effect on burstiness with respect to controls **(A,B)**. **(C)** There was no memory effect for any MB line. **(D)** Approximation of net effect of silencing MB, without the heat effect. Here "Δ=Gal4/*shi* – mean(Controls)" at PT (base of arrow) and RT (head of arrow). Note that ΔB is close to zero for all MB lines at PT, meaning the Gal4/*shi* and controls had similar burstiness when the MB worked normally. Number of flies n=18—32, error bars indicate s.e.m. *Source*: doi:10.1371/journal.pcbi.1002075.g003 (Sorribes et al., 2011).

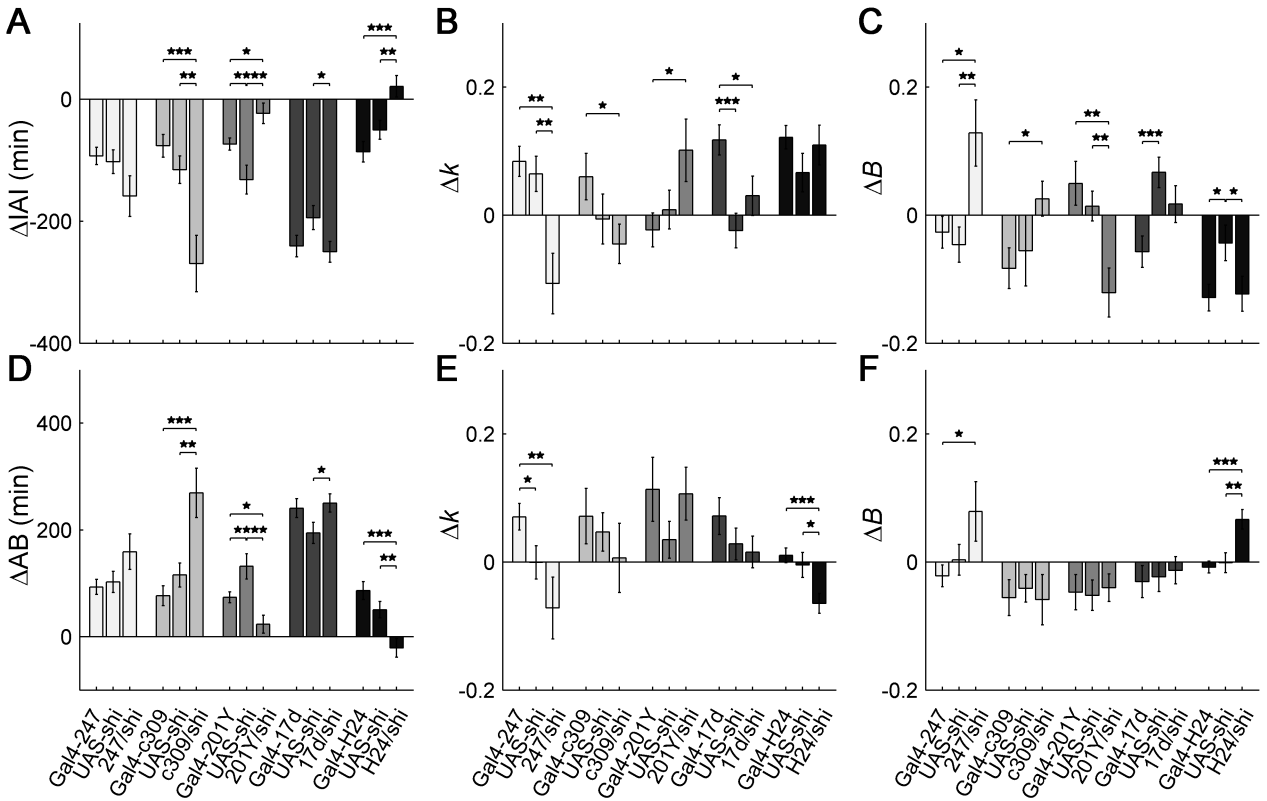

Figure 3.15: Activity levels and burstiness are not correlated when silencing mushroom body (MB) circuitry. Change (Δ) in parameters between permissive and restrictive temperatures (RT−PT). **(A,D)** Average total time spent inactive **(A)** and active **(D)** during the dark period. **(B,C)** Change in burstiness parameters k and B. Same data as in figure 3.14 A,B; here for comparison purposes with activity levels and ABs burstiness. **(E,F)** Burstiness dynamics of activity bouts maintenance. Error bars indicate s.e.m. *Source*: (Sorribes et al., 2011).

The two MB lines where we found statistically significant changes in burstiness, lines 247 and 201Y, show interesting similarities in expression patterns as they both have very strong expression in the α/β lobes and in the γ lobe while they are not expressed in the α'/β' lobes (Aso et al., 2009). In addition, their expression is quite selective, as there is either weak or no expression at all in other parts of the brain. The other MB lines, however, are expressed in a different pattern (Aso et al., 2009). While line 17d has a strong expression in the α/β lobes, it is not expressed in the γ lobe, whereas line H24 has a strong expression in the γ lobe but is only expressed weakly in the α/β lobes. H24 also shows strong expression in other areas of the brain, including the central complex (CCX). Finally, line c309 shows some expression in the α'/β' lobes, as well as expressing in most parts of the brain. Thus, we find our results to be most consistent with an implication of the α/β lobes together with the γ lobe. Interestingly, recent advances on the neuroanatomy of memory formation has established that the acquisition of new memories is predominantly mediated by the γ neurons, while the retrieval of long-term memory is entirely dependent on the α/β lobes (Guven-Ozkan and Davis, 2014). As we mentioned, both lines 247 and 201Y express in the α/β and γ similarly, but the expression in the α/β lobes can be further subdivided into surface and core regions (Aso et al., 2009). A stronger expression in the surface and posterior subdivision of the α/β lobes is found in 247, whereas 201Y has its stronger expression in the core of these lobes. Since both of these lines show a modification of the degree of burstiness, they have opposite effects: 247 increases the burstiness while 201Y decreases it, implying that core and surface regions of the α/β lobes might play a differential role.

Since some of the MB lines also partly show expression in the ellipsoid-body (EB) of the central complex (CCX), and the EB has previously been shown to affect the power-law distributions of walking activity (in absence of light or food) (Martin et al., 1999b, 2001), we complemented our study of burstiness by testing several lines expressing in the EB and the CCX. The line C507-GAL4/UAS-shi^{ts1}('C507'), with expression in the EB (Renn et al., 1999), had also been tested in the decision-making study (Zhang et al., 2007) and found not to affect

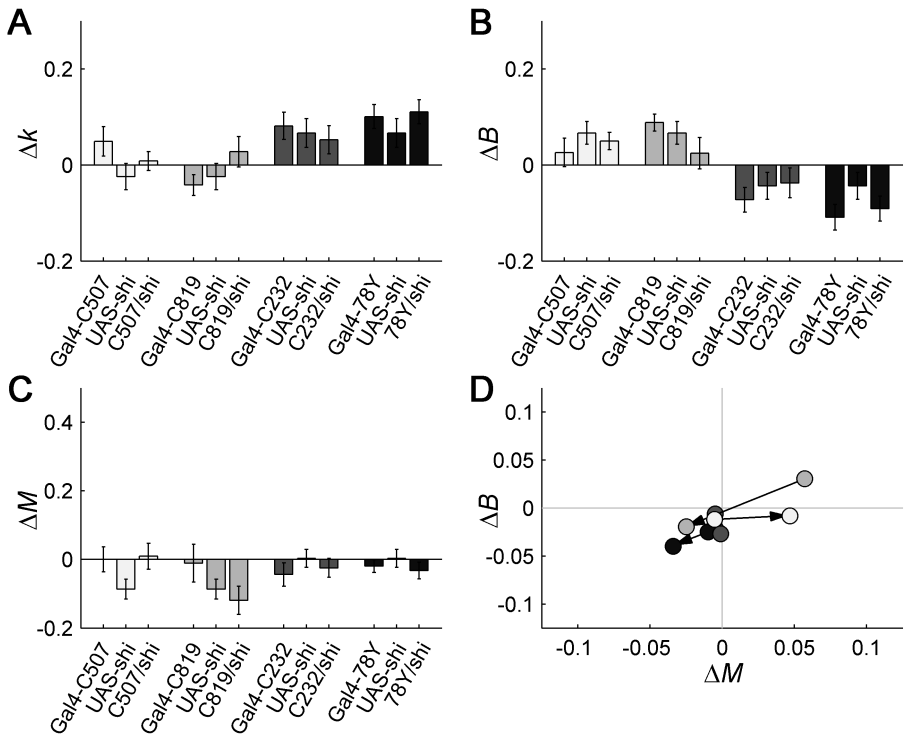

Figure 3.16: Silencing central complex (CCX) circuitry does not affect burstiness. (A–C) Change (Δ) in parameters between permissive and restrictive temperatures (RT−PT). None of the CCX lines had any significant changes in burstiness **(A,B)** or memory **(C)** when silenced. **(D)** Approximation of net effect of silencing CCX, without the heat effect. Here "Δ=Gal4/*shi* – mean(Controls)" at PT (base of arrow) and RT (head of arrow). Note that ΔB is close to zero for all CCX lines at PT, indicating that the Gal4/*shi* and controls had similar burstiness when the CCX worked normally. Importantly, note the change of scale of the axes if comparing with Figure 3.14 (MBs). Number of flies n=25—32, error bars indicate s.e.m. *Source*: (Sorribes et al., 2011).

the decision-making process. Here, we tested for burstiness and memory and found no statistically significant changes in either k, B, or M, Figure 3.16. We extended the analysis to lines C819-GAL4/UAS-*shi*^{ts1}('C819') and C232-GAL4/UAS-*shi*^{ts1}('C232') with expression in EB ring neurons (Connolly et al., 1996; Martin et al., 2001), and 78Y-GAL4/UAS-*shi*^{ts1}('78Y') with wider CCX expression (Martin et al., 1999b), and none of them displayed any significant changes in burstiness or memory, Figure 3.16.

Taken together, thus, we have seen that the mushroom body affected burstiness, while lines expressing in the central complex did not. Importantly, we saw that MB line 247 which was found to have impaired decision-making ability (Zhang et al., 2007) was here also found to have changes in burstiness. Line C507 which is expressed in the ellipsoid-body of the central complex and which was found to have normal choice-behavior in the previously mentioned decision-making assay (Zhang et al., 2007), did not show a change in burstiness. This is in itself quite remarkable, since the central complex has been implicated in the fine locomotor control of walking behavior (Strauss and Heisenberg, 1993; Strauss, 2002), the trait under study here. We thus conclude that the temporal pattern of burstiness is controlled separately from the locomotor control, and that it co-localizes with decision-making processes.

Relating Neuroanatomy to the Bursty Decision-Making Model

Building on the vast literature available on the neuroanatomy and function of different neuropils and neurotransmitters in *Drosophila*, we can suggest a putative relationship between these anatomical structures and the proposed priority-driven model of bursty behavior. The strongest effect on burstiness was found to be increased levels of dopaminergic signaling. Dopaminergic neurons extensively innervate the MB lobes, as well as several other neuropils (Friggi-Grelin et al., 2003; Zhang et al., 2007; Tanaka et al., 2008; Mao and Davis, 2009). The MB α/β lobes have been shown to affect the retrieval of olfactory memories (Krashes et al., 2007) and regulate habituation responses (Acevedo et al., 2007), while the γ lobes have been implicated in the acquisition

of memories (Guven-Ozkan and Davis, 2014). Dopaminergic neurons have on the other hand been shown to disrupt aversive olfactory memory retention (Zhang et al., 2008) and convey motivational state through a modification of the MB memory processing, in an internal-state dependent manner (Krashes et al., 2009). We found in this study that the bursty locomotor behavior decreased when the dopamine signaling was enhanced, that is, the activity became more random with higher dopamine levels. This is consistent with a model where a decision-making process occurs as the weighing of different sensory impulses in combination with the internal motivational states and memories of past outcomes, through the interaction of the mushroom bodies and the dopaminergic systems. Relating it to the priority-based task-executing model (Barabási, 2005; Vázquez et al., 2006), this decision-making process would be what assigns priorities to the different options of attention, impulses or actions. Thus, when the dopamine signaling is hyper-active or the mushroom bodies α/β and γ lobes have impaired function, the relative importance and balance between different options in the decision-making process breaks down and the proper establishment of priorities is disrupted.

It has been shown that the bursty outcome of the priority-list model is valid for as few as two options and independent of the specific function of priority assignment (Barabási, 2005), making the link between decision-making process and burstiness independent of the specific details of that process. Thus, when an animal chooses to act first upon the option that has the highest perceived priority (determined by e.g. salience or other processes), then the behavior will become bursty, while if the animal does not weigh the options and instead acts on impulses as they come, then the behavior will become less bursty and more random – similar to what we saw in the flies with hyper-excited dopamine signaling. Although more detailed studies on the intricacies of the decision-making process are needed to establish causation, we have empirically found that circuitry responsible for decision-making processes also affects burstiness.

3.3.3 Conclusions

We used *Drosophila melanogaster* to experimentally test the link between burstiness and decision-making processes, proposed in the priority-based task execution model (Barabási, 2005; Vázquez et al., 2006). Burstiness was measured by the shape parameter k of the Weibull distribution fit to the inter-activity intervals (IAIs) and by the burstiness parameter B, in addition to measuring the memory parameter M to assess the source of burstiness. Fly lines with altered dopamine signaling or impaired mushroom body (MB) function were selected, as these have previously been shown to regulate decision-making in *Drosophila* (Zhang et al., 2007). In addition, we tested flies with impaired ellipsoid body (EB) or other central complex (CCX) regions since these have been shown to control walking behavior and have previously been found to affect the dynamics of activity (Martin et al., 1999b, 2001; Strauss, 2002).

Burstiness was found to be due mostly to the IAI distributions, and not to memory effect (Figures 3.12-3.16 D). We found that enhanced dopamine signaling exerted the largest effect on burstiness, while decreased levels of dopamine affected the maintenance of the activity bouts (Figure 3.13). The mushroom body line 247, found to have disrupted decision-making (Zhang et al., 2007) also affected burstiness. Line 201Y, with a similar expression pattern as 247 also changed the degree of burstiness, albeit in the opposite direction (Figure 3.14). The other three MB lines (c309, 17d and H24) with a different expression pattern, did not show statistically significant changes in burstiness. We also tested line C507 which expresses in the EB and which was previously found not to affect decision-making circuitry (Zhang et al., 2007), and found that it did not alter the degree of burstiness (Figure 3.16). Other lines with expression patterns in the EB or other parts of the CCX (C819, C232, and 78Y) were found to not affect burstiness either.

We thus found that the impairment of decision-making circuitry impacted the fine-scale dynamics of activity. The co-localization of burstiness and decision-making processes is hence consistent with the proposed model (Barabási, 2005) where priority-based choice of action generates the observed burstiness.

3.3.4 Material and Methods

Fly Strains and Rearing

The *fumin* flies were kindly provided by K. Kume (U. Kumamoto, Japan), and the mushroom body driver c309-GAL4 was obtained from the Bloomington *Drosophila* Stock Center. Lines 247-GAL4, 201Y-GAL4, 17d-GAL4, H24-GAL4, C507-GAL4, C819-GAL4, C232-GAL4, TH-GAL4 and UAS-shi^{ts1} were kindly provided by A. Ferrús (Instituto Cajal, CSIC, Spain) while line 78Y-GAL4 was kindly provided by J.-R. Martin (CNRS, U. Paris-Sud). All the lines of Gal4 and UAS were kept heterozygote on a w^{1118} background throughout.

Fly stocks were maintained on a standard cornmeal food in incubators at 18 °C before commencing the experiment, and at 23 °C for at least one full generation before the experiment. Both the stocks and the experimental flies were housed in incubators on a 12 h light/12 h dark cycle starting at 8:00 AM.

Locomotor Activity Assay

Locomotor activity data were obtained with the DAM2 System, as described in section 2.2.2 *Drosophila Activity Monitor System*. The data were collected in 1-minute bins. One complete 32-channel monitor was used for each genotype, with both male and virgin female flies which were around 3 days old at the start of the experiment. The experiments were performed inside incubators on a LD 12:12 light cycle, at 23 °C for *fumin* and for establishing baseline values. For heat-shock experiments, flies were first monitored for three days at the permissive temperature (PT) 23 °C to establish baseline values, then the temperature of the incubators was raised to the restrictive temperature (RT) 31 °C degrees for an additional three days.

The fly rearing, crossings and experiments with *fumin*, mushroom bodies (MB) and TH flies for this assay were performed by Beatriz G. Armendariz and Diego Lopez-Pigozzi, fellow students in the de Polavieja lab at the time. The fly rearing, genetic crossings and experiments with the central complex (CCX) flies were performed by me, Amanda Sorribes.

Data Analysis

Data analysis was performed with Matlab R2007b (The MathWorks Inc., MA USA) by writing my own custom built code. The recordings from the DAM2 system were divided into inter-activity intervals (IAIs) and activity bouts (AB), as described in section 2.3.1 *Processing Raw Data into Bouts*.

The fitting method to the survival distributions was performed as described in 3.2 *Dynamics of Spontaneous Walking Activity*. Briefly, this consists of constructing the survival distributions and fitting them to the survival Weibull distribution $\exp(-(x/\lambda)^k)$, by linear regression. A linear relation is obtained by applying a double logarithm, transforming the sides into $y' = log(-log(y))$ and $x' = log(x)$, such that $y' = k \cdot x' + C$, where $C = -k \cdot log(\lambda)$. This was found to produce a robust fit, controlled against artificial data drawn from a Weibull distribution with known parameters and a variable number of data points.

To test for the presence of short-term memory (M) effects (described in section 2.3.2 [p. 26]), we compared the empirical values against shuffled versions of the same data. Although a non-zero memory effect seems to indicate that there are memory effects present in the time series, it is important to realize that this is true only when the number of data points is very large (*pers. obs.*). For finite, and relatively small time series as our experimental ones, it is possible (and quite common, actually) to have non-zero memory even in shuffled data, which is why we compare our empirical data to a distribution of shuffled data to determine the presence or not of memory effects.

For experiments where flies were treated with a heat effect, differential values between the restrictive and the permissive temperatures (RT – PT) were calculated individually for each fly, before comparative studies between genotypes were made.

Statistical Analysis

Statistical tests were performed by using the two-tailed Student's t-test with the Bonferroni correction for multiple comparisons between groups. The data were first tested for normality with a Lillie-test, in case of a pass (failure to reject the

null hypothesis) the parametric t-test was used, while if the requirements to pass the normality test were not met by one or more groups the hypothesis testing was performed by bootstrapping the t-statistic (sampling with replacement and computing the t-statistic), using 10.000–100.000 sampling iterations. The p-value of the statistical test is represented in all figures as either one star ($p<0.05$), two stars ($p<0.01$) or three stars ($p<0.001$).

4

Sleep-Wake Dynamics in Model Organisms and Humans

4.1 Introduction & Background

The never ceasing cycle of sleep and wake is an inescapable experience throughout all of our lives. Sleep is a time consuming, complex behavioral state, yet essential for our wellbeing (Rihel et al., 2010). One of the most common reasons for seeking medical attention is problems with sleep (Mahowald and Schenck, 2005). Nonetheless, the function of sleep and how it is regulated by genes, neurons and circuits remains one of the mayor challenges in biology today (Rihel et al., 2010).

Sleep has predominantly been studied in mammalian animals and birds, ever since the discovery that sleep and wake can be observed and objectively measured externally with the electroencephalography (EEG) (Davis et al., 1937). Since the turn of the millennium, however, sleep research has also expanded to "simpler" model organisms by broadening the identification of sleep to behaviorally defined criteria (Hendricks et al., 2000; Shaw et al., 2000; Zhdanova, 2006; Raizen et al., 2008). In this *Introduction & Background* we will start with a brief introduction of the regulatory systems for sleep and wakefulness in mammals. Thereafter we will see an overview of the studies on sleep-wake dynamics so far, and end with a short section on the study of sleep in simpler model organisms.

4.1.1 Regulation of Sleep-Wake Cycles in Mammals

During the course of a normal day an animal must transition between various behavioral states in response to external and internal drives (Chiu and Prober, 2013), of which sleep is the most vulnerable and distinct. Sleep disorders with impaired (or prolonged) sleep consolidation or with disrupted timing of sleep onset have been shown to pose important health risks connected with obesity and diabetes (Knutson, 2010; Nielsen et al., 2011), cardio-vascular disease (Knutson, 2010; Cappuccio et al., 2011), impaired vigilance and cognition (Kronholm et al., 2011) and even death (all-cause mortality) (Cappuccio et al.,

2010). Understanding the transitions, maintenance and dynamics of the sleep-wake episodes is therefore of uttermost importance and currently an active field of research.

On a macroscopic level the transitions between wake and sleep can be understood as the interplay between two main regulatory systems, namely the circadian rhythm and the homeostatic sleep drive (Borbély and Achermann, 1999). The circadian rhythm regulates many physiological processes, such as the body temperature and hormone levels throughout the day, as well as cognitive function and memory (Klein, 1991; Pace-Schott and Hobson, 2002). It also regulates the sleep-wake cycle, making day-time sleeping more difficult for diurnal animals, like humans, leading to problems with insomnia or excessive sleepiness for many night-shift workers (Gumenyuk et al., 2012). The circadian clock is composed of a set of circadian genes which produce proteins that interact in such a way that they oscillate on an approximately 24-hour cycle[1]. The periodicity of the oscillation is entrained to the external natural light cycle through cells in the retina (Pace-Schott and Hobson, 2002), which are connected to the master circadian clock located in the anterior hypothalamus, in a region known as the suprachiasmatic nucleus (SCN) (Clayton et al., 2001; Pace-Schott and Hobson, 2002). The SCN coordinates the circadian rhythm throughout the body and has been shown to regulate the circadian timing of sleep (Schwartz and Roth, 2008).

Although there are many hypotheses about why we need to sleep (Scharf et al., 2008), one of the known properties of sleep is that it is a restorative process, leading e.g. to a replenishment of the cellular energy stores (Scharf et al., 2008; Dworak et al., 2010), as well as playing an important role in learning and memory consolidation (Zisapel, 2007). The homeostatic sleep drive can be described as a "measurement" of the need for this restorative process, where the homeostatic drive increases with prolonged wakefulness and decreases during sleep. The restorative processes of sleep have been shown to be vital, since the

[1] Many advances in what we know about these clock genes and the biochemical time-keeping machinery were first discovered in *Drosophila* (Clayton et al., 2001; Bellen et al., 2010), as described briefly in section 2.1.1 *Drosophila melanogaster as a Model Organism, Introduction*.

detrimental effects of prolonged sleep deprivation have been shown in rats to lead to death (Rechtschaffen and Bergmann, 1995). The homeostatic process of sleep is not yet as well and fully understood as the circadian process, but important pieces of the regulatory machinery have been proposed, in particular the neuromodulators adenosine and nitric oxide (Tonsfeldt and Chappell, 2012; Brown et al., 2012). Adenosine is the basal component of the energy molecule ATP and the end-product when the energy has been completely metabolized (Scharf et al., 2008). High levels of extracellular adenosine have been shown to build up after prolonged wakefulness, which has led to it being proposed as the mediator of the homeostatic sleep drive (Porkka-Heiskanen et al., 1997). Adenosine and nitric oxide act in the cholinergic arousal centers in the basal forebrain and in the brainstem by inhibiting the wake-promoting signaling and are sufficient to facilitate and induce sleep (Portas et al., 1997; Brambilla et al., 2005; Kalinchuk et al., 2010; Porkka-Heiskanen and Kalinchuk, 2011). Interestingly, the central nervous system stimulant caffeine works by temporarily blocking the adenosine receptors of neurons, which prevents adenosine from inhibiting the arousal system and hence prolongs wakefulness (Landolt et al., 2004; Landolt, 2008). Viewed from the two-process model of the interplay between the circadian rhythm and the homeostatic sleep drive (Borbély and Achermann, 1999), the circadian drive for wakefulness during the active phase of the day counteracts the increasing sleep drive of the homeostatic process, thus facilitating sustained wakefulness. Analogously, prolonged sleep consolidation during the inactive phase of the day is accomplished by the circadian drive for sleep while the homeostatic sleep need diminishes (Fuller et al., 2006).

A crucial part to understanding the transitions between wake and sleep has been to map the wake- and sleep-promoting circuits in the brain with ever increasing levels of detail. Briefly, the wake-promoting system is composed of several ascending arousal systems characterized by their distinct neurochemistry and localization. Each of these arousal-promoting systems has been shown to increase wakefulness on its own, but all are needed as a coordinated ensemble to achieve alertness and cortical activation (Zisapel, 2007). The important arousal-promoting systems, defined by neurochemistry, are the monoaminergic neurons,

the hypocretin (also known as orexin) neurons and the previously mentioned cholinergic neurons (Szymusiak and McGinty, 2008; Brown et al., 2012). These arousal-promoting systems originate in the brainstem and posterior hypothalamus and send projections to the basal forebrain and cerebral cortex (Szymusiak and McGinty, 2008; Saper and Lowell, 2014). The sleep-promoting neurons, on the other hand, use the inhibitory neurotransmitters GABA and galanin and are located in the preoptic (anterior) part of the hypothalamus from where they project and inhibit the monoaminergic and hypocretin systems (Zisapel, 2007; Szymusiak and McGinty, 2008). These sleep-promoting neurons in turn are inhibited by the monoaminergic and cholinergic systems through noradrenaline, serotonin and acetylcholine, which all regulate wakefulness (Zisapel, 2007). Sleep-promoting parts of the hypothalamus have been suggested to integrate homeostatic sleep signals (Szymusiak and McGinty, 2008), while the circadian system also projects to these inhibitory, GABA-ergic sleep-promoting neurons (Brown et al., 2012). The sleep-wake transitions are thus regulated by the interactions between the anterior hypothalamus, which integrates both homeostatic sleep need and circadian sleep-regulation, and the wake-promoting neurons in the posterior hypothalamus, brainstem and basal forebrain.

The transitions between sleep and wakefulness can thus be seen as the result of a mutually inhibitory interplay between the wake-promoting and sleep-inducing systems, which in addition, generally happen fast once initiated in healthy individuals (Saper et al., 2010). These observations led to a proposed flip-flop model for sleep-wake transitions, where the arousal and inhibitory systems work analogously to an electronic switch (Saper et al., 2001). In this model the inhibitory GABA-ergic sleep-promoting neurons and the wake-promoting hypocretin (orexin) neurons play an indispensable role for maintaining normal sleep-wake patterns. This conceptual model helps explain the bistability of wakefulness and sleep as well as the fast transitions between the two behavioral states (Saper et al., 2010). The model was later extended to also account for the cycling between NREM (non-rapid-eye-movement, non-REM) sleep, important for the energy restoration and memory consolidation, and REM sleep, associated with dreaming (Lu et al., 2006; Brown et al., 2012).

4.1.2 Sleep-Wake Dynamics

An important step to further our understanding of the transitions between sleep and wake is to explore the temporal properties of these behavioral states. Apart from the overarching circadian rhythmicity of sleep and wake there are also shorter, ultradian cycles within sleep in humans and other mammals, such as the approximately 90-minute cycle of NREM and REM sleep in humans (Pace-Schott and Hobson, 2002; Hobson and Pace-Schott, 2002). The duration of sleep episodes is thus not random, and the disruption and fragmentation of sleep cause both day-time sleepiness, a reduction of cognitive functions and a degradation of mood (Bonnet and Arand, 2003). Experimentally disrupting the natural progression of sleep, while keeping the total amount of sleep constant, has been shown to cause impairment of the next-day performance and alertness (Wesensten et al., 1999) and memory consolidation (Djonlagic et al., 2012), while sleep disorders that cause fragmentation of sleep like narcolepsy and obstructive sleep apnea cause excessive day-time sleepiness and heightened risk for cardio-vascular disease (Mahowald and Schenck, 2005). Similarly, elderly have increased difficulties initiating and maintaining sleep (Floyd et al., 2000), and report frequent nightly awakenings as the most common sleep disturbance (Maggi et al., 1998). It is thus clear that the structure in which sleep occurs is as important as the total amount of sleep. Despite the adversarial effects of induced sleep fragmentation, wake episodes are a normal occurrence during sleeping periods and appear spontaneously in both humans and other mammals (Halász et al., 2004; Lo et al., 2004). It has therefore been proposed that arousals during sleep not only be viewed as a sleep disturbance but that they are an integral part of the normal sleeping process (Halász et al., 2004).

The first study to look at the statistical distributions of sleep and wake bouts was published by Lo et al. (2002). Sleep was recorded in twenty healthy human adults according to standard procedures (Rechtschaffen and Kales, 1968) and all sleep stages of NREM and REM were grouped together into a single sleep state. They found that the wake bout distribution follows a power law ($\Pr(t) \sim t^{-\alpha}$) with a mean exponent of $\alpha = 1.3 \pm 0.4$ (s.d.), and that the

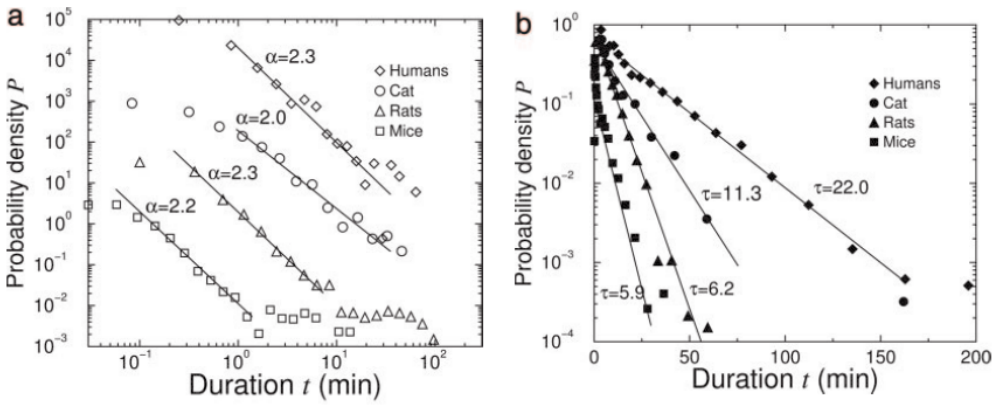

Figure 4.1: Power-law fits to wake bouts and exponential fits to sleep bout distributions for sleep-wake cycles in humans, cats, rats and mice. **(A)** Wake bout distributions plotted on a double-logarithmic scale. All species were found to follow a power law with similar exponents α. Note how wake bouts can last from a few seconds to several tens of minutes. The distributions have been vertically offset for visual clarity. **(B)** Sleep bout distributions from the same animals plotted on a semi-logarithmic scale. The sleep distributions were rescaled to all start from P = 1. Sleep bouts were found to follow an exponential distribution for all animals, with varying time constants τ. *Source*: Modified from (Lo et al., 2004).

sleep bout distribution follows an exponential distribution ($\Pr(t) \sim e^{-t/\tau}$) with $\tau = 20 \pm 5$ minutes – although only in the "large-time region" (t > 5 min). The stretched exponential distribution was tested as an alternative distribution to both sleep and wake bouts with the Levenberg–Marquardt method for non-linear least squares fitting, but found to provide a lesser fit[2]. In their highly influential follow up study, Lo et al. (2004) extended the analysis and compared the sleep and wake bout distributions of human sleep to other mammalian species' sleep-wake distributions (Figure 4.1). The sleep and wake bout distributions were

[2]It is however not stated if both the exponential distribution and stretched exponential were tested against all sleep bout durations or only to the large-time region t > 5 min.

collected from adults in each of humans, cats, rats and mice, and from each species' respective inactive/sleep periods as humans are diurnal while the other three species are nocturnal. They found that wake bouts follow a power law with an exponent in the range of α = [2.0 2.3] for all species, including humans. Unfortunately, no mention or comparison was made with the previously found result (by some of the same authors) of $\alpha = 1.3$ for human wake bouts (Lo et al., 2002). Sleep bouts, on the other hand, were found to follow an exponential distribution in all animals with a characteristic time constant τ, which was found to correlate with the species brain and/or body mass. Sleep and wake were thus found to be regulated independently with clearly differing statistics, where wake bouts follow a power-law distribution with a common scale-invariant pattern while sleep bouts follow an exponential distribution with a species-dependent characteristic time constant.

In a study published shortly thereafter, Blumberg et al. (2005) explored the dynamic properties of the sleep and wake bout distributions during development and maturation in infant rats. Since the sleep and wake states alternate much faster at a young age when the circadian system has not yet been fully established, it opens the possibility to examine the control of the sleep-wake regulation before it has been properly developed (Blumberg et al., 2005). They found that sleep bouts follow an exponential distribution at all ages (0–3 weeks post-natal), with an increasing characteristic time constant τ as the sleep bouts become longer with increasing age and maturation. For wake bouts, however, they found that the power-law distribution is not yet present in the very young individuals – where instead the exponential distribution gave a better fit – and that the power law only emerged at the older ages as sleep became more consolidated.[3] This finding is a valuable addition to our understanding of how the control and regulation of the sleep-wake cycle is established, and correlates with the increasing modulatory effect of the basal forebrain over the brainstem in the developing brain (Blumberg et al., 2005; Mohns et al., 2006). These findings were followed by a study of wild-type mice and knock-out mice with a non-functioning hypocretin (orexin) receptor (Blumberg et al., 2007). A

[3]No other alternative distributions to the power law and exponential were however tested.

defective hypocretin transmission had quite recently been established as the biological basis for the human disease narcolepsy, which we saw in the previous section causes severe sleep fragmentation and acute sleepiness (Taheri et al., 2002). Hypocretin is produced by neurons in the hypothalamus, which projects to the locus coeruleus and other nuclei in the brainstem that control the sleep-wake cycle (Taheri et al., 2002). Blumberg et al. (2007) found that the developmental progress of the sleep-wake transitions in mice is very similar to that of rats, as the sleep bouts follow an exponential distribution for all ages whereas the wake bouts only develop a power-law distribution during the third post-natal week. They also found that a lack of hypocretin delays the maturation of the power-law distribution, but it does not completely abolish the transition. In the next study on the topic, however, the locus coeruleus was selectively targeted with a neurotoxin and found to halter the emergence of the power-law structure of wake bouts (Gall et al., 2009). The locus coeruleus is part of the monoaminergic arousal system which controls the wake process, and was thus shown by Gall et al. to be an important and interesting piece of the intrinsic sleep-wake regulation. In the latest study on the statistical properties of sleep and wake bouts during development, Karlsson et al. (2011) assessed the dynamics of sleep-wake distributions along early development but this time in prenatal sheep, to compare the development of the sleep-wake cycling during the gestational period in a precocial species (which when born are autonomous and can feed themselves) to the post-natal period of the altricial rodents (which are born undeveloped, with the eyes unopened and initially in need of care and feeding by their parents). Karlsson et al. found a similar development of the sleep-wake distributions in prenatal sheep as in rats and mice, where sleep bouts were found to follow an exponential distribution for all gestational ages with an increasing characteristic time scale as the sleep and wake bouts consolidated throughout development, whereas wake bouts showed exponential distributions for all ages and only tended towards a power-law distribution for the oldest age, close to parturition.

As we saw in the studies of the impaired locus coeruleus circuit and the animal model of narcolepsy (with knocked-out hypocretin system), the ex-

amination of the temporal aspect of the sleep-wake cycle shows great utility for finding critical regulatory systems and investigating the effect of disease on the sleep-wake dynamics. In this line, several studies have analyzed the effect of obstructive sleep apnea (Chervin et al., 2009; Chu-Shore et al., 2010; Bianchi et al., 2010) and chronic fatigue syndrome (Kishi et al., 2008) on the sleep and wake bout distributions. Since these studies have been focused on human disease, the choice of methodology has been to also utilize the internal fine-structure within the sleeping state, such as REM sleep and NREM sleep, and sometimes also the different stages (I-IV) within NREM sleep. This makes the results of these studies less easily comparable with the ones we saw previously, which centered on studying the transitions between wake and sleep as these are more easily generalizable between species. Nevertheless, the results are interesting as Kishi et al. (2008) found that the deeper sleep stages were more complex than the other stages of sleep: while REM sleep episodes and stage I of NREM sleep followed an exponential function, stage II followed a stretched exponential distribution and finally, the deep sleep stages III and IV followed a power-law distribution. Like in previous studies, the wake bout distribution was also found to follow a power-law distribution. The results presented by Bianchi et al. (2010) are also interesting, albeit different: they found that both REM and NREM sleep bouts were better fit by a multi-exponential rather than by a mono-exponential distribution, and that wake bouts could be explained by a multi-exponential distribution just as well as by a power law. The model selection was done by using the Akaike Information Criterion (AIC) and comparing the exponential fits pair-wise in increasing order of complexity.

A notable difference between these newer results and the original studies in humans (Lo et al., 2002, 2004) is that, as mentioned above, the NREM and REM were joined into a single sleeping state in the previous studies while the more recent ones considered the substages of sleep separately (Kishi et al., 2008; Bianchi et al., 2010). An additional difference is that Bianchi et al. (2010) fit the entire distribution, while Lo et al. (2002) only considered the exponential distribution to be good fit for $t > 5$ minutes. Rather than a difference, however, this could also be seen as a similarity, in that the sleep bouts do seem to show

more complexity (Lo et al., 2002; Kishi et al., 2008; Bianchi et al., 2010) than what they appear to have when described only as following an exponential distribution (Lo et al., 2004; Blumberg et al., 2005, 2007; Gall et al., 2009; Karlsson et al., 2011). Notably, only Lo et al. (2002, 2004), Kishi et al. (2008) and Bianchi et al. (2010) considered other distributions than the exponential and the power law, and the fitting methods and model selection technique of the other studies were based on linear regression of the semi-logarithm and double-logarithm and comparing these two r^2 fits – a practice that was common, but in the last few years has been deemed unsatisfactory for determining the quality of the fits and the suitability of the model, at least without further validation (see e.g. Clauset et al. 2009, and section 3.1.1 *Modeling Animal Movement Patterns* for further references). It should therefore, in my view, not be seen as a contradiction to find that sleep bouts might have more structure than previously described, since it was usually never even tested if sleep bouts might have this complexity (in the form of heavier tails than an exponential but less so than a power law). Therefore I suggest that we consider sleep bouts to be "exponential-like" and wake bouts to be "power law-like" for the time being, while recognizing the power that these descriptors have had in characterizing the general trends and differences between the regulation of sleep and wake bouts. While the exact functional forms are desirable for a full understanding and for modeling efforts, it is not yet possible without detailed targeted experimentation to distinguish between a generating model where the circuitry is seen as a self-organized critical system giving rise to scale-free power laws (Lo et al., 2004) or a generating model where the combination of random stochastic processes generate a multi-exponential distribution (Bianchi et al., 2010; Chu-Shore et al., 2010).

Regardless of the difficulties, we should again highlight the remarkable findings that we have seen throughout this section: that sleep bouts follow exponential-like distributions that scale as the brain mass and developmental maturity, while wake bouts follow power law-like distributions that consolidate throughout development, and with a similar exponent across species. Hopefully more experiments with continually increasing details about the circadian regu-

lation, sleep homeostasis, sleep-promoting system and the arousal systems that control the sleep-wake transitions can shed further light on the dynamics and the underlying generating mechanisms.

4.1.3 Sleep in "Simpler" Model Organisms

Sleep has primarily been studied in mammalian and avian animals, and sleep in animals of other orders was generally not considered to occur (Campbell and Tobler, 1984; Tobler, 1995; Hendricks et al., 2000). Traditionally, sleep has been defined as a coordinated set of physiological changes measured by electroencephalography (EEG), electromyography (EMG) and electrooculography (EOG) (Brown et al., 2012). However, in large review-surveys covering studies of sleep in most of the animal orders by Campbell and Tobler (1984) and Tobler (1995), they identified the need for establishing a behaviorally based definition of sleep, so that sleep could also be identified in species that do not possess a cerebral cortex (and thus do not produce an EEG signal) or in species that are water-based (which makes electrical recordings difficult). Based on this work, the proposed behavioral criteria that need to be met in order for an animal to be considered to have a sleep state are: i) immobile periods regulated by the circadian rhythm, ii) homeostatic regulation of these quiescent periods, iii) reversibility to wakefulness (distinguishing it from coma or stupor), iv) reduced sensory responsiveness when in the quiescent state (an increased arousal threshold to stimuli), and v) a preferred posture and/or resting place (Campbell and Tobler, 1984; Tobler, 1995; Hendricks et al., 2000).

Based on these criteria, two research groups independently and almost simultaneously published the findings that *Drosophila* fulfills them all and can thus be considered to have a sleeping state (Hendricks et al., 2000; Shaw et al., 2000). Since then part of the sleep-wake circuitry has been mapped and it has been shown that *Drosophila* shares much of the signaling and molecular machinery governing sleep and arousal in mammals, e.g. caffeine and adenosine have the same effects in *Drosophila*, and monoaminergic and GABA-ergic signaling are important regulators in flies as well (Rihel and Schier, 2013). Both

sleep homeostasis and the connection between memory consolidation and sleep are being investigated in *Drosophila* (Donlea et al., 2014; Michel and Lyons, 2014). Besides *Drosophila*, sleep has also been identified in two more genetically tractable model organisms: in the zebrafish *Danio rerio* (Zhdanova et al., 2001; Prober et al., 2006; Yokogawa et al., 2007) and in the nematode *Caenorhabditis elegans* (Raizen et al., 2008; Van Buskirk and Sternberg, 2007). The small worm *C. elegans* is helping shed light on the most ancient and conserved mechanisms of sleep, while the zebrafish has quickly grown to become an important model animal since as a vertebrate it shares many of the mammalian neural substrates, while at the same time it has a much faster reproductive and experimental cycle than other more complex mammalian models like rodents (Rihel et al., 2010). The research on sleep in simpler model organisms has contributed with many advances on the genetic and molecular basis of sleep regulation and disorders also to the human sleep research, and has been recognized to have been the catalyzer for the rapid progress seen in sleep research during the twenty-first century (Zimmerman et al., 2008; Sehgal and Mignot, 2011; Saper and Sehgal, 2013).

4.2 Ontogeny of Sleep-Wake Dynamics in Zebrafish and Humans

4.2.1 Introduction

Sleep is a fundamental and vital process, essential in all stages of life. The amount of sleep needed throughout ontogeny is not constant, however, and all species wherein sleep has been studied have been found to need more sleep in the early part of the lifespan (Roffwarg et al., 1966; Jouvet-Mounier et al., 1970; McGinty et al., 1977; Shaw et al., 2000; Jenni et al., 2004; Blumberg et al., 2005; Jenni et al., 2006) (with the exception of cetaceans (Lyamin et al., 2005)). The amount of time dedicated to sleep then decreases throughout development and consolidates to adult levels as an individual matures. In humans for example, it has been shown that infants sleep for about two thirds of the 24-hour day; then gradually the waking hours increase until sleep only takes up about one third of the day in adulthood (Roffwarg et al., 1966).

Another common feature of the sleep development among species is the initial high level of sleep and wake fragmentation in early life (Blumberg et al., 2005; Arnardóttir et al., 2010; Karlsson et al., 2011). In humans a significant consolidation of sleep and wakefulness occurs during infancy and the first couple of years of living (Jenni et al., 2006; Arnardóttir et al., 2010). In rats there is a similar development as sleep bout durations quadruple during the first two post-natal weeks (Blumberg et al., 2005). The sleep and wake bouts thus consolidate during early development, while the total amount of sleep needed throughout the day decreases.

The consolidation of sleep and wake bouts during development happens concurrently with a shift of the sleep and wake bout distributions (Blumberg et al., 2005, 2007), as we saw in the *Introduction & Background* to this chapter, 4.1.2 *Sleep-Wake Dynamics*. While the sleep bout distribution follows an exponential distribution with a characteristic time constant τ that increases as the sleep bouts lengthen during development, the wake bout distribution undergoes

a shift from initially an exponential distribution to a power-law distribution as the animal matures (Blumberg et al., 2005, 2007). The mature distributions parallel the findings in adults for several species, where sleep bouts were found to exhibit an exponential distribution with a characteristic time constant τ that is developmental- and species-dependent, while the wake bouts were found to follow a power law with a common species-invariant exponent α (Lo et al., 2002, 2004; Blumberg et al., 2005, 2007).

While this pattern of exponential sleep bout distributions and power-law distributed wake bout durations has been found across several species, both nocturnal and diurnal, all of the species examined so far have been mammalian (Lo et al., 2002, 2004; Blumberg et al., 2005, 2007; Karlsson et al., 2011). Sleep research has however advanced immensely during the last ten–fifteen years with the introduction and utilization of genetically tractable "simpler" model organisms, in particular *Drosophila* and the zebrafish *Danio rerio* (Zimmerman et al., 2008; Sehgal and Mignot, 2011; Saper and Sehgal, 2013). The zebrafish is a diurnal vertebrate that has become a popular model organism due to its small size and easy handling, fast development cycle with transparent embryos and larvae, and rich behavioral repertoire (Spence et al., 2008). It is well suited for large-scale genetic and pharmacologic screens and the zebrafish genome has been fully sequenced (Lessman, 2011; Howe et al., 2013; Chiu and Prober, 2013). The transparency of the embryo and larva has further made it ideal for studying development and neuronal circuits (Spence et al., 2008; Portugues et al., 2013).

In sleep research, the zebrafish has been shown to fulfill all the five behavioral criteria that characterize sleep, exhibiting a reversible immobile state with an increased arousal threshold and a characteristic posture that is under circadian and homeostatic regulation (Zhdanova et al., 2001; Prober et al., 2006; Yokogawa et al., 2007). Zebrafish larvae have also been shown to sleep, with an observable sleep behavior emerging by the fifth day of development (Prober et al., 2006). As a vertebrate animal model, it has been found to share all of the known signaling systems that regulate sleep and wakefulness in humans, despite developmental differences in some brain regions (Panula et al., 2010).

In addition, it has been shown to be affected by stimulants and hypnotics in much the same way as mammals (Rihel and Schier, 2013).

The zebrafish has thus become an important model organism for sleep research as it shares many of the advantages of an invertebrate model like *Drosophila*, while its brain anatomy and neurochemistry resembles those of mammal species. To further probe the characteristics of sleep and wakefulness in zebrafish, we studied the development of sleep and wake across ontogeny and compared it with the sleep and wake development over the human lifespan. Additionally, we studied the dynamics of sleep and wake bouts in zebrafish and also contrasted that to the human sleep-wake dynamics. We found that sleep and wake in zebrafish follow a similar course across ontogeny as in humans and other mammals, where sleep levels are highest in the early stages of life and then decrease with age. We further found that wake bouts follow a power-law distribution in both zebrafish and humans of all ages, whereas the sleep bouts were better fit by a stretched exponential distribution in both zebrafish and humans, except for the oldest ages which were better fit by a power law. We thereby show that zebrafish have a similar regulation of sleep and wake as humans, and further validate zebrafish as an important model organism for unraveling the intricacies of the sleep-wake process.

4.2.2 Results & Discussion

To compare the ontogeny of sleep and wake in zebrafish and humans we analyzed the sleep-wake behavior during the night, since both species are diurnal. In both humans and zebrafish we measured the nightly sleep and wake episodes in subjects representing a wide range of ages across the lifespan. Human sleep was measured according to standard procedure (Rechtschaffen and Kales criteria (Rechtschaffen and Kales, 1968)), after which all the sleep stages were merged into a single sleeping state.

The analysis is divided into two main parts: first, a characterization of the sleep and wake structure in humans and zebrafish, that is, the total amount of sleep and wake, the mean duration of sleep and wake bouts, the number of

transitions per night and the fragmentation indices (defined as the number of bouts divided by the total amount of time of each sleep and wake during the night). In the second part we studied the sleep-wake dynamics by analyzing the distributions of sleep and wake bouts in the different age groups of the human participants and of zebrafish.

Human Sleep and Wake Structure Across Ontogeny

We analyzed nightly recordings of sleep and wake from 50 participants between the ages of 2 and 74. The data have been published previously in (Arnardóttir et al., 2010), but in this study we have employed different analysis methods and divided the participants into age groups differently. The participants were divided into four groups: "Children" (ages 2–8, n=15), "Preteens and Teens" (ages 11–16, n=9), "Adults" (ages 23–43, n=15) and "Adults 50+" (ages 49–74, n=11), representing roughly the different stages of human life, Figure 4.2.

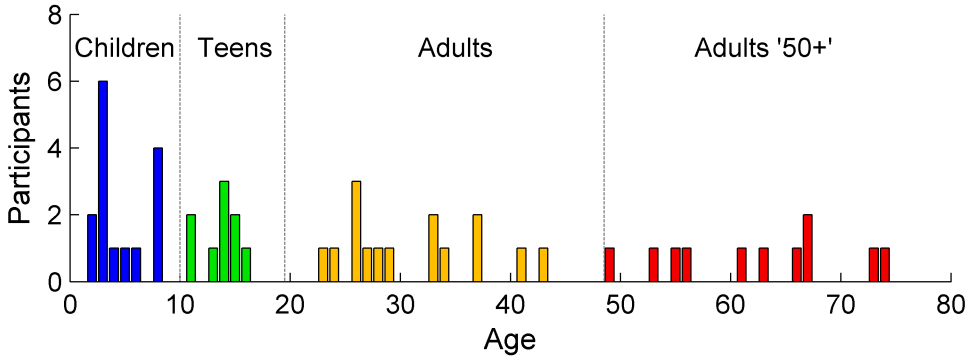

Figure 4.2: Division of human participants into age groups. 50 human participants were divided into four groups according to their age. In the youngest age group "Children" there were 15 participants between ages 2–8. The next group was chosen to comprise of the 9 preteens and teenagers, between ages 11–16, in the text referred to as "Preteens and Teens" and here referred to as "Teens". The adult participants were divided into two age groups, "Adults" with 15 participants between 23–43 and "Adults '50+'" with 11 participants of ages 49–74.

When measuring the sleep levels throughout the night, we found the sleep ratio (the percentage of time asleep during night) to be reduced across age ($F(3,46)=11.69$, $p<0.0001$). The sleep ratio of the Adults 50+ age group was lower compared to Children ($p<0.01$), Preteens and Teens ($p<0.01$) and Adults ($p<0.01$), Figure 4.3 A. The average duration of sleep bouts, number of sleep bouts and sleep fragmentation were however unchanged across age, Figure 4.3 B–D.

Turning to wake during the night, the wake ratio (percentage of time awake during the night) concomitantly changed with age ($F(3,46)=11.69$, $p<0.0001$). Thus, the Adults 50+ showed a significant increase of time awake during the night when compared to that of Children ($p<0.01$), Preteens and Teens ($p<0.01$) and Adults ($p<0.01$), Figure 4.3 E. Another effect of age on the wake structure was the lengthening of the average wake bout durations ($F(3,46)=9.08$, $p<0.0001$), longer in the age group Adults 50+ compared to Children ($p<0.0001$) and Preteens and Teens ($p<0.0001$), Figure 4.3 F, while no change across age was found in the number of wake bouts, Figure 4.3 G. We found a decrease with age in wake fragmentation, defined as the number of awakenings divided by the total time awake ($F(3,46)=6.94$, $p<0.001$), Figure 4.3 H. The Adults 50+ age group showed reduced wake fragmentation (i.e. a longer wake bout duration once awake) compared to Children ($p<0.0001$), Preteens and Teens ($p<0.001$) and Adults ($p<0.0001$).

We thus found that the sleep and wake structure is affected by age in humans, and confirm previous findings of decreased sleep levels in the elderly (Floyd et al., 2000). While we did not find that the youngest participants sleep significantly more than the two older age groups, it is important to note that the youngest children were already 2 years old and that a rapid development of the sleep-wake pattern occurs during infancy (the first 12 months of life) with a considerable consolidation of sleep and wake and a shift towards night-time sleeping (Jenni et al., 2004, 2006; Peirano et al., 2003). We further found a significant effect of age on wake fragmentation in the elderly, which was due to longer, but not more numerous wake bouts during the night.

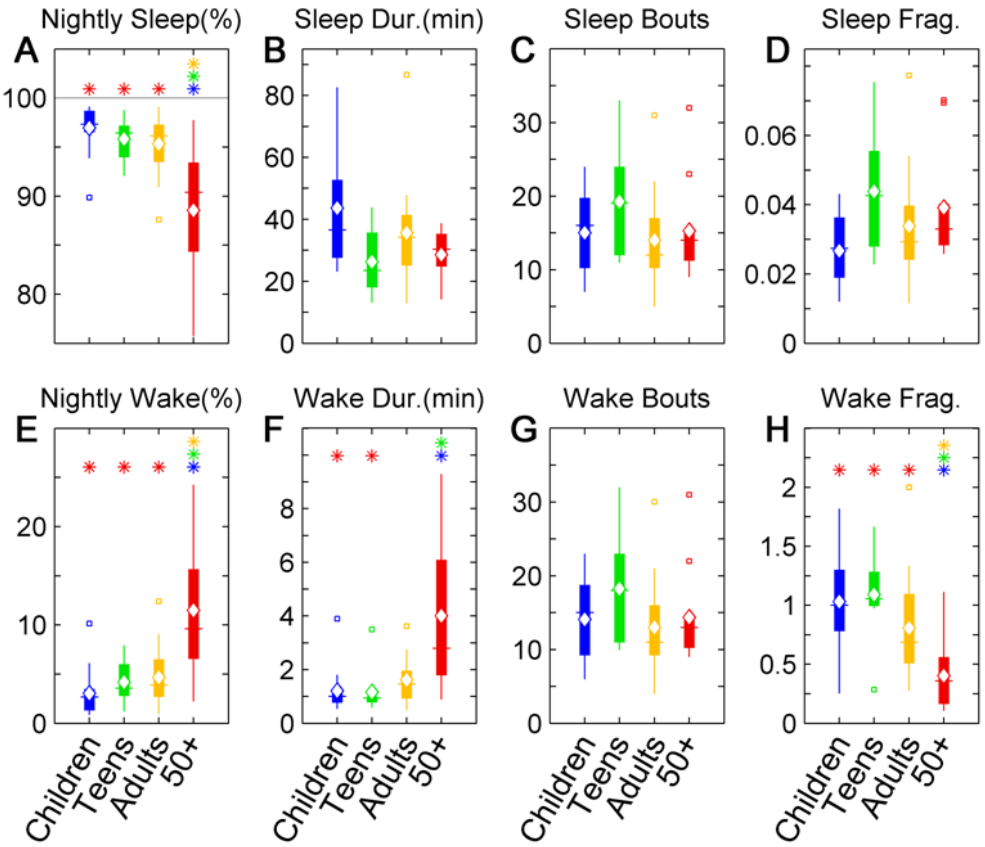

Figure 4.3: Human sleep-wake structure across age groups. Upper row (A–D) shows parameters of sleep structure and lower row (E–H) shows parameters of wake structure. The age groups are Children (blue), Preteens and Teens ("Teens", green), Adults (yellow) and Adults 50+ ("50+", red). **(A)** Percent of time asleep during the night. Adults 50+ sleep less time during the night than the younger participants. **(B)** Mean sleep bout duration, **(C)** mean number of sleep bouts per night and **(D)** sleep fragmentation (number of bouts/total time of sleep) are not significantly different between groups. **(E)** Percent of time awake during the night. Adults 50+ spend more time awake than the younger age groups. The awakenings during the night appear as longer wake bouts **(F)** while the number of awakenings remains unaffected **(G)**. Adults 50+ show a more fragmented sleep than the younger age groups **(H)**. Diamond, white line, and squares indicate mean, median, and outlier values, respectively, while a star indicates $p<0.05$. *Source*: Modified from (Sorribes et al., 2013).

Zebrafish Sleep and Wake Structure Across Ontogeny

To study the ontogeny of the sleep-wake structure in zebrafish four age groups were defined to represent approximately the larval, juvenile, adult and senior phases of the zebrafish lifespan. A total of sixty-one zebrafish of the Tübingen stock strain were recorded in the following age groups: 6–10 days-post-fertilization (n=16); 4–6 weeks old (n=16); 4–6 months old (n=14); and over 12 months old (n=15). While these groups were chosen to represent different stages of the zebrafish lifespan in order to study the ontogeny of sleep-wake regulation in zebrafish and how it relates to mammal sleep-wake regulation, it is not currently known if or how well these age groups correspond to the age groups defined above for the human participants in the sleep study.

Sleep in zebrafish is classified according to behavioral criteria, established by video recordings of larvae and fish which are housed in individual compartments for the entire duration of the recording. Sleep in zebrafish has been established to occur after the sixth second of immobility, both in adult fish (Yokogawa et al., 2007; Zhdanova et al., 2008; Singh et al., 2013) and larvae (Sigurgeirsson et al., 2011). Sleep was thus classified as all immobile 1-second bins starting from and including the 7th immobile second, while all non-sleeping bins were classified as wake. The activity of zebrafish was recorded under white and IR lights on a 14:10 light:dark cycle with lights on at 07:00 and lights off at 21:00, with a 28.5 °C water temperature. The recordings lasted 48 hours following a 24-hour acclimation period, and only night-time data were considered since zebrafish show a diurnal circadian pattern of activity and sleep.

We found that in zebrafish the nightly sleep ratio, defined as the percentage of time spent asleep during the night, decreased with age ($F(3,57)=6.87$, $p<0.001$), Figure 4.4 A. Both adult age groups showed a significantly lower sleep ratio compared to the larval and juvenile groups. When comparing the sleep ratio of the 4–6 month olds to the 6–10 day olds it was significantly decreased ($p<0.001$) as well as in comparison to the 4–6 week olds ($p<0.01$). The sleep ratio of the 12 month+ group was also shown to be lower than those of the 6–10 day old group ($p<0.01$) and 4–6 week old group ($p<0.05$).

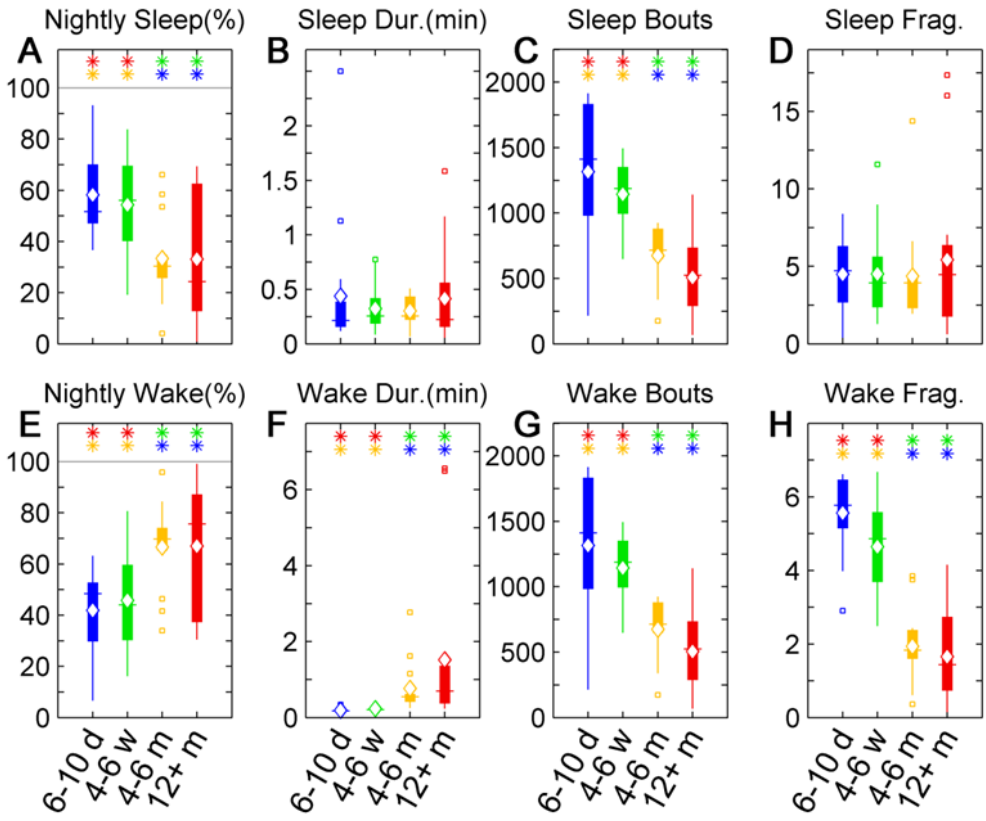

Figure 4.4: Zebrafish sleep-wake structure across age groups. Upper row (A–D) shows parameters of sleep structure and lower row (E–H) shows parameters of wake structure. The age groups are 6–10 days (blue), 4–6 weeks (green), 4–6 months (yellow) and 12+ months (red). **(A)** Percent of time asleep during the night, **(B)** mean sleep bout duration, **(C)** mean number of sleep bouts per night and **(D)** sleep fragmentation (number of bouts/total time of sleep). The two older groups sleep less and have fewer sleep bouts than the two younger groups. **(E)** Percent of time awake during the night, **(F)** mean wake bout duration, **(G)** mean number of wake bouts per night and **(H)** wake fragmentation (number of bouts/total time of wake). The two older, adult, age groups spend more time awake during the night in longer but fewer wake bouts, with a resulting decreased fragmentation of wake as compared to the larval and juvenile age groups. Diamond, white line, and squares indicate mean, median, and outlier values, respectively, while a star indicates $p<0.05$. *Source*: Modified from (Sorribes et al., 2013).

No statistically significant difference was found in the mean duration of sleep bouts between the age groups, Figure 4.4 B, whereas the number of sleep bouts significantly decreased with age ($F(3,57)=17.25$, $p<0.0001$). The sleep-wake transitions were significantly less frequent in the 4–6 month old group compared to the 6–10 day old ($p<0.001$) and 4–6 week old ($p<0.0001$), while the 12+ month old group also displayed fewer sleep bouts as compared to the 6–10 day olds ($p<0.0001$) and 4–6 week olds ($p<0.0001$), Figure 4.4 C. Despite the decreased number of sleep bouts in the two adult age groups as compared to the larvae and juvenile fish, the fragmentation of sleep was not different between the age groups, Figure 4.4 D, as the effect was compensated by a concomitant decrease of the time spent asleep, Figures 4.4 A–D.

Considering the structure of wake bouts in zebrafish next, we found a significant increase of the nightly wake ratio with age ($F(3,57)=6.87$, $p<0.001$). The 4–6 month old group increased significantly with respect to the 6–10 day ($p<0.001$) and the 4–6 week olds ($p<0.01$), as did the 12+ month olds with respect to the 6–10 day old larvae ($p<0.01$) and the 4–6 week old fish ($p<0.05$), Figure 4.4 E. The increase in wake ratio was accompanied by an increase of the mean wake bout duration with age ($F(3,57)=5.05$, $p<0.01$). The 4–6 month group and the 12+ month group had significantly longer wake bout durations than the 6–10 day group (both with $p<0.0001$) and longer than the 4–6 week group ($p<0.0001$ for both), Figure 4.4 F. Regarding the sleep-wake transitions, the number of wake bouts per night were significantly fewer in the two older groups as compared to the two younger groups ($F(3,57)=17.29$, $p<0.0001$), with the 4–6 month and 12+ month olds having fewer wake bouts than the 6–10 day olds ($p<0.001$ and $p<0.0001$, respectively) and 4–6 week olds ($p<0.0001$, both), Figure 4.4 G. The wake fragmentation also displayed a clear decrease with age in zebrafish ($F(3,57)=45.8$, $p<0.0001$). Both the 4–6 month and the 12+ month olds had a significantly lower wake fragmentation than the 6–10 day olds ($p<0.0001$) and the 4–6 month olds ($p<0.0001$), Figure 4.4 H. We thus see that the wake structure is more complex than the sleep structure in zebrafish, as all four parameters of wake structure change across age, Figures 4.4 E–H.

We thus conclude that the internal structure of the sleeping state across the lifespan of zebrafish does not change much with age – the mean sleep bout durations and sleep fragmentation remain constant across age. The significant difference, however, emerges in the total amount of sleep during the night, higher in younger and lower in older fish, achieved through a decrease of the number of sleep bouts along the night with age.

The wake ratio per night and the number of wake bouts are intrinsically tied to the sleep ratio per night and the number of sleep bouts, as these by definition are complementary and alternate with the sleep-wake transitions throughout the night. Therefore we find the analogous results that older zebrafish spend more time awake during the night than the younger ones, with wake spread across fewer bouts. While sleep bout durations remain approximately the same throughout the lifespan and the sleep fragmentation is stable across age, the structure of wake is more susceptible to the effect of age, with longer wake periods during the night and a decreased fragmentation in the adult zebrafish when compared to larval and juvenile fish.

Comparison of Sleep-Wake Structure in Zebrafish and Humans

We can thus compare the ontology of the sleep-wake structure in zebrafish with that in humans, and conclude that they follow a highly similar pattern across the age groups. In both zebrafish and humans there is a generalized decrease of the sleep ratio during the night, which is the same as to say that older individuals spend more time awake during the night. In both zebrafish and humans there is no change in sleep bout durations or sleep fragmentation with age, while wake undergoes differences in both mean wake duration and fragmentation with age. In both species the wake bouts become longer with age and the wake fragmentation decreases. The only aspect which differed was the number of sleep-wake transitions during the night, which in zebrafish decreased with age while in humans it remained stable across age. We can therefore conclude that the developmental pattern of the sleep-wake structure in zebrafish mirrors that of humans to a great extent.

Sleep-Wake Dynamics: Models and Approach

To study the dynamics of the sleep and wake bout distributions, we tested them against four simple functional forms commonly used to study complex dynamics: the exponential distribution, the power law, the stretched exponential and the log-normal distribution (Newman, 2004; Goh and Barabási, 2008). The exponential and the power law distributions have previously been found to describe sleep bouts and wake bouts respectively, as we saw extensively in the introduction to this chapter, section 4.1.2 *Sleep-Wake Dynamics*. The stretched exponential has been found to describe the heavy-tailed activity dynamics in *Drosophila* well (Sorribes et al., 2011 and 3.2 *Dynamics of Spontaneous Walking Activity*), while the log-normal distribution is a commonly found heavy-tailed alternative to especially to the power law distribution (Mitzenmacher, 2004). The analytical expressions of these distributions are given by

$$f(x;\tau) = 1/\tau \cdot \exp(-x/\tau) \tag{4.1}$$

$$f(x;\alpha, x_{low}) = (\alpha - 1) \cdot x_{low}^{\alpha-1} \cdot x^{\alpha} \tag{4.2}$$

$$f(x;k,\lambda) = (k/\lambda) \cdot (x/\lambda)^{k-1} \cdot \exp(-(x/\lambda)^{k}) \tag{4.3}$$

$$f(x;\mu,\sigma) = (1/x)(\sigma^2 2\pi)^{-1/2} \cdot \exp(-(\ln(x) - \pi)^2/2\sigma^2) \tag{4.4}$$

where Equation 4.1 is the exponential distribution, Eq. 4.2 is the power law, Eq. 4.3 the stretched exponential and Eq. 4.4 the log-normal distribution. These four distributions represent different generating mechanisms for the state transitions, where the power law is indicative of complex scale-free dynamics, while the log-normal arises from random events that have a multiplicative effect. Both of these are heavy-tailed and bursty, while the exponential distribution is indicative of a memoryless random (Poisson) process with a characteristic time scale. The stretched exponential distribution on the other hand, is more flexible and can capture both bursty and random dynamics depending on its scale parameter k (Eq. 4.3). When $k{=}1$ the expression simplifies and describes a (simple) exponential distribution, while when $k{<}1$ the stretched exponential distribution becomes heavy tailed. An interpretation of the heavy tailed stretched exponential distribution applied to state transitions is that there

is an initial settling period for the dynamics. Before the system has settled the probability of transitioning out of the state is high, but once settled, the system tends to remain in its current state.

We applied the model selection procedure presented by Clauset et al. (2009). In this procedure the following steps were detailed for each model, namely i) finding the best fit to the data and its corresponding Kolmogorov-Smirnov (KS) distance, ii) drawing a large number (N=10,000) of random samples from the model distribution using the estimated parameters from the data, each random sample being the same size as the data, and iii) performing a 'plausibility' or consistency test by comparing the empirical KS distance to the ones from the randomly sampled data, and thus obtaining a p-value. The final step, iv) is to find the model that is the most consistent with the data among the different plausible models, using the Akaike Information Criterion with a correction for finite sample sizes (AICc) and/or the Bayesian Information Criterion (BIC).

To determine the best fit to the data we estimated the parameters using maximum likelihood estimators (MLE) for the exponential, power-law and log-normal distributions, while for the stretched exponential distribution we used the linear fit between log(x) and log(-log(y)), where y is the survival distribution, as we have previously shown in section 3.9 *The Linear Fit Correctly Estimates the Parameters*, that it robustly estimates the parameters of the stretched exponential distribution for small sample sizes. The power-law exponent α and the lower cut-off x_{low} were estimated following the best practices recommended in (Clauset et al., 2009) for estimating the parameters of a power law. All the distributions were shifted in time so that the distributions start at the smallest bout duration determined by the experimental conditions (t_{min}), such that $x = t - t_{min}$, where t_{min} is 30 seconds for human sleep and wake bouts, while 6 and 1 seconds respectively for zebrafish sleep and wake bouts.

Human Sleep-Wake Dynamics Across Ontogeny

To accurately determine the possible functional forms of the distributions of sleep and wake bouts, the numbers of unique bout durations is an important

factor since the number of bouts with different durations determine the number of points in the survival distributions. In humans we found, however, that the sleep-wake dynamics are characterized by relatively few transitions and that the variation in bouts durations is fairly limited. The number of sleep bout durations was on average 13.6 (range: 7–21 among all individuals in the age group) for Children, 16.6 (range: 10–28) for Preteens and Teens, 12.5 (range: 5–21) for Adults and 13.6 (range: 9–25) for Adults 50+. An even lower number of unique wake bout durations was found, indicating that most awakenings are short with most wake bout durations falling in the 30-sec or 60-sec bins. The average number of unique wake bout durations for Children was 3.9 (range: 2–7), for Preteens and Teens 4.2 (range: 2–6), for Adults 4.5 (range: 1–8) and for the Adults 50+ group 6.4 (range: 3–11).

While it is important to perform fits on an individual level, it is also important that the underlying distributions have enough statistics to do so. To perform meaningful model fits we thus established the criteria that the empirical distributions had to have at least 5 points (5 unique bouts durations) to be considered. In the different age groups, however, only 5 Children, 4 Preteens and Teens, 8 Adults and 8 Adults 50+ met this requirement. As a consequence, we also considered the pooled distributions of each age group for model selection.

The pooled sleep bouts distributions were found to be well fit by stretched exponential distribution for Children (k=0.79, λ=31.6 minutes), Preteens and Teens (k=0.78, λ=19.6 minutes) and the Adults group (k=0.76, λ=23.0 minutes), Figures 4.5 A–B [p. 113], whereas a power law distribution was favored for sleep of the Adults 50+ group (α=2.2, x_{low}=2.5 minutes). From the fits to each individual survival distribution we obtained k=0.84 $\pm$ 0.06 for Children, k=0.84 $\pm$ 0.05 for Preteens and Teens and k=0.79 $\pm$ 0.07 for Adults, Figure 4.5 A, with no statistically significant differences between the age groups. We thus find that sleep bouts exhibit heavy-tailed distributions and hence have more structure than in the random dynamics case when they follow an exponential distribution (Lo et al., 2002, 2004), consistent with more recent finding that also found more complex dynamics (Chu-Shore et al., 2010). Apart from heavier tails than previously reported, the scale parameters are similar to the

previously reported value of 22 minutes in healthy adult participants (Lo et al., 2002), especially the Preteens and Teens and the Adult groups.

The pooled wake bout distributions were found to be consistent with a power law for all age groups, with the exponent for Children estimated at α=2.4 (x_{low}=2.5 minutes), Preteens and Teens α=2.7 (x_{low}=1 minutes), Adults α=2.2 (x_{low}=1.5 minutes) and Adults 50+ α=2.2 (x_{low}=2.5 minutes), Figures 4.5 C–D. The group mean exponents were α=1.78 $\pm$ 0.04 for Children, α=1.90 $\pm$ 0.04 for Preteens and Teens, α=1.71 $\pm$ 0.03 for Adults and α=1.83 $\pm$ 0.13 for Adults 50+, with no statistically significant differences between the age groups, Figure 4.5 D. These results thus match previously reported findings of wake bouts following a power law distribution with an exponent $\alpha \approx 2$ (Lo et al., 2002, 2004).

Zebrafish Sleep-Wake Dynamics Across Ontogeny

The dynamics of the zebrafish sleep-wake cycle, on the other hand, are dominated by many more transitions during the night. A comparison of sleep-wake dynamics between humans and zebrafish reveals that the transitions occurring in the fish during the night are 10–100 times more frequent than in human night sleep (cf. Figures 4.3 C and 4.4 C). In zebrafish the number of unique sleep bouts were on average 94.7 (range: 58–164) for the 6–10 day group, 94.3 (range: 27–154) for the 4–6 week group, 81.9 (range: 22–131) for the 4–6 month group and 75.6 (range: 11–134) for the 12+ month group. As observed in human sleep-wake dynamics, the unique wake bout durations were less numerous, averaging 42.8 (range: 23–88) for the 6–10 day olds, 51.8 (range: 23–98) for the 4–6 week group, 85.9 (range: 56–128) for the 4–6 month olds and 85.3 (range: 39–130) for the 12+ month olds.

The comparatively large number of unique sleep and wake bout durations in zebrafish allowed us to perform model estimations on an individual level. For each zebrafish, thus, each of the four model distributions (the exponential, stretched exponential, power law and log-normal distributions) was fit to the sleep and wake bout length distributions, following the steps i–iii outlined

above. Briefly, the steps consist of estimating the parameters from the empirical distribution and calculating a goodness-of-fit (GoF) measure; drawing a large number of synthetic random samples from the distribution with the empirical estimated parameters and calculating the GoF for each of the random samples; and calculating how 'extreme' the empirical GoF is in comparison to the synthetic GoFs in the form of a p-value. This p-value then quantifies how plausible it is that the empirical distribution stems from the model distribution, and by this method we thus obtain a plausibility measure for each of the four model distributions. The last step is the model selection, where all of the plausible models are compared with the AICc and/or BIC to determine the best model for the data. This procedure has been used to validate and debunk power laws in a wide variety of empirical distributions, but usually these consist of a single distribution for each phenomenon (Newman, 2004; Clauset et al., 2009). In our case we have multiple individual distributions in each age group and would thus quantify which of the model distributions is the best fit to the most individuals in each group, to compare the age groups.

However, out of the 61 fits to the empirical sleep bout distributions across all ages only about half (33 of 61, or 54%) were found to be plausibly consistent with one or more models, and of these, 26 were only consistent with a single model. Similarly, while 36% of the wake bout distributions were consistent with one or more models, the majority, 91%, of those proved to be consistent with one model only. The last step of using AICc or BIC to select among models was thus generally superfluous, and we instead directly quantified which model was found to be the most plausible in each of the age groups.

The low level of plausibility for any of the four models might create the temptation to try with a wider array of distributions with a higher degree of complexity, to capture features that the simpler models seem to not be able to incorporate. There are however two main downsides to this approach. First, the introduction of complex functional forms that have more parameters makes it more complicated to interpret the distribution parameters and what they say about the sleep-wake dynamics. Second, there is a clear risk of over fitting when employing complex models to noisy data. With an increased number

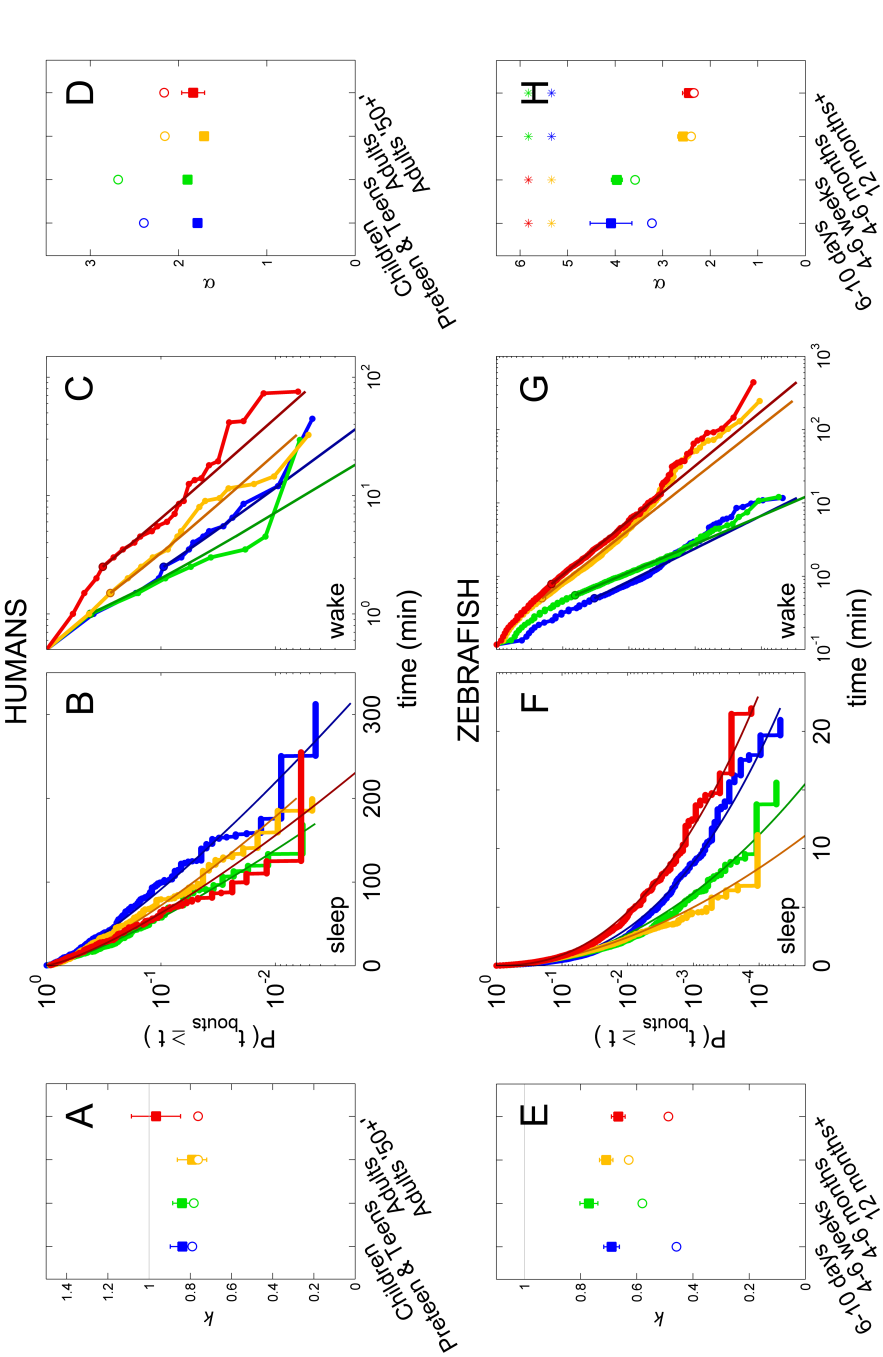

Figure 4.5: Sleep-Wake Dynamics in Humans and Zebrafish. **(B, F)** Sleep bout distribution of pooled values on log-lin axes, with stretched exponential fits in darker shades. **(C, G)** Wake bout distribution of pooled values on log-log axes, with power law fits in darker shades. **(A, E)** Shape k of the stretched exponential fits and **(D, H)** exponent α from the power-law fits. Open circles indicate the parameter value from the fits to the pooled distributions, while filled squares show the mean value of the individual fits. Error bars indicate s.e.m. and a star $p<0.05$. *Source:* (Sorribes et al., 2013).

of parameters the complex models are more flexible and will thus be able to better fit the kinks and twists of the individual distributions, but the information gained will generally not be generalizable.

Many of our empirical sleep and wake bout distributions are indeed quite noisy, as we can see in Figure 4.6. It is therefore quite unlikely that they would be plausibly consistent with any reasonably simple functional form that we might try. Importantly, though, is to consider that a failed plausibility test only indicates that the empirical distribution does not purely follow the exact functional form of the model, and that real-world noisy systems seldom do (Alstott et al., 2014). This does not exclude that the models can still be useful for parameterizing and comparing distributions that have a reasonable, albeit noisy fit. This can probably most easily be seen visually in Figure 4.6, where the models quite accurately capture the shape of the distributions despite the many failed plausibility tests and noisy data.

The fits to the sleep bout distributions were thus found to most often be described by the stretched exponential distribution in the 6–10 day olds (k=0.69 $\pm$ 0.03, λ=20 $\pm$ 7 sec), 4–6 week olds (k=0.77 $\pm$ 0.03, λ=16 $\pm$ 2 sec) and 4–6 month olds (k=0.71 $\pm$ 0.02, λ=14 $\pm$ 2 sec), Figures 4.5 E–F [p. 113]. Neither the shapes k nor the scales λ showed any statistically significant differences between the means of the age groups. The 12+ month olds, however, had a larger proportion of power law and log-normal fits, tied with an equal number of plausible cases. To determine the best model for this group we applied AICc to the two cases where both models had been found plausible, which favored the power law model over the log-normal, with α=2.8 $\pm$ 0.2. We thus conclude that the sleep dynamics are heavy-tailed in all age groups, characterized by longer sleep bouts being more frequent than in the random (exponential distribution) case.

The wake bout distributions, in turn, were consistent with the power law for all age groups, with α=4.1 $\pm$ 0.4 for 6–10 day olds, α=4.0 $\pm$ 0.1 for the 4–6 week group, α=2.6 $\pm$ 0.1 for the 4–6 month olds and α=2.4 $\pm$ 0.1 for the 12+ month olds, Figures 4.5 G–H. We observed that with age the power law exponent α was reduced ($F(3,57)=12.1$, $p<0.0001$). Adult fish (4–6 month

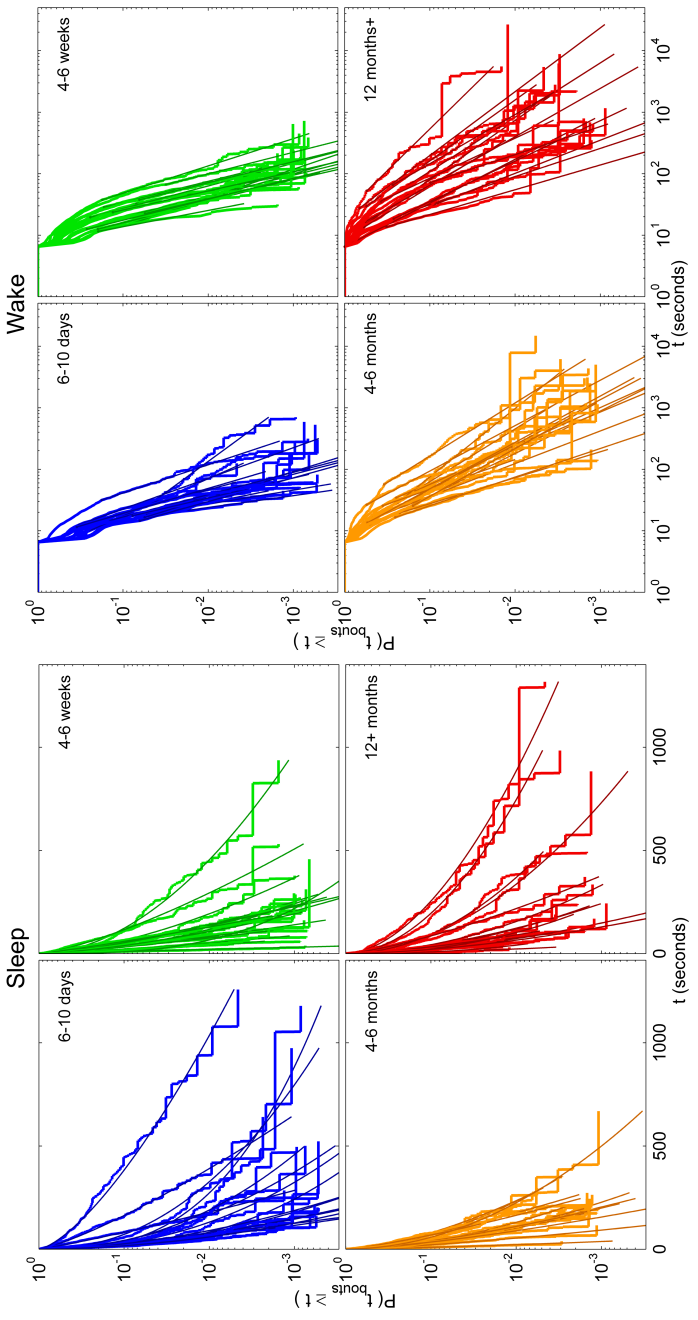

Figure 4.6: Individual Sleep-Wake Distribution in Zebrafish. Left panel shows sleep distributions with stretched exponential fits on log-lin axes. A straight line on these plots indicates an exponential distribution of bout lengths. Right panel shows wake distributions with power-law fits on log-log axes. A straight line on these plots can be indicative of a power-law distribution. *Source*: (Sorribes et al., 2013).

and 12+ month groups) exhibited significantly ($p<0.0001$) lower exponents of the power-law fits to the wake bout distributions than the larval and juvenile stages (6–10 day and 4–6 week groups), Figure 4.5 H. The wake bouts thus exhibit markedly heavy-tailed distributions, where with age the likelihood of soon falling asleep anew after having woken up becomes lower.

Comparison of Sleep-Wake Dynamics in Zebrafish and Humans

We can now compare the dynamics of sleep and wake across ontogeny in zebrafish and humans. The sleep bout distributions were best fit by the stretched exponential distribution in all age groups except the oldest, in both zebrafish and humans (Figure 4.5). The distributions were found to be burstier than random with $k<1$ in all age groups across species.

The wake bout distributions were found to follow a power law for all age groups in both zebrafish and humans (Figure 4.5). In humans the power-law exponent α was found to be around 2, like reported previously for humans, cats, rats and mice (Lo et al., 2004). In zebrafish we found a similar power-law exponent for the two adult fish ages, while the larval and juvenile ages showed markedly steeper power-law relationships, indicative of a less bursty dynamics – which is probably tied to increased sleep pressure and the shorter wake bouts in the younger individuals. Although we found a clear power-law structure of the wake bouts in the young larvae and juvenile fish, the shift towards a burstier wake dynamics with age resembles that found in young rats, mice and sheep, where newly born (or prenatal in the case of sheep) exhibit exponential(-like) distributions in the early ages which turn into power laws as the animals mature and grow (Blumberg et al., 2005, 2007; Karlsson et al., 2011).

Clearly, an important sleep-wake maturation takes place between the 4–6 weeks and 4–6 months of age in zebrafish (Figures 4.4 and 4.5), opening the door for further studies of the sleep-wake dynamics during this critical time. In humans the youngest participants were already 2 years old, when much of the important sleep-wake maturation has already occurred. It would be interesting to thoroughly study the development of the sleep-wake dynamics

in even younger children, even though it poses important methodological difficulties as the sleep-wake dynamics are highly non-stationary and undergo important changes from around-the-clock sleeping to predominantly nightly sleep as the sleep-wake cycle comes under circadian control during the first year of infancy (Jenni et al., 2004, 2006; Peirano et al., 2003).

Despite some differences in early development, we conclude that the dynamics of both sleep and wake are very similar in zebrafish and humans across ontogeny.

4.2.3 Conclusions

We studied the sleep-wake cycles of humans and zebrafish at different ages along the lifespan. In humans the different life stages were represented by the age groups of Children, Preteens and Teens, Adults and Adults '50+', while in zebrafish the groups comprised of larvae, juvenile fish, young adults and adult fish. By combining the different sub-stages of human sleep and only considering the state transitions between sleep and wake, meaningful comparisons become available also to species with behaviorally defined sleep criteria.

We first studied the structure of sleep and wake in humans and zebrafish. We found that older individuals spend less time asleep during the night than the younger groups in both humans and zebrafish, while there is no change in sleep bout durations or sleep fragmentation with age. The wake bouts on the other hand become longer with age and the wake fragmentation decreases in both species. Apart from a difference in the number of sleep-wake transitions with age, the sleep-wake structure in zebrafish resembles that of humans to a great extent across ontogeny.

We next studied the dynamics of sleep and wake, by fitting the sleep and wake bout distributions against four common modeling distributions: the exponential, stretched exponential, power law and log-normal. In humans we were able to replicate and extend previous findings, while in zebrafish it had never been studied before. In both humans and zebrafish the sleep bout distributions were best fit by a stretched exponential distribution for all age

groups except the oldest, which was better fit by a power law. We thus found that the sleep bout dynamics exhibit more structure than had generally been found previously. The wake bout distributions were best fit by the power-law distribution, in accordance with previous findings, which we have now shown extends to zebrafish as well.

The findings that both the sleep-wake structure and dynamics in zebrafish resembles that of humans to such a high degree points to a conserved evolutionary control of the sleep-wake control and the underlying neural circuitry. We have thus shown that the zebrafish sleep state is very similar to human sleep across ontogeny, and thus further validated the zebrafish as a valuable animal model for sleep research.

4.2.4 Material and Methods

Human Sleep Data

Nightly sleep-wake data were provided by Karl Æ. Karlsson from the University of Reykjavik, Iceland. Briefly, the procedure to acquire the human sleep-wake recordings was as follows.

Possible candidates for the study were drawn from a randomized sample from the national registry of Iceland of 1000 inhabitants from the Reykjavik area. Of the over 250 contacted candidates, 78 accepted to partake in the study. After screening for sleep-related health issues, 57 healthy participants were included and underwent an unattended ambulatory polysomnography (PSG) with a digital recording system (Medcare Inc., Iceland). 1 participant was excluded due to suspected hypothyroidism and 6 PSGs were unusable for technical reasons, leaving 50 participants between the ages of 2 and 74 participating in the study.

The unattended ambulatory PSGs were recorded at home between 22:00 and 08:00, and the participants were instructed to follow their normal daily sleep routine as closely as possible. The recordings were scored by an accredited sleep technologist in 30-s epochs as either non-REM sleep stages 1–4, REM sleep, or

wake, in accordance with the Rechtschaffen and Kales criteria (Rechtschaffen and Kales, 1968). For subsequent analysis the non-REM and REM sleeping stages were unified into a single sleeping state.

For further detail on the data acquisition process, please see (Sorribes et al., 2013) for a longer description of the Recruitment, Questionnaire and Procedure used to obtain the human sleep-wake data. In addition, the data collection has also been described in detail in (Arnardóttir et al., 2010). The study was approved by the Icelandic National Bioethics Committee (permit VSNb2007100011/03-15).

Zebrafish Sleep Data

Nightly sleep-wake data were provided by Karl Æ. Karlsson from the University of Reykjavik, Iceland. Briefly, the procedure to acquire the zebrafish sleep-wake recordings was as follows.

Zebrafish of the Tübingen reference strain were obtained from the University of Oregon Zebrafish International Resource Center. Four age groups were selected to approximately represent the different stages along the zebrafish life: larvae, just after they have developed an observable sleep-wake pattern (6–10 days old), juvenile fish (4–6 weeks old), young adults (4–6 months old) and adult fish (12+ months). The typical lifespan of zebrafish in captivity is 2–3 years (Spence et al., 2008).

The zebrafish were entrained to a daily cycle of 14:10 light:dark with lights on at 07:00 and off at 21:00, and with daily feeding at 12:00 (noon). The experimental set-ups were blocked from natural light and instead illuminated from below with white light (255 lx) during the lights-on period and infrared light (0 lx) during the lights off period. Recordings started at noon and continued for 48 hours, after the first day of acclimatization. Larvae were recorded in 24 well plates and the juvenile fish in 12 well plates, while the adult fish were recorded in individualized compartments inside an opaque tank. All recordings were performed at a 28.5 °C water temperature, with circulating water.

The movements of the zebrafish were recorded with the Ethovision XT 7.0

behavioral tracking system (Noldus Information Technology), which allows the velocity of each fish to be tracked in two dimensions. After the recordings, the velocity data were divided into 1-second bins and classified as either movement or non-movement according to an age-dependent velocity threshold. The velocity thresholds were found to scale with body mass, determined and verified by three independent human raters. The velocity thresholds were 0.5 cm/s for the 6–10 days (Sigurgeirsson et al., 2011), 0.75 cm/s for the 4–6 weeks, 1.0 cm/s for the 4–6 months, and 1.5 cm/s for the 12+ month olds. Subsequently, the movement/non-movement data were dichotomized into sleep and wake using the established criteria of sleep occurring after 6 seconds of immobility, in both larvae and adult fish (Yokogawa et al., 2007; Zhdanova et al., 2008; Sigurgeirsson et al., 2011; Singh et al., 2013).

For further detail on the data acquisition process, please see (Sorribes et al., 2013) for a longer description of the Fish, Procedure and Data Preprocessing used to obtain the zebrafish sleep-wake data. All the procedures of the study were in compliance with the regulations of the National Bioethics Committee of Iceland, with a permit issued to Karl Æ. Karlsson on 19th May 2008 (no number).

Statistical Analysis

All data on human and zebrafish sleep-wake bouts were imported into Matlab 2010a (The MathWorks Inc.) for analysis. To test the influence of age on the sleep and wake structure parameters (ratio percentage, bout duration, number of bouts and fragmentation index) analysis of variance (ANOVA) was used, with the null hypothesis that all of the means across the age groups were the same. Two-tailed Student's t-tests were used to test the specific pair-wise difference between age groups, using the Holm-Bonferroni correction for multiple comparisons. The family-wise type I error rate was set to α=0.05 for both the ANOVA and the sets of multiple pair-wise comparisons.

The two-tailed Student's t-test was implemented with care to fulfill the prerequisites of the standard parametric tests. For each pair-wise test, the two

groups were tested with the Lilliefors test of normality and with the two-sample F-test for equal variances. If both groups were normally distributed (or rather, failed to be rejected as coming from a normal distribution) and the variances were not unequal (i.e. "equal") the standard parametric Student's t-test was used, while if the variances were unequal, the Welch's t-test was used. If however one (or both) of the two group samples did not pass the normality test the t-statistic was bootstrapped with a resampling of 10,000 to calculate the probability of finding a result at least as extreme as the test t-statistic.

All values in the text are presented as the mean $\pm$ standard error of the mean (s.e.m.), unless otherwise noted. In the figures containing box plots, the whiskers extend to the lowest and highest values within the 1.5 interquartile range (IQR), which corresponds approximately to ± 2.7 standard deviations and 99.3% coverage if the data are normally distributed. Values outside the 1.5 IQR are considered outliers, and are plotted with square symbol outside of the whisker range.

5

Activity-Rest Dynamics and Neuronal Excitability of *DmIh*

5.1 Introduction & Background

In this chapter we will take a somewhat different approach and make an in-depth exploration into the neuronal current I_h, known as the "pacemaker" current, and see its effect on neuronal excitability in *Drosophila*. But first we will learn a bit more about the I_h current and the HCN channels and see how it got the name of "pacemaker" by regulating rhythmic electrical activity.

5.1.1 The I_h Current

The I_h current is a slow inward ionic current which activates at hyperpolarization and depolarizes the membrane (Robinson and Siegelbaum, 2003). It arises through hyperpolarization-activated cyclic nucleotide-gated (HCN) channels (Robinson and Siegelbaum, 2003). The HCN channels are selectively permeable to the monovalent cations Na^+ and K^+, but not to Li^+ or divalent cations (Pape, 1996). Unusually for voltage channels, the HCN channels are modulated by cyclic nucleotides which bind to the channel and shift the voltage dependence towards more positive potentials (Wahl-Schott et al., 2014). Neurotransmitters and hormones can thus modulate the dynamic properties of the channel through the secondary messenger cAMP (Tsien, 1974; DiFrancesco and Tortora, 1991).

The HCN channels are structurally composed of four subunits, which are in turn each composed of six transmembrane helices (He et al., 2014). In mammals there exist four different kinds of subunits, each encoded by a different gene (HCN1–4) (Ludwig et al., 1998; Santoro et al., 1998). The HCN channels can be homomerically or heteromerically assembled in a cell specific pattern, and confer different electrical properties (Altomare et al., 2003).

The I_h current was first discovered three–four decades ago rather concurrently in rod photoreceptors, hippocampal pyramidal neurons as well as in sino-atrial node cells and Purkinje fibers of the mammalian heart (Pape, 1996). The current has primarily been studied in mammals, where it has been found throughout the nervous system and heart. The study of the I_h current has

however also extended to the zebrafish *Danio rerio* and the fruit fly *Drosophila melanogaster* (Baker et al., 1997; Marx et al., 1999). In *Drosophila*, I_h seems to be located throughout the nervous system and in the aorta, but advancements have been hampered by the lack of effective antibodies to identify the HCN channels (Marx et al., 1999; Monier et al., 2005).

The electrical properties and the resulting physiological effect of the I_h current have been perplexing since the very beginning. When the current was first discovered, it was named I_f for "funny" in the heart (Brown et al., 1979) and I_q for "queer" in hippocampal neurons (Halliwell and Adams, 1982), but the name I_h was later settled on for its hyperpolarized activation. The activation upon hyperpolarization and deactivation by depolarization is what especially sets this current apart – and that a substantial degree of HCN channels remain open and depolarize the membrane at resting potentials (Wahl-Schott et al., 2014). These electrical properties, in conjunction with its permeability to Na^+ and K^+ and modulation by cAMP, are what is thought to confer I_h its ability to control rhythmic activity in the heart and nerve populations (Wahl-Schott et al., 2014).

Physiologically, I_h has been found to have several different functions, including controlling and limiting the resting potential, controlling the membrane resistance and the signal integration in dendrites, regulate synaptic transmission, and controlling pacemaker activity in the heart and brain (Robinson and Siegelbaum, 2003). The pacemaker function is not only important for establishing and maintaining a correct heart rhythm, but also in the brain, where specialized pacemaker cells generate spontaneous rhythmic activity that underlies the coordinated activity of behavioral states (Santoro et al., 1998). I_h is found in many regions and neuronal types throughout the brain, and is important for regulating arousal and sleep; learning and memory; and perceptual representation and consciousness (Lewis and Chetkovich, 2011).

5.1.2 Activity-Rest Patterns of *DmIh* Null Mutant

An important cell type that expresses the I_h channel are the dopaminergic neurons. Dopamine has been shown to be important in many higher order brain functions, like sleep and wake, learning and memory and consciousness (Palmiter, 2011). Dopaminergic neurons exhibit spontaneous rhythmic activity patterns, which can be modulated by neuronal inputs. The I_h current has been found to be important in regulating the firing rate of the spontaneous activity (Seutin et al., 2001; Neuhoff et al., 2002; Zolles et al., 2006), and the HCN channels have been identified as key targets through which neurotransmitters can alter the dopaminergic firing rate (Cathala and Paupardin-Tritsch, 1997; Liu et al., 2003; Arencibia-Albite et al., 2007). In addition, HCN channels have also been implicated in several dopamine-related disorders like Parkinson's disease (Chan et al., 2011) or schizophrenia (Arnsten, 2007).

As mentioned in the previous section, there exist four genes that encode subunits for the I_h channel in mammals (HCN1–4). While most studies have centered on the I_h current in the heart, a few studies have investigated the consequences of blocking one of the HCN genes in neuronal populations (Lewis and Chetkovich, 2011; Herrmann et al., 2007). Taking advantage of the fact that the *Drosophila* genome only contains a single I_h gene, named *DmIh*, a collaborating group created a null mutation for this gene (*DmIh*$^-$) by deleting a core region of the channel and thus creating a non-functioning variant of the HCN channel (Gonzalo-Gómez et al., 2012).

With this I_h null mutation Gonzalo-Gómez et al. (2012) were able to study the effects of complete abolishment of the I_h current throughout the entire organism. In particular, their study centered on the behavioral effects of missing the I_h current on the activity-rest pattern, and how it relates to dopamine. To establish baseline results they first measured the levels of dopamine in wild-type flies, and found that it cycles throughout the day. In the *DmIh* null mutants, however, dopamine lost the cyclicity during the day (light period) but with overall normal levels, while the dopamine levels increased significantly during the night (dark period).

The behavioral consequences of the *DmIh*$^{-}$ induced dopamine alteration were studied next. The I_h current null mutants had overall lower activity levels during the day, in particular during the characteristic “dawn” activity peak. Measuring sleep-wake parameters during the day and night, they found that sleep levels were increased during the day, while not significantly different during the night. The sleep fragmentation was however affected during both day and night, with shorter and more numerous sleep bouts. We studied the activity dynamics in these flies, and found a strong effect on burstiness during the night, and a weak effect during the day. Taken together, the results suggest that the I_h current in *Drosophila* is necessary for preventing an overproduction of dopamine during the night, while I_h is necessary for a correct cycling of dopamine during the day.

5.2 Electrophysiological Study of the *DmIh* NMJ

5.2.1 Introduction

The null mutation for the I_h current creates a behavioral phenotype in adult *Drosophila*, affecting the activity-rest patterns by modulating the dopaminergic signaling (Gonzalo-Gómez et al., 2012). In addition there was a differential effect on the activity intensity (mid-point crossings/active minute) during day and night. At day, the flies showed a decreased walking intensity during the active periods, while at night it reversed, with an increased walking intensity during active episodes compared to control flies.

To better understand the physiological effect of a missing I_h current in *Drosophila*, the larvae were examined for a possibly similar phenotype, since the *Drosophila* larvae have a much simpler nervous system than the adult flies. The null mutation mutants *DmIh*$^-$ were indeed found to have a locomotor phenotype, as well as an altered morphology of the neuromuscular junction. Both walking speed and the total distance traveled were lower than in controls, as well as the number of stops and turns – which in the *Drosophila* larvae are search and decision-making events (Wang et al., 1997).

Since the *Drosophila* larval neuromuscular junction is an ideal system for electrophysiological examination due to its simple constitution of easily accessible muscles and motoneurons, as well as having a simple and easily quantifiable morphology and locomotor behavior, we decided to further investigate how the I_h current affects locomotion in the *Drosophila* larva together with our collaborators at the laboratory of Dr. Inmaculada Canal (Universidad Autónoma de Madrid).

To this extent, our collaborators generated a dominant negative isoform IhDN, which dominates and disrupts the normal I_h channel function in *Drosophila*. With this dominant negative isoform we could express the blocking of the I_h current with Gal4/UAS constructs selectively in either motoneurons (*D42-Gal4/UAS-IhDN*) or muscles (*24B-Gal4/UAS-IhDN*).

Morphologically, the *DmIh*$^{-}$ null mutants showed a drastic decrease in the number of synaptic boutons, which is usually a sign of reduced excitability (hypoexcitability). The size of the synaptic boutons was larger than in the control strain (henceforth called 'ISO' for isogenic), which was surprising as the opposite result would be expected for a hypoexcitable strain (Lnenicka et al., 2003). When analyzing the number of active sites per bouton, however, it was found that the increase in size was not accompanied by a proportional increase of synaptic release sites, as the number of active sites was lower than in controls. To further probe the effect of abolishing the I_h current, the IhDN was expressed in either motoneurons or muscles, after having confirmed with RNA *in situ* hybridization that *Drosophila* larval muscles also express the I_h channel. Both targeted expressions yielded an identical pattern to the *DmIh*$^{-}$, indicating that the I_h current is needed both pre- and postsynaptically for a normal maturation of the neuromuscular junction.

Turning to behavior, the *DmIh*$^{-}$ null mutation had a slower crawl speed, more frequent pauses as well as decision-making events, and an overall shorter crawl path, as mentioned above. The presynaptic mutant (*D42/IhDN*) showed a similar phenotype with slower crawl speed and shorter overall distances, but did not show a difference in the number of pauses and decision-making events compared to controls. This indicates that the locomotor movement is affected in the presynaptic mutant, but not the decision-making phenotype which is controlled in the central nervous system (Peron et al., 2009). The targeted expression of the dominant negative in the postsynaptic muscles (*24B/IhDN*) did not however display any locomotor defects, despite the morphological phenotype.

In addition to the effects on the displacement parameters, the *DmIh*$^{-}$ and presynaptic mutant also had an aberrant body movement, in the form of altered peristaltic waves. Both mutants had an increased peristaltic contraction frequency, while only the general mutant (*DmIh*$^{-}$) had a concomitant reduction of the stride length, which often occurs in ion channel mutants (Wang et al., 2002). These results are particularly interesting given the role of I_h in the maintenance of rhythmic activity.

In conjunction with these results, we performed an electrophysiological study of the effects of the general, presynaptic and postsynaptic silencing of the I_h current in *Drosophila* larvae. To control for developmental effects, we also used the I_h specific pharmacological blocker ZD7288 to test the immediate effect of blocking the I_h current on the synaptic transmission at the larval neuromuscular junction.

This study has been done in collaboration with members of the laboratory of Dr. Inmaculada Canal (Universidad Autónoma de Madrid), in particular with Alicia Gonzalo Gómez who generated the mutants and performed the morphological study, and JM Barcia who performed and analyzed the locomotor assays.

5.2.2 Results & Discussion

Spontaneous and Evoked Junction Potentials

To test the physiological effects of genetically removing the I_h current from either the whole animal, only presynaptically in motoneurons or only postsynaptically in the muscles, we performed intracellular recordings from muscles 6 & 7 in segments A3 and A4 of wandering third instar *Drosophila melanogaster* larvae. To study the spontaneous neurotransmitter we severed the innervating nerve and recorded the miniature end-plate potentials (mEPPs) caused by presynaptic spontaneous release of vesicles. The mEPP amplitude distributions were significantly shifted towards higher values in *DmIh*$^{-}$ and *D42/IhDN* (general expression and presynaptically), with a mean increase of 28% and 34% respectively (p_{DmIh}=0.003 and p_{D42}=0.001), while no significant change was observed postsynaptically in *24B/IhDN* (p=0.41), Figure 5.1. No statistically significant changes in frequencies of mEPPs were found (p_{DmIh}=0.086, p_{D42}=0.94, p_{24B}=0.97). The resting potential of the muscle membranes were also not statistically different between genotypes (p_{DmIh}=0.086, p_{D42}=0.94, p_{24B}=0.97).

Evoked junction potentials (EJPs) were measured by stimulating the severed nerve at a 0.5 Hz frequency. No significant differences between genotypes were

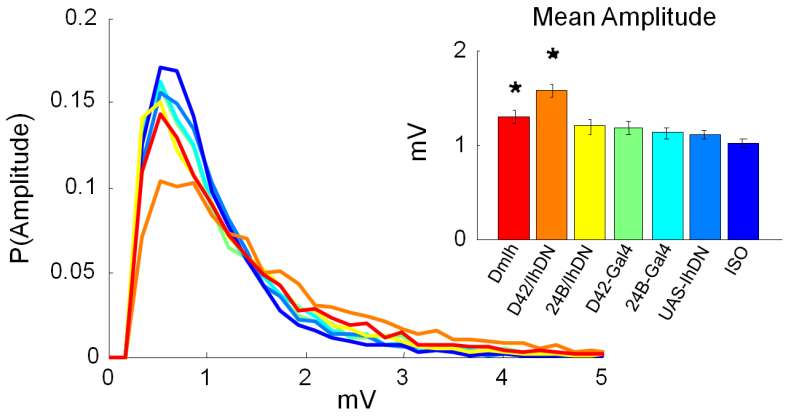

Figure 5.1: Miniature Spontaneous Neurotransmitter Release. Main Panel: Distribution of mEPP amplitudes for the general *DmIh* null mutant (red), presynaptic (orange) and postsynaptic (yellow) mutants, and their controls. The distribution of amplitudes is shifted towards larger values in the presynaptic and general mutants. Inset: Comparing the mean mEPP amplitudes reveals that the general and presynaptic lack of I_h leads to statistically significantly larger miniature potentials, as compared to their respective controls. Error bars indicate s.e.m. while asterisk p<0.05.

observed in muscle resting potential (p_{DmIh}=0.29, p_{D42}=0.83, p_{24B}=0.48) and the average resting potential was -70 mV across genotypes. No significant differences were found among the EJP amplitudes (p_{DmIh}=0.65, p_{D42}=0.11, p_{24B}=0.57), with a mean amplitude across genotypes of 49 mV. Considering that there were differences in the mEPP amplitudes, but not in the EJP amplitudes, we next calculated the quantal content (the number of effective vesicles released in response to a nerve impulse) as the mean EJP amplitude divided by the mean mEPP amplitude, which was found to be 13% lower in *DmIh*$^-$ (p=0.03) and 26% lower in *D42/IhDN* (p=0.0002) compared to controls, while *24B/IhDN* had no apparent difference (-1.2%, p=0.91), Figure 5.2 A. This means that *DmIh*$^-$ and *D42/IhDN* release fewer vesicles but with more neurotransmitter content than the controls in order to produce comparable EJPs.

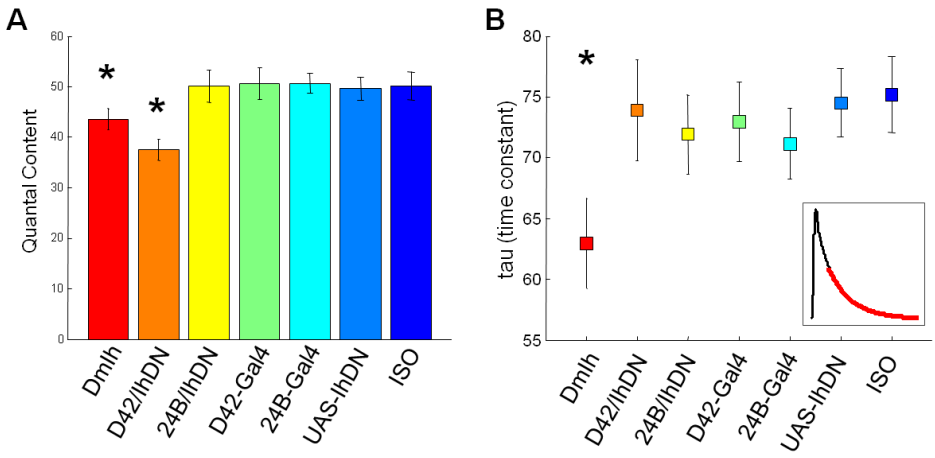

Figure 5.2: Characteristics of the Evoked Junction Potentials. (A) Quantal content, defined as the mean EJP amplitude divided by the mean mEPP amplitude, measures the number of effective vesicles released in response to a nerve impulse. **(B)** The time constant τ of an exponential fit to the decay shape of the EJPs. A lower time constant indicates that the EJPs decay faster. Error bars indicate s.e.m. while asterisk $p<0.05$.

The latencies between stimuli and EJP responses were found to be similar in all genotypes, while the shape, quantified by the time constant of an exponential fit to the tail of the EJP (Figure 5.2 B:Inset), was found to be reduced by 16.2% in $DmIh^{-}$ ($p=0.045$), i.e., the EJPs decayed slightly faster, Figure 5.2 B.

Adaptation Effect of the EJP Responses

The presence of a 'hysteresis' effect of the NMJ response was assayed by a stairs protocol which, in essence, stepwise incremented the stimuli for each repetition (15 traces at 0.5 Hz, with 2 s pause in between) until reaching a maximum EJP response and then symmetrically decreased it. The facilitation (or depression) was then calculated as the difference between the EJP responses to the stimuli during the decrease and increase phases. $DmIh^{-}$ showed depression, i.e., a

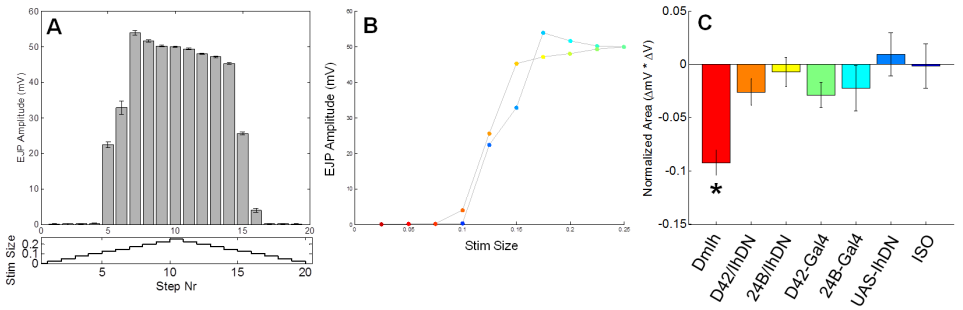

Figure 5.3: Adaptation Effect to a Variable Stimulus. A 'hysteresis' protocol was employed to assess the level of adaptation depending on previous stimuli. **(A)** Lower panel: The stimulus size was step-wise incremented until reaching a maximum, and then decreased symmetrically. Main panel: Example EJP amplitude response to the stimulus steps. **(B)** The same example EJP responses plotted as EJP amplitude vs. stimulus size. The color indicates the stim. sequence, starting at blue and ending at red. **(C)** The normalized area between the ascending and descending curves in (B) quantifies the degree of adaptation. Error bars indicate s.e.m. while asterisk $p<0.05$.

loss of responsiveness to stimuli depending on the previous stimulus strength history ($p<0.001$ with respect to zero, $p<0.001$ with respect to control), while *D42/IhDN* and *24B/IhDN* showed no adaptation ($p_{D42}=0.12$, $p_{24B}=0.72$ with respect to zero), Figure 5.3.

Taken together, thus, these results indicate a presynaptic effect of disrupting the I_h current, as *D42/IhDN* has increased mEPP amplitude and lower quantal content, *DmIh*$^-$ has increased mEPP amplitude, lower quantal content and shows adaptation, while physiologically the *24B/IhDN* mutant is indistinguishable from its corresponding controls.

Pharmacological I_h Channel Blocker

To further probe the physiological effect of the I_h channel in *Drosophila* , we used the I_h channel blocker ZD7288 to help distinguish between possible

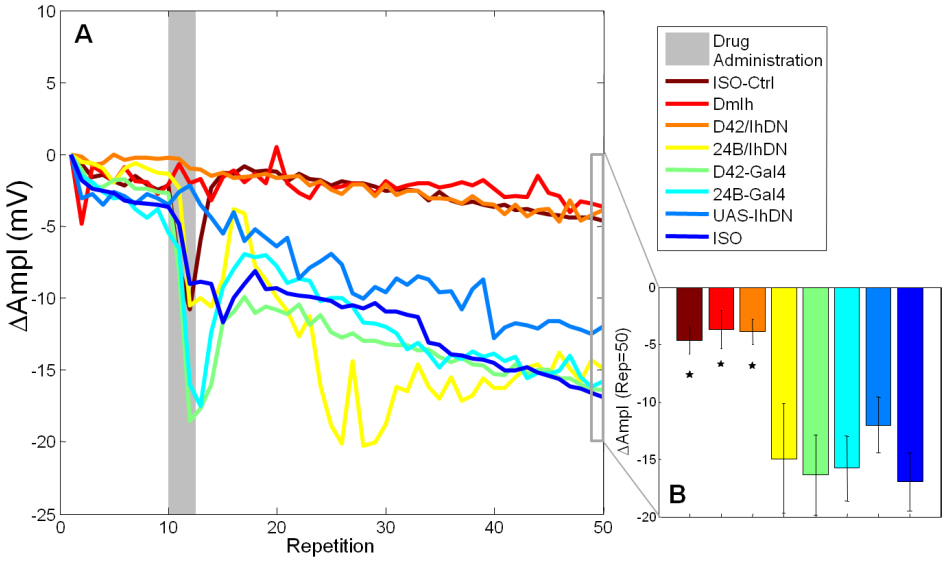

Figure 5.4: Effect of Pharmacological I_h Blocker. Pharmacologically blocking the I_h channel reveals a presynaptic function for the I_h current. **(A)** The mean EJP amplitude was measured over 50 sets of repetitions (each set 10 stimulations at 0.5 Hz), with the I_h blocker added after the 10th repetition (gray area). **(B)** The effect of the pharmacological blocking of the I_h channel was assessed at the 50th repetition, revealing a significant decrease of the EJP amplitude in the genotypes with a pre-experimental functioning presynaptic I_h current. Error bars indicate s.e.m. while asterisk $p<0.05$.

developmental compensatory effects of a continuous lack of I_h current and the direct functional effect of blocking the I_h channel. ZD7288 has been used previously in mammal preparations (Neuhoff et al., 2002; Puopolo et al., 2007; George et al., 2009), but never before in *Drosophila*.

Briefly, the protocol consisted of 50 repetitions of 10 traces at 0.5 Hz stimulation, with 2 s pause between each repetition. 110% of the lowest voltage shock that produced full EJP amplitude responses was used as the stimulus. The first 10 repetitions served as baseline recordings, with the ZD7288-saline

mixture slowly added to the bath starting at the 11th repetition. An additional set of experiments were also performed on ISO larvae to control for the method, where only the vehicle (saline with no drug) was added instead, henceforth referred to as 'ISO-Ctrl'. ISO-Ctrl showed a slight decrease of the EJP amplitudes over the course of the stimulations, while ISO showed a significantly larger decrease of the EJP amplitudes when applying ZD7288, compared to ISO-Ctrl ($p<0.001$), Figure 5.4. When the drug was applied to *DmIh*$^{-}$ it had no measurable effect, seen as a non-significant difference with ISO-Ctrl, concurrently with a large significant difference with ISO ($p<0.001$), showing that ZD7288 is a specific blocker of the I_h current also in *Drosophila*. Similarly, *D42/IhDN* did not significantly differ in comparison to the ISO-Ctrl ($p=0.71$), while its controls *UAS-IhDN* and *D42-Gal4* both had significantly smaller EJPs ($p<0.01$). Lastly, *24B/IhDN* EJPs were not significantly different than its controls ($p=0.89$), which in turn were all significantly smaller than ISO-Ctrl ($p<0.021$). We thus further conclude that the effect of the I_h blocker on the EJP amplitudes must be presynaptic, since the I_h blocker caused no effect in *D42/IhDN*, which has the *IhDN* expressed in the motoneurons, while causing a differential effect in *24B/IhDN*, with the directed disruption of I_h channels in the muscles. The decreased amplitudes of the EJP responses point towards a decreased excitability of the motoneurons when functioning without the I_h current.

5.2.3 Conclusions

We studied the functional role of the null mutation of the I_h current in the *Drosophila* larval neuromuscular junction, motivated by an observed locomotor and decision-making phenotype coupled with a morphological phenotype in these larvae.

First we studied the spontaneous release of neurotransmitter vesicles in the neuromuscular junction, and found that the generally I_h-lacking (*DmIh*$^{-}$) and the presynaptically I_h-lacking (*D42/IhDN*) genotypes had larger miniature endplate potentials (mEPPs) than their control strains, while the postsynaptically I_h-lacking (*24B/IhDN*) genotype were indistinguishable from the controls. This

translated to an identical presynaptic effect on the quantal content, i.e. the number of effective vesicles released in response to stimulus, since there were no significant different of the evoked junction potentials (EJPs) among the groups. The only noticeable difference of the EJPs was a faster decay rate in the generally expressed *DmIh*$^{-}$.

We next assayed the dynamical properties of the adaptation response to a variable stimulus sequence, by applying a symmetric stimulus 'stair' protocol. This allowed us to measure the 'hysteresis' effect as the difference in response to a stimulus depending on the intensity history of the stimuli. We found that the general *DmIh*$^{-}$ null mutant exhibited a desensitization, or fatigue syndrome, as compared to the control, with less ample EJPs in response to the same stimuli but after having recently received stronger stimuli. The other selectively expressed pre- and postsynaptic *IhDN* did not exhibit a similar effect.

Lastly, we examined the role of developmental adaptation to the lack of I_h current, by applying a pharmacological I_h-channel blocker. Since the electrical properties of the larval neuromuscular junction during development are established dynamically, channel defects or other irregularities can be corrected and compensated for during development (Collins and DiAntonio, 2007). Using a pharmacological agent to externally block the channel function therefore reveals the immediate effect of missing the I_h current. We found that the EJP amplitudes gradually decreased over the course of repeated stimulation in all the genotypes that had a functioning I_h channel prior to applying the blocker, while the blocker had no effect on the genotypes with an already genetically non-functioning I_h channel.

We thus conclude that the locomotive phenotype is due to a defective presynaptic neuronal function, and not due to reduced excitability of the muscles. The lack of I_h current causes a reduced excitability to prolonged and varied stimuli, causing a fatigue syndrome, responsible for the slower crawl velocities and the shorter overall distances covered by the larvae.

5.2.4 Material and Methods

Dissection

The neuromuscular electrophysiological experiments were performed on third instar wandering larvae using the standard "open-book" preparation (Broadie, 2000). Briefly, the larvae were pinned down on a sylgard coated petridish, were covered in ice cold extracellular saline and a longitudinal mid-dorsal incision was made, permitting the edges to be pinned down, spreading out the surface and exposing the body wall musculature. Internal organs including the CNS were carefully removed with fine dissection scissors, with particular care given to cleanly cutting the segmental nerves of segments A3–A4. The saline HL3 was used as extracellular saline (Broadie, 2000), consisting of (in mM): 70 NaCl, 5 KCl, 1.5 $CaCl_2$, 20 $MgCl_2$, 10 $NaHCO_3$, 5 Trehalose, 115 Sucrose, 5 HEPES, adjusted to a pH of 7.2.

Electrophysiology

Intracellular recordings were performed on muscles 6 or 7 from segments A3–A4 with microelectrodes containing 3 M KCl electrolyte and with tip resistances $\leq$50 MΩ (mean: 31.8 MΩ) in a room with a controlled temperature of 18–20° C. The custom-built BioSyst software (Juusola and de Polavieja, 2003) (National Instruments board interface MATDAQ, (c) HPC Robinson, 1997–99) was used to perform all experiments. Only recordings with a resting potential -60 mV were used.

Spontaneous neurotransmitter release events (mEPPs) were passively recorded for 1 minute at 10 kHz, after a low-pass filtering at 0.3 kHz (LPBF-01G, npi instruments). The raw recordings were then passed through a simple smoothing function with a window of 22.5 ms and subsequently down-sampled by 1/10. mEPPs were identified as all those peaks above 0.3 mV (minimum amplitude threshold) that had a fast rise time (so as to exclude mEPPs from neighboring muscles). The mEPP minimum amplitude threshold was determined by analyzing the noise histograms of proximal extracellular recordings. The

number of recordings was as follows (with number of different larvae in parenthesis): 25 (15) *DmIh*, 23 (14) *D42/IhDN*, 23 (14) *24B/IhDN*, 28 (16) *D42-Gal4*, 30 (16) *24B-Gal4*, 28 (17) *UAS-IhDN*, 23 (10) ISO. When possible, recordings were performed on both the left and right side of each larva.

For the evoked responses, suction pipettes with diameters of 5–10 μm were used to stimulate the severed nerve ends (ISO-STIM 01M, npi instruments). EJPs were acquired at 0.1 kHz using a dynamic protocol of variable steps of stimulation intensities, where each step consisted of 15 identical nerve stimulations at a 0.5 Hz frequency, with 2 seconds pause between each step. The stimulation intensity was increased step-wise until at least one EJP amplitude $\geq$ 40 mV (or after a maximum number of attempts once the muscle started responding), stepped up 3 more steps for a reliable response of both the Ib and Is motoneurons and then stepped down with the same stimuli intensities used for the ascent. During the posterior analysis the mean amplitude of each set was calculated for all EJPs $\geq$ 30 mV where the response was confirmed to be of Ib+Is type (both the Is and Ib identified separately). The total number of recordings was as follows (with number of different larvae in parenthesis): 30 (15) *DmIh*, 30 (15) *D42/IhDN*, 29 (15) *24B/IhDN*, 35 (16) *D42-Gal4*, 34 (16) *24B-Gal4*, 30 (17) *UAS-IhDN*, 23 (10) ISO.

For the I_h channel blocker experiments, 100 μM ZD7288 mixed with 1 ml HL3 saline was administered through a Pasteur pipette by slowly and steadily injecting the mixture into the extracellular saline, close ($\sim$1 cm) to the recording site. A similar step-up protocol as described above for finding the adequate stimulation intensity was used, but with 50 sets of 10 traces at 0.5 Hz and 2 seconds pause between. The drug (or control saline) was administered right after the 10th stimulation set, leaving the first 10 sets as control reference and the remaining 40 sets for assessing the drug effect. During the posterior analysis the mean amplitude for each set was calculated over all the traces of the set. The number of recordings was as follows: 6 ISO-Ctrl, 6 *DmIh*, 8 *D42/IhDN*, 5 *24B/IhDN*, 6 *D42-Gal4*, 7 *24B-Gal4*, 4 *UAS-IhDN*, 24 ISO. Since drug (or saline) was administered during the recordings only one recording per larva was possible.

Statistical Analysis

All values are presented as mean $\pm$ s.e.m. (standard error of the mean). The statistical significance level α was set to 0.05 and a significant difference is denoted with an asterisk (*). The two-tailed Student's t-test was used throughout with the Bonferroni correction for multiple comparisons. If both samples passed the Lillie test of normality the standard two sample t-test was used, otherwise the t-statistic was bootstrapped with a resampling of 10,000. All the electrophysiological data analysis was performed in MATLAB R2009a (The MathWorks Inc., Natick, MA).

Conclusions

- The *Drosophila melanogaster* walking activity dynamics are bursty with heavy-tailed distributions. Both the initiation of activity (inter-activity intervals) and the maintenance of activity (activity bout durations) have bursty dynamics. The activity dynamics are almost memoryless.

- The *Drosophila* inter-activity interval distribution is well described by the stretched exponential function (Weibull distribution). The fitting method was shown to be accurate by validating with artificial data.

- The bursty dynamics in *Drosophila* is affected in mutants with an impaired decision-making process. Enhanced levels of dopamine affect burstiness the strongest, making behavior more random. The Mushroom Bodies also affect behavioral burstiness, while the Central Complex did not.

$\sim$

- Human sleep-wake structure is affected by age, with a decreased wake fragmentation and longer nightly awakenings, leading to a shorter overall sleep. The sleep bout distributions show bursty (and not random) dynamics, with stretched exponential and power law fits. The wake bout distributions show even burstier dynamics, with overall power law fits.

- Zebrafish sleep-wake structure is affected by age, decreasing the wake fragmentation and the number of sleep-wake transitions per night, while increasing the wake durations and the total time awake. The sleep bout distributions show bursty dynamics with stretched exponential and power law fits, while the wake bout distributions show even burstier dynamics, with power law fits to all age groups.

- The ontogeny of the zebrafish sleep-wake cycle show a very high degree of similarity to that of humans, suggesting a conserved mechanism of sleep-wake regulation and further validating the zebrafish as a valuable 'simple' model organism for the study of sleep.

$\sim$

- The locomotive phenotype of *DmIh* is due to a defective presynaptic neuronal function, and not to reduced excitability of the muscles. The lack of I_h current leads to a decreased neuronal excitability of the motoneuron, especially visible when applying a pharmacological blocker of the I_h channel.

Conclusiones

- La dinámica de actividad de *Drosophila melanogaster* cuando camina es rafagosa con una distribución de cola pesada. Tanto la iniciación de actividad (los intervalos de interactividad) y el mantenimiento de actividad (las duraciones de actividad) tienen una dinámica rafagosa. La dinámica de actividad no tiene casi memoria.

- La distribución de intervalos de interactividad en *Drosophila* se describe bien por la distribución de exponencial estirada (la distribución de Weibull). El método de ajuste fue validado con datos artificiales y mostrado ser correcto.

- La dinámica rafagosa de *Drosophila* se ve afectada en mutantes con el proceso de toma de decisiones silenciada. Niveles aumentados de dopamina afecta a la rafagosidad, haciendo el comportamiento más aleatorio. El cuerpo de setas también afecta a la rafagosidad, mientras el complejo central no lo afectó.

$\sim$

- La estructura de sueño-vigilia es afectada por la edad en humanos, con un decrecimiento de la fragmentación y un alargamiento de las duraciones de vigilia, dando lugar a menos sueño durante la noche. La distribución de episodios de sueño tiene una dinámica rafagosa (y no aleatoria), ajustada por la exponencial estirada y ley de potencias. La distribución de episodios de vigilia es aún más rafagosa, ajustada por ley de potencias.

- La estructura de sueño y vigilia se ve afectado por la edad en el pez cebra, con una disminución de la fragmentación de vigilia y del número de transiciones de sueño vigilia nocturno, mientras las duraciones y el tiempo total de vigilia aumentan. La distribución de episodios de sueño muestra dinámica rafagosa con ajustes de exponencial estirada y ley de potencias, mientras la distribución de episodios de vigilia es más rafagosa aún, viniendo ajustada por ley de potencias para todas las edades.

- La ontogenia de los ciclos de sueño-vigilia en el pez cebra muestra un alto grado de similitud con la de humanos, sugiriendo un mecanismo conservado de regulación de sueño-vigilia, por tanto validando el pez cebra como valioso animal modelo 'simple' para el estudio del sueño.

$\sim$

- El fenotipo de locomoción de *DmIh* se debe a una función neuronal defectuosa presináptica, y no a una excitabilidad reducida del músculo. La falta de corriente I_h da lugar a una disminuición de la excitabilidad de la motoneurona, especialmente visible cuando se bloquea farmacológicamente el canal I_h .

Bibliography

Acevedo S.F., Froudarakis E.I., Kanellopoulos A. and Skoulakis E.M.C. (2007) *Protection from premature habituation requires functional mushroom bodies in Drosophila.* Learning & memory (Cold Spring Harbor, N.Y.) 14(5):376–84. doi: 10.1101/lm.566007.

Adams M.D., Celniker S.E., Holt R.A. et al (2000) *The genome sequence of Drosophila melanogaster.* Science (New York, N.Y.) 287(5461):2185–2195. doi: 10.1126/science.287.5461.2185.

Allen M.J., Godenschwege T.A., Tanouye M.A. and Phelan P. (2006) *Making an escape: development and function of the Drosophila giant fibre system.* Seminars in cell & developmental biology 17(1):31–41. doi: 10.1016/j.semcdb.2005.11.011.

Alstott J., Bullmore E. and Plenz D. (2014) *Powerlaw: a Python package for analysis of heavy-tailed distributions.* PloS one 9(1):e85777. doi: 10.1371/journal.pone.0085777.

Altomare C., Terragni B., Brioschi C., Milanesi R., Pagliuca C., Viscomi C., Moroni A., Baruscotti M. and DiFrancesco D. (2003) *Heteromeric HCN1-HCN4 channels: a comparison with native pacemaker channels from the rabbit sinoatrial node.* The Journal of physiology 549(Pt 2):347–59. doi: 10.1113/jphysiol.2002.027698.

Arencibia-Albite F., Paladini C., Williams J.T. and Jiménez-Rivera C.A. (2007) *Noradrenergic modulation of the hyperpolarization-activated cation current (Ih) in dopamine neurons of the ventral tegmental area*. Neuroscience 149(2):303–314. doi: 10.1016/j.neuroscience.2007.08.009.

Arnardóttir H., Thorsteinsson H. and Karlsson K.Æ. (2010) *Dynamics of sleep-wake cyclicity at night across the human lifespan.* Frontiers in neurology 1:156. doi: 10.3389/fneur.2010.00156.

Arnsten A.F.T. (2007) *Catecholamine and Second Messenger Influences on Prefrontal Cortical Networks of "Representational Knowledge": A Rational Bridge between Genetics*

and the Symptoms of Mental Illness. Cerebral Cortex 17(suppl 1):i6–i15. doi: 10.1093/cercor/bhm033.

Aso Y., Grübel K., Busch S., Friedrich A.B., Siwanowicz I. and Tanimoto H. (2009) *The mushroom body of adult Drosophila characterized by GAL4 drivers.* Journal of neurogenetics 23(1):156–172. doi: 10.1080/01677060802471718.

Atkinson R.P.D., Rhodes C.J., Macdonald D.W. and Anderson R.M. (2002) *Scale-free dynamics in the movement patterns of jackals*. Oikos 98(1):134–140. doi: 10.1034/j.1600-0706.2002.980114.x.

Austin D., Bowen W. and McMillan J. (2004) *Intraspecific variation in movement patterns: modeling individual behaviour in a large marine predator*. Oikos 105(1):15–30. doi: 10.1111/j.0030-1299.1999.12730.x.

Baker K., Warren K.S., Yellen G. and Fishman M.C. (1997) *Defective "pacemaker" current (Ih) in a zebrafish mutant with a slow heart rate.* Proceedings of the National Academy of Sciences of the United States of America 94(9):4554–9.

Barabási A.L. (2005) *The origin of bursts and heavy tails in human dynamics*. Nature 435(7039):207–211. doi: 10.1038/nature03459.

Bazazi S., Bartumeus F., Hale J.J. and Couzin I.D. (2012) *Intermittent motion in desert locusts: behavioural complexity in simple environments.* PLoS computational biology 8(5):e1002498. doi: 10.1371/journal.pcbi.1002498.

Behnia R. and Desplan C. (2015) *Visual circuits in flies: beginning to see the whole picture*. Current Opinion in Neurobiology 34:125–132. doi: 10.1016/j.conb.2015.03.010.

Bellen H.J., Tong C. and Tsuda H. (2010) *100 years of Drosophila research and its impact on vertebrate neuroscience: a history lesson for the future*. Nature Reviews Neuroscience 11(7):514–522. doi: 10.1038/nrn2839.

Benhamou S. (2007) *How many animals really do the Lévy walk?* Ecology 88(8):1962–1969. doi: 10.1890/06-1769.1.

Bénichou O., Loverdo C., Moreau M. and Voituriez R. (2006) *Two-dimensional intermittent search processes: An alternative to Lévy flight strategies*. Physical Review E 74(2):020102. doi: 10.1103/PhysRevE.74.020102.

Bianchi M.T., Cash S.S., Mietus J., Peng C.K. and Thomas R. (2010) *Obstructive sleep apnea alters sleep stage transition dynamics.* PLoS ONE 5(6):e11356. doi: 10.1371/journal.pone.0011356.

Bloomington Drosophila Stock Center (a) *Drosophila Media Recipes and Meth-*

ods. Retrieved from URL `http://flystocks.bio.indiana.edu/Fly{_}Work/media-recipes/media-recipes.htm` on 2015-08-04.

Bloomington Drosophila Stock Center (b) *A Brief History of the Collection*. Retrieved from URL `http://flystocks.bio.indiana.edu/Inst/history.htm` on 2015-08-04.

Bloomington Drosophila Stock Center, Web () *http://flystocks.bio.indiana.edu*. Retrieved on 2015-08-04.

Blumberg M.S., Seelke A.M.H., Lowen S.B. and Karlsson K.a.E. (2005) *Dynamics of sleep-wake cyclicity in developing rats.* Proceedings of the National Academy of Sciences of the United States of America 102(41):14860–4. doi: 10.1073/pnas.0506340102.

Blumberg M.S., Coleman C.M., Johnson E.D. and Shaw C. (2007) *Developmental divergence of sleep-wake patterns in orexin knockout and wild-type mice.* The European journal of neuroscience 25(2):512–518. doi: 10.1111/j.1460-9568.2006.05292.x.

Bonini N.M. (2008) *A tribute to Seymour Benzer, 1921–2007.* Genetics 180(3):1265–73. doi: 10.1534/genetics.104.97782.

Bonnet M.H. and Arand D.L. (2003) *Clinical effects of sleep fragmentation versus sleep deprivation.* Sleep medicine reviews 7(4):297–310.

Borbély A.A. and Achermann P. (1999) *Sleep homeostasis and models of sleep regulation.* Journal of biological rhythms 14(6):557–68.

Borst A. and Egelhaaf M. (1989) *Principles of visual motion detection.* Trends in neurosciences 12(8):297–306. doi: 10.1016/0166-2236(89)90010-6.

Bovet P. and Benhamou S. (1988) *Spatial analysis of animals' movements using a correlated random walk model*. Journal of Theoretical Biology 131(4):419–433. doi: 10.1016/S0022-5193(88)80038-9.

Brambilla D., Chapman D. and Greene R. (2005) *Adenosine mediation of presynaptic feedback inhibition of glutamate release.* Neuron 46(2):275–83. doi: 10.1016/j.neuron.2005.03.016.

Brand A.H. and Perrimon N. (1993) *Targeted gene expression as a means of altering cell fates and generating dominant phenotypes.* Development 118(2):401–15. doi: 10.1101/lm.1331809.

Breed G.A., Severns P.M. and Edwards A.M. (2014) *Apparent power-law distributions in animal movements can arise from intraspecific interactions*. Journal of The Royal Society Interface 12(103):20140927–20140927. doi: 10.1098/rsif.2014.0927.

Brembs B. (2008) *Operant learning of Drosophila at the torque meter.* Journal of visualized experiments : JoVE (16). doi: 10.3791/731.

Brembs B. (2009) *Mushroom Bodies Regulate Habit Formation in Drosophila*. Current Biology 19(16):1351–1355. doi: 10.1016/j.cub.2009.06.014.

Brembs B. (2013) *Invertebrate behavior-actions or responses?* Frontiers in neuroscience 7:221. doi: 10.3389/fnins.2013.00221.

Broadbent S.R. and Kendall D.G. (1953) *The random walk of Trichostrongylus retortaeformis*. Biometrics 9(4):460–466.

Broadie K.S. (2000) *Electrophysiological approaches to the neuromusculature*. In Sullivan W., Ashburner M. and Hawley R.S., editors, *Drosophila Protocols* pages 273–295. Cold Spring Harbor Laboratory Press.

Brown H.F., DiFrancesco D. and Noble S.J. (1979) *How does adrenaline accelerate the heart?* Nature 280(5719):235–236. doi: 10.1038/280235a0.

Brown R.E., Basheer R., McKenna J.T., Strecker R.E. and McCarley R.W. (2012) *Control of Sleep and Wakefulness*. Physiological Reviews 92(3):1087–1187. doi: 10.1152/physrev.00032.2011.

Campbell S. and Tobler I. (1984) *Animal sleep: a review of sleep duration across phylogeny*. Neurosci. Biobehav. Rev. 8:269–300.

Cappuccio F.P., D'Elia L., Strazzullo P. and Miller M.A. (2010) *Sleep duration and all-cause mortality: a systematic review and meta-analysis of prospective studies.* Sleep 33(5):585–92.

Cappuccio F.P., Cooper D., D'Elia L., Strazzullo P. and Miller M.A. (2011) *Sleep duration predicts cardiovascular outcomes: a systematic review and meta-analysis of prospective studies.* European heart journal 32(12):1484–92. doi: 10.1093/eurheartj/ehr007.

Cathala L. and Paupardin-Tritsch D. (1997) *Neurotensin inhibition of the hyperpolarization-activated cation current (Ih) in the rat substantia nigra pars compacta implicates the protein kinase C pathway.* The Journal of physiology 503 (Pt 1: 87–97.

Chan C.S., Glajch K.E., Gertler T.S. et al (2011) *HCN channelopathy in external globus pallidus neurons in models of Parkinson's disease*. Nature Neuroscience 14(1):85–92. doi: 10.1038/nn.2692.

Chervin R.D., Fetterolf J.L., Ruzicka D.L., Thelen B.J. and Burns J.W. (2009) *Sleep stage dynamics differ between children with and without obstructive sleep apnea.* Sleep 32

(10):1325–1332.

Chippindale A., Archer M., Gass E., Rose M. and Mueller L. (1999) *Laboratory manual of Drosophila*.

Chiu C.N. and Prober D.A. (2013) *Regulation of zebrafish sleep and arousal states: current and prospective approaches.* Frontiers in neural circuits 7:58. doi: 10.3389/fncir.2013.00058.

Chu-Shore J., Westover M.B. and Bianchi M.T. (2010) *Power law versus exponential state transition dynamics: Application to sleep-wake architecture*. PLoS ONE 5(12): e14204. doi: 10.1371/journal.pone.0014204.

Cirelli C. and Bushey D. (2008) *Sleep and wakefulness in Drosophila melanogaster*. Annals of the New York Academy of Sciences 1129(608):323–329. doi: 10.1196/annals.1417.017.

Claridge-Chang A., Roorda R.D., Vrontou E., Sjulson L., Li H., Hirsh J. and Miesenböck G. (2009) *Writing Memories with Light-Addressable Reinforcement Circuitry*. Cell 139 (2):405–415. doi: 10.1016/j.cell.2009.08.034.

Clauset A., Shalizi C.R. and Newman M.E.J. (2009) *Power-Law Distributions in Empirical Data*. SIAM Review 51(4):661. doi: 10.1137/070710111.

Clayton J.D., Kyriacou C.P. and Reppert S.M. (2001) *Keeping time with the human genome*. Nature 409(6822):829–831. doi: 10.1038/35057006.

Codling E.A. and Plank M.J. (2011) *Turn designation, sampling rate and the misidentification of power laws in movement path data using maximum likelihood estimates*. Theoretical Ecology 4(3):397–406. doi: 10.1007/s12080-010-0086-9.

Codling E.A., Plank M.J. and Benhamou S. (2008) *Random walk models in biology.* Journal of the Royal Society 5(25):813–834. doi: 10.1098/rsif.2008.0014.

Cole B. (1995) *Fractal time in animal behaviour: the movement activity of Drosophila*. Animal Behaviour 50(5):1317–1324. doi: 10.1016/0003-3472(95)80047-6.

Collett T.S. and Land M.F. (1975) *Visual control of flight behaviour in the hoverfly, Syritta pipiens*. L. J. comp. Physiol. 99:1–66.

Collins C. and DiAntonio A. (2007) *Synaptic development: insights from Drosophila*. Current Opinion in Neurobiology 17(1):35–42. doi: 10.1016/j.conb.2007.01.001.

Connolly J.B., Roberts I.J.H., Armstrong J.D., Kaiser K., Forte M., Tully T. and O'Kane C.J. (1996) *Associative learning disrupted by impaired Gssignaling in Drosophila*

mushroom bodies. Science 274(5295):2104–2107.

Coughlin D.J., Strickler J.R. and Sanderson B. (1992) *Swimming and search behaviour in clownfish, Amphiprion perideraion, larvae*. Animal Behaviour 44(3):427–440. doi: 10.1016/0003-3472(92)90053-C.

Crittenden J.R., Skoulakis E.M.C., Han K.A., Kalderon D. and Davis R.L. (1998) *Tripartite mushroom body architecture revealed by antigenic markers*. Learning & memory (Cold Spring Harbor, N.Y.) 5(1):38. doi: 10.1101/lm.5.1.38.

Crosby M.A., Goodman J.L., Strelets V.B., Zhang P. and Gelbart W.M. (2007) *FlyBase: genomes by the dozen*. Nucleic acids research 35(Database issue):D486–91. doi: 10.1093/nar/gkl827.

Davis H., Davis P.A., Loomis A.L., Harvey E.N. and Hobart G. (1937) *Changes in human brain potentials during the onset of sleep*. Science 86(2237):448–450.

DiFrancesco D. and Tortora P. (1991) *Direct activation of cardiac pacemaker channels by intracellular cyclic AMP.* Nature 351(6322):145–7. doi: 10.1038/351145a0.

Djonlagic I., Saboisky J., Carusona A., Stickgold R. and Malhotra A. (2012) *Increased sleep fragmentation leads to impaired off-line consolidation of motor memories in humans.* PloS one 7(3):e34106. doi: 10.1371/journal.pone.0034106.

Donlea J.M., Pimentel D. and Miesenböck G. (2014) *Neuronal machinery of sleep homeostasis in Drosophila.* Neuron 81(4):860–72. doi: 10.1016/j.neuron.2013.12.013.

Dudley R. (2000) *The Biomechanics of Insect Flight: Form, Function, Evolution*. Princeton University Press reprinted edition. ISBN 978-0691094915.

Duffy J.B. (2002) *GAL4 system in Drosophila: A fly geneticist's swiss army knife*. genesis 34(1-2):1–15. doi: 10.1002/gene.10150.

Dworak M., McCarley R.W., Kim T., Kalinchuk A.V. and Basheer R. (2010) *Sleep and brain energy levels: ATP changes during sleep.* The Journal of neuroscience : the official journal of the Society for Neuroscience 30(26):9007–16. doi: 10.1523/1423-10.2010.

Edwards A.M. (2011) *Overturning conclusions of Lévy flight movement patterns by fishing boats and foraging animals*. Ecology 92(6):1247–1257. doi: 10.1890/10-1182.1.

Edwards A.M., Phillips R.A., Watkins N.W. et al (2007) *Revisiting Lévy flight search patterns of wandering albatrosses, bumblebees and deer.* Nature 449(7165):1044–8. doi: 10.1038/nature06199.

Edwards A.M., Freeman M.P., Breed G.A. and Jonsen I.D. (2012) *Incorrect likelihood methods were used to infer scaling laws of marine predator search behaviour.* PloS one 7(10):e45174. doi: 10.1371/journal.pone.0045174.

Fenchel T. (2004) *Orientation in two dimensions: chemosensory motile behaviour of Euplotes vannus*. European Journal of Protistology 40(1):49–55. doi: 10.1016/j.ejop.2003.09.001.

Floyd J.A., Medler S.M., Ager J.W. and Janisse J.J. (2000) *Age-related changes in initiation and maintenance of sleep: a meta-analysis.* Research in nursing & health 23 (2):106–17.

Friggi-Grelin F., Coulom H., Meller M., Gomez D., Hirsh J. and Birman S. (2003) *Targeted gene expression in Drosophila dopaminergic cells using regulatory sequences from tyrosine hydroxylase*. Journal of neurobiology 54(4):618–27. doi: 10.1002/neu.10185.

Fuller P.M., Gooley J.J. and Saper C.B. (2006) *Neurobiology of the Sleep-Wake Cycle: Sleep Architecture, Circadian Regulation, and Regulatory Feedback*. Journal of Biological Rhythms 21(6):482–493. doi: 10.1177/0748730406294627.

Gall A.J., Joshi B., Best J., Florang V.R., Doorn J.A. and Blumberg M.S. (2009) *Developmental emergence of power-law wake behavior depends upon the functional integrity of the locus coeruleus.* Sleep 32(7):920–6.

Ganguly-Fitzgerald I., Donlea J. and Shaw P.J. (2006) *Waking experience affects sleep need in Drosophila.* Science (New York, N.Y.) 313(5794):1775–81. doi: 10.1126/science.1130408.

Gautestad A.O. (2013) *Animal space use: distinguishing a two-level superposition of scale-specific walks from scale-free Lévy walk*. Oikos 122(4):612–620. doi: 10.1111/j.1600-0706.2012.19998.x.

George M.S., Abbott L.F. and Siegelbaum S. (2009) *HCN hyperpolarization-activated cation channels inhibit EPSPs by interactions with M-type K(+) channels.* Nature neuroscience 12(5):577–584. doi: 10.1038/nn.2307.

Gerber B., Tanimoto H. and Heisenberg M. (2004) *An engram found? Evaluating the evidence from fruit flies.* Current opinion in neurobiology 14(6):737–744. doi: 10.1016/j.conb.2004.10.014.

Goh K.I. and Barabási A.L. (2006) *Burstiness and Memory in Complex Systems*. ArXiv 0 (1):4.

Goh K.I. and Barabási A.L. (2008) *Burstiness and memory in complex systems*. EPL (Europhysics Letters) 81(4):48002. doi: 10.1209/0295-5075/81/48002.

Gonzalo-Gómez A., Turiegano E., León Y., Molina I., Torroja L. and Canal I. (2012) *Ih current is necessary to maintain normal dopamine fluctuations and sleep consolidation in Drosophila.* PloS one 7(5):e36477. doi: 10.1371/journal.pone.0036477.

Götz K.G. (1964) *Optomotorische Untersuchung des visuellen Systems einiger Augenmutanten der Fruchtfliege Drosophila*. Kybernetik 2:77–92.

Götz K.G. (1972) *Principles of optomotor reactions in insects*. Bibliotheca Ophthalmologica 82:411–417.

Grigliatti T.A., Hall L., Rosenbluth R. and Suzuki D.T. (1973) *Temperature-sensitive mutations in Drosophila melanogaster - XIV. A selection of immobile adults*. MGG Molecular & General Genetics 120(2):107–114. doi: 10.1007/BF00267238.

Gu Z., Cavalcanti A., Chen F.C., Bouman P. and Li W.H. (2002) *Extent of Gene Duplication in the Genomes of Drosophila, Nematode, and Yeast*. Molecular Biology and Evolution 19(3):256–262. doi: 10.1093/oxfordjournals.molbev.a004079.

Gumenyuk V., Roth T. and Drake C.L. (2012) *Circadian phase, sleepiness, and light exposure assessment in night workers with and without shift work disorder.* Chronobiology international 29(7):928–36. doi: 10.3109/07420528.2012.699356.

Guven-Ozkan T. and Davis R.L. (2014) *Functional neuroanatomy of Drosophila olfactory memory formation.* Learning & memory (Cold Spring Harbor, N.Y.) 21(10):519–26. doi: 10.1101/lm.034363.114.

Halász P., Terzano M., Parrino L. and Bódizs R. (2004) *The nature of arousal in sleep*. Journal of sleep research 13(1):1–23.

Halliwell J.V. and Adams P.R. (1982) *Voltage-clamp analysis of muscarinic excitation in hippocampal neurons*. Brain Research 250(1):71–92. doi: 10.1016/0006-8993(82)90954-4.

Hassenstein B. and Reichardt W.Z. (1956) *System theoretical analysis of time, sequence and sign analysis of the motion perception of the snout-beetle Chlorophanus*. Z Naturforsch. B 11:513–524.

He C., Chen F., Li B. and Hu Z. (2014) *Neurophysiology of HCN channels: from cellular functions to multiple regulations.* Progress in neurobiology 112:1–23. doi: 10.1016/j.pneurobio.2013.10.001.

Heisenberg M. (2001) *Flexibility in a Single Behavioral Variable of Drosophila*. Learning

& Memory 8(1):1–10. doi: 10.1101/lm.8.1.1.

Heisenberg M. and Wolf R. (1979) *On the fine structure of yaw torque in visual flight orientation of Drosophila melanogaster*. Journal of Comparative Physiology A 130(2): 113–130. doi: 10.1007/BF00611046.

Heisenberg M., Heusipp M. and Wanke C. (1995) *Structural plasticity in the Drosophila brain*. J. Neurosci. 15(3):1951–1960.

Heisenberg M. (1983) *Initiale aktivität und willkürverhalten bei tieren*. Naturwissenschaften 20:70–78.

Heisenberg M. (2015) *Outcome learning, outcome expectations, and intentionality in Drosophila.* Learning & memory (Cold Spring Harbor, N.Y.) 22(6):294–8. doi: 10.1101/lm.037481.114.

Heisenberg M. and Wolf R. (1984) *Vision in Drosophila* volume 12 of *Studies of Brain Function*. Springer-Verlag Berlin Heidelberg Berlin, Heidelberg. ISBN 978-3-642-69937-5.

Hendricks J.C., Finn S.M., Panckeri K.a., Chavkin J., Williams J.a., Sehgal A. and Pack A.I. (2000) *Rest in Drosophila is a sleep-like state.* Neuron 25(1):129–138. doi: 10.1016/S0896-6273(00)80877-6.

Herrmann S., Stieber J. and Ludwig A. (2007) *Pathophysiology of HCN channels*. Pflügers Archiv - European Journal of Physiology 454(4):517–522. doi: 10.1007/s00424-007-0224-4.

Hidalgo C.a. (2006) *Conditions for the emergence of scaling in the inter-event time of uncorrelated and seasonal systems*. Physica A: Statistical Mechanics and its Applications 369(2):877–883. doi: 10.1016/j.physa.2005.12.035.

Hirsch H.V. and Tompkins L. (1994) *The flexible fly: experience-dependent development of complex behaviors in Drosophila melanogaster.* The Journal of experimental biology 195:1–18.

Hobson J.A. and Pace-Schott E.F. (2002) *The cognitive neuroscience of sleep: neuronal systems, consciousness and learning.* Nature reviews. Neuroscience 3(9):679–93. doi: 10.1038/nrn915.

Howe K., Clark M.D., Torroja C.F. et al (2013) *The zebrafish reference genome sequence and its relationship to the human genome.* Nature 496(7446):498–503. doi: 10.1038/nature12111.

Humphries N.E., Queiroz N., Dyer J.R.M. et al (2010) *Environmental context explains*

Lévy and Brownian movement patterns of marine predators. Nature 465(7301): 1066–1069. doi: 10.1038/nature09116.

Humphries N.E., Weimerskirch H., Queiroz N., Southall E.J. and Sims D.W. (2012) *Foraging success of biological Levy flights recorded in situ*. Proceedings of the National Academy of Sciences 109(19):7169–7174. doi: 10.1073/pnas.1121201109.

Humphries N.E., Weimerskirch H. and Sims D.W. (2013) *A new approach for objective identification of turns and steps in organism movement data relevant to random walk modelling*. Methods in Ecology and Evolution pages n/a–n/a. doi: 10.1111/2041-210X.12096.

IHGSC I.H.G.S.C. (2004) *Finishing the euchromatic sequence of the human genome.* Nature 431(7011):931–45. doi: 10.1038/nature03001.

James A. and Plank M.J. (2007) *On fitting power laws to ecological data*. ArXiv.

James A., Plank M.J. and Edwards A.M. (2011) *Assessing Levy walks as models of animal foraging*. Journal of The Royal Society Interface 8(62):1233–1247. doi: 10.1098/rsif.2011.0200.

Jan Y.N. and Jan L. (2008) *Retrospective: Seymour Benzer (1921-2007)*. Science (New York, N.Y.) 319(5859):45. doi: 10.1126/science.1154050.

Jenett A., Rubin G.M., Ngo T.T.B. et al (2012) *A GAL4-Driver Line Resource for Drosophila Neurobiology*. Cell Reports 2(4):991–1001. doi: 10.1016/j.celrep.2012.09.011.

Jenni O.G., Borbély A.A. and Achermann P. (2004) *Development of the nocturnal sleep electroencephalogram in human infants*. American Journal of Physiology - Regulatory Integrative and Comparative Physiology 286(3 55-3).

Jenni O.G., Deboer T. and Achermann P. (2006) *Development of the 24-h rest-activity pattern in human infants*. Infant Behavior and Development 29(2):143–152. doi: 10.1016/j.infbeh.2005.11.001.

Jo H.H., Karsai M., Kertesz J. and Kaski K. (2012) *Circadian pattern and burstiness in mobile phone communication*. New Journal of Physics 14. doi: 10.1088/1367-2630/14/1/013055.

Jouvet-Mounier D., Astic L. and Lacote D. (1970) *Ontogenesis of the states of sleep in rat, cat, and guinea pig during the first postnatal month.* Developmental psychobiology 2 (4):216–39. doi: 10.1002/dev.420020407.

Juusola M. and de Polavieja G.G. (2003) *The rate of information transfer of naturalistic stimulation by graded potentials.* The Journal of general physiology 122(2):191–206.

doi: 10.1085/jgp.200308824.

Kalinchuk A.V., McCarley R.W., Porkka-Heiskanen T. and Basheer R. (2010) *Sleep deprivation triggers inducible nitric oxide-dependent nitric oxide production in wake-active basal forebrain neurons.* The Journal of neuroscience : the official journal of the Society for Neuroscience 30(40):13254–64. doi: 10.1523/JNEUROSCI.0014-10.2010.

Kareiva P.M. and Shigesada N. (1983) *Analysing insect movement as a correlated random walk*. Oecologia 56:234–238.

Karlsson K.Æ.K., Arnardóttir H., Robinson S.R. and Blumberg M.S. (2011) *Dynamics of sleep-wake cyclicity across the fetal period in sheep (Ovis aries)*. Developmental Psychobiology 53(1):89–95. doi: 10.1002/dev.20495.

Kishi A., Struzik Z.R., Natelson B.H., Togo F. and Yamamoto Y. (2008) *Dynamics of sleep stage transitions in healthy humans and patients with chronic fatigue syndrome*. AJP: Regulatory, Integrative and Comparative Physiology 294(6):R1980–R1987. doi: 10.1152/ajpregu.00925.2007.

Kitamoto T. (2001) *Conditional modification of behavior in Drosophila by targeted expression of a temperature-sensitive shibire allele in defined neurons*. Journal of Neurobiology 47(2):81–92. doi: 10.1002/neu.1018.

Klafter J., Shlesinger M.F. and Zumofen G. (1996) *Beyond Brownian Motion*. Physics Today 49(2):33. doi: 10.1063/1.881487.

Klein D.C. (1991) *Suprachiasmatic Nucleus: The Mind's Clock*. Oxford Univ. Press New York.

Knutson K.L. (2010) *Sleep duration and cardiometabolic risk: a review of the epidemiologic evidence.* Best practice & research. Clinical endocrinology & metabolism 24(5):731–43. doi: 10.1016/j.beem.2010.07.001.

Konopka R.J. and Benzer S. (1971) *Clock mutants of Drosophila melanogaster.* Proceedings of the National Academy of Sciences of the United States of America 68(9):2112–6.

Krashes M.J., Keene A.C., Leung B., Armstrong J.D. and Waddell S. (2007) *Sequential use of mushroom body neuron subsets during drosophila odor memory processing.* Neuron 53(1):103–15. doi: 10.1016/j.neuron.2006.11.021.

Krashes M.J., DasGupta S., Vreede A., White B., Armstrong J.D. and Waddell S. (2009) *A neural circuit mechanism integrating motivational state with memory expression in*

Drosophila. Cell 139(2):416–27. doi: 10.1016/j.cell.2009.08.035.

Kronholm E., Sallinen M., Era P., Suutama T., Sulkava R. and Partonen T. (2011) *Psychomotor slowness is associated with self-reported sleep duration among the general population.* Journal of sleep research 20(2):288–97. doi: 10.1111/j.1365-2869.2010.00899.x.

Kume K., Kume S., Park S.K., Hirsh J. and Jackson F.R. (2005) *Dopamine is a regulator of arousal in the fruit fly.* The Journal of neuroscience : the official journal of the Society for Neuroscience 25(32):7377–84. doi: 10.1523/JNEUROSCI.2048-05.2005.

Landolt H.P. (2008) *Sleep homeostasis: a role for adenosine in humans?* Biochemical pharmacology 75(11):2070–9. doi: 10.1016/j.bcp.2008.02.024.

Landolt H.P., Rétey J.V., Tönz K., Gottselig J.M., Khatami R., Buckelmüller I. and Achermann P. (2004) *Caffeine Attenuates Waking and Sleep Electroencephalographic Markers of Sleep Homeostasis in Humans*. Neuropsychopharmacology 29(10):1933–1939. doi: 10.1038/sj.npp.1300526.

Lessman C.A. (2011) *The developing zebrafish (Danio rerio): A vertebrate model for high-throughput screening of chemical libraries*. Birth Defects Research Part C: Embryo Today: Reviews 93(3):268–280. doi: 10.1002/bdrc.20212.

Levandowsky M., Klafter J. and White B.S. (1988a) *Feeding and Swimming Behavior in Grazing Microzooplankton 1 , 2*. The Journal of Protozoology 35(2):243–246. doi: 10.1111/j.1550-7408.1988.tb04334.x.

Levandowsky M., Klafter J. and White B.S. (1988b) *Swimming behavior and chemosensory responses in the protistan microzooplankton as a function of the hydrodynamic regime*. Bulletin of Marine Science 43:758–763.

Lewis A.S. and Chetkovich D.M. (2011) *HCN channels in behavior and neurological disease: Too hyper or not active enough?* Molecular and Cellular Neuroscience 46(2):357–367. doi: 10.1016/j.mcn.2010.11.007.

Liu Z., Bunney E.B., Appel S.B. and Brodie M.S. (2003) *Serotonin reduces the hyperpolarization-activated current (Ih) in ventral tegmental area dopamine neurons: involvement of 5-HT2 receptors and protein kinase C.* Journal of neurophysiology 90(5):3201–12. doi: 10.1152/jn.00281.2003.

Lnenicka G., Spencer G.M. and Keshishian H. (2003) *Effect of reduced impulse activity on the development of identified motor terminals in Drosophila larvae.* Journal of neurobiology 54(2):337–45. doi: 10.1002/neu.10133.

Lo C.C., Amaral L.a.N., Havlin S. et al (2002) *Dynamics of sleep-wake transitions during sleep*. Europhysics Letters 57(March):625–631. doi: 10.1209/epl/i2002-00508-7.

Lo C.C., Chou T., Penzel T., Scammell T.E., Strecker R.E., Stanley H.E. and Ivanov P.C. (2004) *Common scale-invariant patterns of sleep-wake transitions across mammalian species.* Proceedings of the National Academy of Sciences of the United States of America 101(50):17545–8. doi: 10.1073/pnas.0408242101.

Lomholt M.A., Koren T., Metzler R. and Klafter J. (2007) *The advantage of L\'evy strategies in intermittent search processes*. page 4.

Lu J., Sherman D., Devor M. and Saper C.B. (2006) *A putative flip-flop switch for control of REM sleep.* Nature 441(7093):589–94. doi: 10.1038/nature04767.

Ludwig A., Zong X., Jeglitsch M., Hofmann F. and Biel M. (1998) *A family of hyperpolarization-activated mammalian cation channels.* Nature 393(6685):587–91. doi: 10.1038/31255.

Lyamin O., Pryaslova J., Lance V. and Siegel J. (2005) *Animal behaviour: Continuous activity in cetaceans after birth*. Nature 435(7046):1177–1177. doi: 10.1038/4351177a.

Maarell A., Ball J.P. and Hofgaard A. (2002) *Foraging and movement paths of female reindeer: insights from fractal analysis, correlated random walks, and Lévy flights*. Canadian Journal of Zoology 80(5):854–865. doi: 10.1139/z02-061.

Maggi S., Langlois J.A., Minicuci N., Grigoletto F., Pavan M., Foley D.J. and Enzi G. (1998) *Sleep complaints in community-dwelling older persons: prevalence, associated factors, and reported causes.* Journal of the American Geriatrics Society 46(2):161–8.

Mahowald M.W. and Schenck C.H. (2005) *Insights from studying human sleep disorders.* Nature 437(7063):1279–85. doi: 10.1038/nature04287.

Malmgren R.D., Stouffer D.B., Motter A.E. and Amaral L.A.N. (2008) *A Poissonian explanation for heavy tails in e-mail communication.* Proceedings of the National Academy of Sciences of the United States of America 105(47):18153–8. doi: 10.1073/pnas.0800332105.

Malmgren R.D., Stouffer D.B., Campanharo A.S.L.O. and Amaral L.a.N. (2009) *On universality in human correspondence activity.* Science (New York, N.Y.) 325(5948):1696–700. doi: 10.1126/science.1174562.

Mandelbrot B.B. (1982) *The Fractal Geometry of Nature*. W. H. Freeman and Company 1 edition. ISBN 0-7167-1186-9.

Mao Z. and Davis R.L. (2009) *Eight different types of dopaminergic neurons innervate the Drosophila mushroom body neuropil: anatomical and physiological heterogeneity.* Frontiers in neural circuits 3(July):5. doi: 10.3389/neuro.04.005.2009.

Martin J.R., Ernst R. and Heisenberg M. (1998) *Mushroom bodies suppress locomotor activity in Drosophila melanogaster.* Learning & memory (Cold Spring Harbor, N.Y.) 5 (1-2):179–191. doi: 10.1101/lm.5.1.179.

Martin J.R., Ernst R. and Heisenberg M. (1999a) *Temporal pattern of locomotor activity in Drosophila melanogaster.* Journal of comparative physiology. A, Sensory, neural, and behavioral physiology 184(1):73–84.

Martin J.R., Raabe T. and Heisenberg M. (1999b) *Central complex substructures are required for the maintenance of locomotor activity in Drosophila melanogaster*. Journal of Comparative Physiology - A Sensory, Neural, and Behavioral Physiology 185(3): 277–288. doi: 10.1007/s003590050387.

Martin J.R., Faure P. and Ernst R. (2001) *The power law distribution for walking-time intervals correlates with the ellipsoid-body in Drosophila.* Journal of neurogenetics 15 (3-4):205–19.

Marx T., Gisselmann G., Störtkuhl K.F., Hovemann B.T. and Hatt H. (1999) *Molecular cloning of a putative voltage- and cyclic nucleotide-gated ion channel present in the antennae and eyes of Drosophila melanogaster.* Invertebrate neuroscience 4(1):55–63. doi: 10.1007/s101589900006.

Maye A., Hsieh C.H.H., Sugihara G. and Brembs B. (2007) *Order in spontaneous behavior.* PloS one 2(5):e443. doi: 10.1371/journal.pone.0000443.

McGinty D.J., Stevenson M., Hoppenbrouwers T., Harper R.M., Sterman M.B. and Hodgman J. (1977) *Polygraphic studies of kitten development: Sleep state patterns*. Developmental Psychobiology 10(5):455–469. doi: 10.1002/dev.420100506.

McGuire S.E., Le P.T., Osborn A.J., Matsumoto K. and Davis R.L. (2003) *Spatiotemporal rescue of memory dysfunction in Drosophila.* Science (New York, N.Y.) 302(5651): 1765–8. doi: 10.1126/science.1089035.

Michel M. and Lyons L.C. (2014) *Unraveling the complexities of circadian and sleep interactions with memory formation through invertebrate research*. Frontiers in System Neuroscience 8:133. doi: 10.3389/fnsys.2014.00133.

Mitzenmacher M. (2001) *A brief history of generative models for power law and lognormal distributions*. Internet Mathematics 1(2):226 – 251.

Mitzenmacher M. (2004) *A Brief History of Generative Models for Power Law and Lognormal Distributions*. Internet Mathematics 1(2):226–251. doi: 10.1080/15427951.2004.10129088.

Mohns E.J., Karlsson K.Æ. and Blumberg M.S. (2006) *The preoptic hypothalamus and basal forebrain play opposing roles in the descending modulation of sleep and wakefulness in infant rats.* The European journal of neuroscience 23(5):1301–10. doi: 10.1111/j.1460-9568.2006.04652.x.

Monier B., Astier M., Sémériva M. and Perrin L. (2005) *Steroid-dependent modification of Hox function drives myocyte reprogramming in the Drosophila heart.* Development (Cambridge, England) 132(23):5283–5293. doi: 10.1242/dev.02091.

NASA (2004) *The Fruit Fly in You*. Retrieved from URL `http://science.nasa.gov/science-news/science-at-nasa/2004/03feb{_}fruitfly/` on 2015-08-13.

Neckameyer W.S. and Argue K.J. (2013) *Comparative approaches to the study of physiology: Drosophila as a physiological tool.* American journal of physiology. Regulatory, integrative and comparative physiology 304(3):R177–88. doi: 10.1152/ajpregu.00084.2012.

Neuhoff H., Neu A., Liss B. and Roeper J. (2002) *I(h) channels contribute to the different functional properties of identified dopaminergic subpopulations in the midbrain.* The Journal of neuroscience : the official journal of the Society for Neuroscience 22(4):1290–302. doi: 22/4/1290[pii].

Newman M.E.J. (2004) *Power laws, Pareto distributions and Zipf's law*. October (x):28. doi: 10.1080/00107510500052444.

Nielsen L.S., Danielsen K.V. and Sørensen T.I.A. (2011) *Short sleep duration as a possible cause of obesity: critical analysis of the epidemiological evidence.* Obesity reviews : an official journal of the International Association for the Study of Obesity 12(2):78–92. doi: 10.1111/j.1467-789X.2010.00724.x.

Nobel Lectures (1965) *Thomas H. Morgan - Biographical*. In *Physiology or Medicine 1922-1941*. Elsevier Publishing Company Amsterdam.

Oliveira J.G. and Barabási A.L. (2005) *Human dynamics: Darwin and Einstein correspondence patterns.* Nature 437(7063):1251. doi: 10.1038/4371251a.

Oxford Dictionaries (2015) *http://www.oxforddictionaries.com/definition/english/animal*. Retrieved on 2015-11-01.

Pace-Schott E.F. and Hobson J.A. (2002) *The neurobiology of sleep: genetics, cellular*

physiology and subcortical networks. Nature reviews. Neuroscience 3(8):591–605. doi: 10.1038/nrn895.

Palmiter R.D. (2011) *Dopamine signaling as a neural correlate of consciousness.* Neuroscience 198:213–20. doi: 10.1016/j.neuroscience.2011.06.089.

Palyulin V.V., Chechkin A.V. and Metzler R. (2014) *Levy flights do not always optimize random blind search for sparse targets.* Proceedings of the National Academy of Sciences of the United States of America 111(8):2931–6. doi: 10.1073/pnas.1320424111.

Panula P., Chen Y.C., Priyadarshini M., Kudo H., Semenova S., Sundvik M. and Sallinen V. (2010) *The comparative neuroanatomy and neurochemistry of zebrafish CNS systems of relevance to human neuropsychiatric diseases.* Neurobiology of disease 40(1):46–57. doi: 10.1016/j.nbd.2010.05.010.

Pape H.C. (1996) *Queer Current and Pacemaker: The Hyperpolarization-Activated Cation Current in Neurons*. Annual Review of Physiology 58(1):299–327. doi: 10.1146/annurev.ph.58.030196.001503.

Patlak C.S. (1953) *Random walk with persistence and external bias*. The Bulletin of Mathematical Biophysics 15(3):311–338. doi: 10.1007/BF02476407.

Peirano P., Algarín C. and Uauy R. (2003) *Sleep-wake states and their regulatory mechanisms throughout early human development*. In *Journal of Pediatrics* volume 143 (2003).

Peng C.K., Buldyrev S.V., Havlin S., Simons M., Stanley H.E. and Goldberger A.L. (1994) *Mosaic organization of DNA nucleotides*. Physical Review E 49(2):1685–1689. doi: 10.1103/PhysRevE.49.1685.

Peng C.K., Havlin S., Stanley H.E. and Goldberger A.L. (1995) *Quantification of scaling exponents and crossover phenomena in nonstationary heartbeat time series.* Chaos (Woodbury, N.Y.) 5(1):82–87. doi: 10.1063/1.166141.

Peron S., Zordan M., Magnabosco A., Reggiani C. and Megighian A. (2009) *From action potential to contraction: Neural control and excitation-contraction coupling in larval muscles of Drosophila*. Comparative Biochemistry and Physiology - A Molecular and Integrative Physiology 154(2):173–183. doi: 10.1016/j.cbpa.2009.04.626.

Petrovskii S., Mashanova A. and Jansen V.A.A. (2011) *Variation in individual walking behavior creates the impression of a Levy flight*. Proceedings of the National Academy of Sciences 108(21):8704–8707. doi: 10.1073/pnas.1015208108.

Pierce B.A. (2004) *Genetics: A Conceptual Approach*. W. H. Freeman 2nd ed edition. ISBN 978-0-7167-8881-2.

Plank M.J. and Codling E.A. (2009) *Sampling rate and misidentification of Lévy and non-Lévy movement paths*. Ecology 90:3546–3553. doi: 10.1890/09-0079.1.

Poggio T. (2011) *Werner Reichardt: the man and his scientific legacy*. In Geiger G., editor, *MIT-CSAIL-TR-2011-011/CBCL-297*. Massachusetts Institute of Technology Cambridge, MA.

Porkka-Heiskanen T., Strecker R.E., Thakkar M., Bjorkum A.A., Greene R.W. and McCarley R.W. (1997) *Adenosine: a mediator of the sleep-inducing effects of prolonged wakefulness.* Science (New York, N.Y.) 276(5316):1265–8.

Porkka-Heiskanen T. and Kalinchuk A.V. (2011) *Adenosine, energy metabolism and sleep homeostasis*. Sleep Medicine Reviews 15(2):123–135. doi: 10.1016/j.smrv.2010.06.005.

Portas C.M., Thakkar M., Rainnie D.G., Greene R.W. and McCarley R.W. (1997) *Role of adenosine in behavioral state modulation: a microdialysis study in the freely moving cat.* Neuroscience 79(1):225–35.

Portugues R., Severi K.E., Wyart C. and Ahrens M.B. (2013) *Optogenetics in a transparent animal: circuit function in the larval zebrafish.* Current opinion in neurobiology 23 (1):119–26. doi: 10.1016/j.conb.2012.11.001.

Prober D.A., Rihel J., Onah A.A., Sung R.J. and Schier A.F. (2006) *Hypocretin/orexin overexpression induces an insomnia-like phenotype in zebrafish.* The Journal of neuroscience : the official journal of the Society for Neuroscience 26(51):13400–10. doi: 10.1523/JNEUROSCI.4332-06.2006.

Proekt A., Banavar J.R., Maritan A. and Pfaff D.W. (2012) *Scale invariance in the dynamics of spontaneous behavior*. Proceedings of the National Academy of Sciences 109(26):10564–10569. doi: 10.1073/pnas.1206894109.

Puopolo M., Raviola E. and Bean B.P. (2007) *Roles of subthreshold calcium current and sodium current in spontaneous firing of mouse midbrain dopamine neurons.* The Journal of neuroscience : the official journal of the Society for Neuroscience 27(3): 645–656. doi: 10.1523/JNEUROSCI.4341-06.2007.

Raichlen D.A., Wood B.M., Gordon A.D., Mabulla A.Z.P., Marlowe F.W. and Pontzer H. (2014) *Evidence of Levy walk foraging patterns in human hunter-gatherers*. Proceedings of the National Academy of Sciences 111(2):728–733. doi: 10.1073/pnas.

1318616111.

Raizen D.M., Zimmerman J.E., Maycock M.H., Ta U.D., You Y.j., Sundaram M.V. and Pack A.I. (2008) *Lethargus is a Caenorhabditis elegans sleep-like state.* Nature 451 (7178):569–72. doi: 10.1038/nature06535.

Ramos-Fernández G., Mateos J.L., Miramontes O., Cocho G., Larralde H. and Ayala-Orozco B. (2004) *Lévy walk patterns in the foraging movements of spider monkeys (Ateles geoffroyi)*. Behavioral Ecology and Sociobiology 55(3):223–230. doi: 10.1007/s00265-003-0700-6.

Rechtschaffen A. and Kales A. (1968) *A manual of standardised terminology, techniques, and scoring system for sleep stages of human subjects*.

Rechtschaffen A. and Bergmann B.M. (1995) *Sleep deprivation in the rat by the disk-over-water method*. Behavioural Brain Research 69(1-2):55–63. doi: 10.1016/0166-4328(95)00020-T.

Reichardt W. and Wenking H. (1969) *Optical detection and fixation of objects by fixed flying flies (Musca domestica)*. Naturwissenschaften 56(8):424–425.

Reichardt W. and Poggio T. (1976) *Visual control of orientation behaviour in the fly*. Quarterly Review of Biophysics 9(3):311–375.

Reiter L.T., Potocki L., Chien S., Gribskov M. and Bier E. (2001) *A systematic analysis of human disease-associated gene sequences in Drosophila melanogaster.* Genome research 11(6):1114–25. doi: 10.1101/gr.169101.

Renn S.C.P., Armstrong J.D., Yang M., Wang Z., An X., Kaiser K. and Taghert P.H. (1999) *Genetic analysis of the Drosophila ellipsoid body neuropil: Organization and development of the central complex*. Journal of Neurobiology 41(2):189–207. doi: 10.1002/(SICI)1097-4695(19991105)41:2<189::AID-NEU3>3.0.CO;2-Q.

Reynolds A.M. (2009) *Adaptive Lévy walks can outperform composite Brownian walks in non-destructive random searching scenarios*. Physica A: Statistical Mechanics and its Applications 388(5):561–564. doi: 10.1016/j.physa.2008.11.007.

Reynolds A.M. (2010) *Balancing the competing demands of harvesting and safety from predation: Lévy walk searches outperform composite Brownian walk searches but only when foraging under the risk of predation*. Physica A: Statistical Mechanics and its Applications 389(21):4740–4746. doi: 10.1016/j.physa.2010.06.027.

Reynolds A.M. (2014) *Lévy flight movement patterns in marine predators may derive from turbulence cues.* Proceedings. Mathematical, physical, and engineering sciences

/ the Royal Society 470(2171):20140408. doi: 10.1098/rspa.2014.0408.

Reynolds A.M. (2012) *Distinguishing between Lévy walks and strong alternative models*. Ecology 93(5):1228–1233. doi: 10.1890/11-1815.1.

Reynolds A.M. and Rhodes C.J. (2009) *The Lévy flight paradigm: Random search patterns and mechanisms*. Ecology 90(4):877–887. doi: 10.1890/08-0153.1.

Reynolds A.M. (2015) *Liberating Lévy walk research from the shackles of optimal foraging*. Physics of Life Reviews 14(0):59–83. doi: 10.1016/j.plrev.2015.03.002. Retrieved from URL `http://linkinghub.elsevier.com/retrieve/pii/S1571064515000536http://dx.doi.org/10.1016/j.plrev.2015.03.002`.

Riemensperger T., Isabel G., Coulom H. et al (2011) *Behavioral consequences of dopamine deficiency in the Drosophila central nervous system.* Proceedings of the National Academy of Sciences of the United States of America 108(2):834–839. doi: 10.1073/pnas.1010930108.

Rihel J. and Schier A.F. (2013) *Sites of action of sleep and wake drugs: insights from model organisms*. Current Opinion in Neurobiology 23(5):831–840. doi: 10.1016/j.conb.2013.04.010.

Rihel J., Prober D.A. and Schier A.F. (2010) *Monitoring Sleep and Arousal in Zebrafish*. In *Methods in cell biology* volume 100 pages 281–294. doi: 10.1016/B978-0-12-384892-5.00011-6.

Robinson R.B. and Siegelbaum S.A. (2003) *Hyperpolarization-activated cation currents: from molecules to physiological function.* Annual review of physiology 65:453–80. doi: 10.1146/annurev.physiol.65.092101.142734.

Roffwarg H.P., Muzio J.N. and Dement W.C. (1966) *Ontogenetic Development of the Human Sleep-Dream Cycle*. Science 152(3722):604–619. doi: 10.1126/science.152.3722.604.

Rosato E. and Kyriacou C.P. (2006) *Analysis of locomotor activity rhythms in Drosophila.* Nature protocols 1(2):559–568. doi: 10.1038/nprot.2006.79.

Rowell C.H.F. (1988) *Mechanisms of flight steering in locust*. Experientia 44:389–395.

Rubin G.M. and Lewis E.B. (2000) *A Brief History of Drosophila's Contributions to Genome Research*. Science 287(5461):2216–2218. doi: 10.1126/science.287.5461.2216.

Santoro B., Liu D.T., Yao H., Bartsch D., Kandel E.R., Siegelbaum S.A. and Tibbs G.R. (1998) *Identification of a Gene Encoding a Hyperpolarization-Activated Pacemaker Channel of Brain*. Cell 93(5):717–729. doi: 10.1016/S0092-8674(00)81434-8.

Saper C.B. and Lowell B.B. (2014) *The hypothalamus*. Current Biology 24(23):R1111–R1116. doi: 10.1016/j.cub.2014.10.023.

Saper C.B. and Sehgal A. (2013) *New perspectives on circadian rhythms and sleep*. Current opinion in neurobiology 23(5):721–3. doi: 10.1016/j.conb.2013.07.005.

Saper C.B., Chou T.C. and Scammell T.E. (2001) *The sleep switch: hypothalamic control of sleep and wakefulness*. Trends in Neurosciences 24(12):726–731. doi: 10.1016/S0166-2236(00)02002-6.

Saper C.B., Fuller P.M., Pedersen N.P., Lu J. and Scammell T.E. (2010) *Sleep state switching*. Neuron 68(6):1023–42. doi: 10.1016/j.neuron.2010.11.032.

Sareen P., Wolf R. and Heisenberg M. (2011) *Attracting the attention of a fly*. Proceedings of the National Academy of Sciences 108(17):7230–7235. doi: 10.1073/pnas.1102522108.

Sayeed O. and Benzer S. (1996) *Behavioral genetics of thermosensation and hygrosensation in Drosophila*. Proceedings of the National Academy of Sciences of the United States of America 93(12):6079–6084. doi: 10.1073/pnas.93.12.6079.

Scharf M.T., Naidoo N., Zimmerman J.E. and Pack A.I. (2008) *The energy hypothesis of sleep revisited*. Progress in Neurobiology 86(3):264–280. doi: 10.1016/j.pneurobio.2008.08.003.

Schwartz J. and Roth T. (2008) *Neurophysiology of Sleep and Wakefulness: Basic Science and Clinical Implications*. Current Neuropharmacology 6(4):367–378. doi: 10.2174/157015908787386050.

Sehgal A. and Mignot E. (2011) *Genetics of sleep and sleep disorders*. Cell 146(2):194–207. doi: 10.1016/j.cell.2011.07.004.

Seutin V., Massotte L., Renette M.F. and Dresse A. (2001) *Evidence for a modulatory role of Ih on the firing of a subgroup of midbrain dopamine neurons*. Neuroreport 12(2):255.

Shaw P.J., Cirelli C., Greenspan R.J. and Tononi G. (2000) *Correlates of Sleep and Waking in Drosophila melanogaster*. Science 287(5459):1834–1837. doi: 10.1126/science.287.5459.1834.

Shlesinger M.F. and Klafter J. (1986) *Lévy Walks Versus Lévy Flights*. In *On Growth and Form* pages 279–283. Springer Netherlands Dordrecht. doi: 10.1007/978-94-009-5165-5{_}29.

Sigurgeirsson B., Þorsteinsson H., Arnardóttir H., Jóhannesdóttir I.. and Karlsson K.Æ.

(2011) *Effects of Modafinil on Sleep–Wake Cycles in Larval Zebrafish*. Zebrafish 8(3): 133–140. doi: 10.1089/zeb.2011.0708.

Silies M., Gohl D.M. and Clandinin T.R. (2014) *Motion-detecting circuits in flies: coming into view.* Annual review of neuroscience 37:307–27. doi: 10.1146/annurev-neuro-071013-013931.

Sims D.W., Reynolds A.M., Humphries N.E., Southall E.J., Wearmouth V.J., Metcalfe B. and Twitchett R.J. (2014) *Hierarchical random walks in trace fossils and the origin of optimal search behavior*. Proceedings of the National Academy of Sciences 111(30): 11073–11078. doi: 10.1073/pnas.1405966111.

Sims D.W. and Humphries N.E. (2012) *Lévy flight search patterns of marine predators not questioned : a reply*. ArXiv pages 1–18.

Sims D.W., Southall E.J., Humphries N.E. et al (2008) *Scaling laws of marine predator search behaviour.* Nature 451(7182):1098–102. doi: 10.1038/nature06518.

Singh A., Subhashini N., Sharma S. and Mallick B.N. (2013) *Involvement of the α1-adrenoceptor in sleep-waking and sleep loss-induced anxiety behavior in zebrafish.* Neuroscience 245:136–47. doi: 10.1016/j.neuroscience.2013.04.026.

Siniff D.B. and Jessen C.R. (1969) *A Simulation Model of Animal Movement Patterns*. Advances in Ecological Research 6:185–219. doi: 10.1016/S0065-2504(08)60259-7.

Skellam J.G. (1951) *Random dispersal in theoretical populations.* Biometrika 38(1-2): 196–218. doi: 10.1016/S0092-8240(05)80044-8.

Snook R.R. and Hosken D.J. (2004) *Sperm death and dumping in Drosophila.* Nature 428(6986):939–41. doi: 10.1038/nature02455.

Sokolowski M.B. (2001) *Drosophila: genetics meets behaviour.* Nature reviews. Genetics 2(11):879–90. doi: 10.1038/35098592.

Sorribes A., Armendariz B.G., Lopez-Pigozzi D., Murga C. and de Polavieja G.G. (2011) *The origin of behavioral bursts in decision-making circuitry*. PLoS Computational Biology 7(6):e1002075. doi: 10.1371/journal.pcbi.1002075.

Sorribes A., Thornorsteinsson H., Arnardóttir H., Jóhannesdóttir I.., Sigurgeirsson B., de Polavieja G.G. and Karlsson K.Æ. (2013) *The ontogeny of sleep-wake cycles in zebrafish: a comparison to humans.* Frontiers in neural circuits 7(November):178. doi: 10.3389/fncir.2013.00178.

Spence R., Gerlach G., Lawrence C. and Smith C. (2008) *The behaviour and ecology of the zebrafish, Danio rerio.* Biological reviews of the Cambridge Philosophical Society

83(1):13–34. doi: 10.1111/j.1469-185X.2007.00030.x.

St Johnston D. (2002) *The art and design of genetic screens: Drosophila melanogaster.* Nature reviews. Genetics 3(3):176–188. doi: 10.1038/nrg751.

Stocker H. and Gallant P. (2008) *Getting started: an overview on raising and handling Drosophila.* Methods in molecular biology (Clifton, N.J.) 420:27–44. doi: 10.1007/978-1-59745-583-1{_}2.

Stouffer D.B., Malmgren R.D. and Amaral L.a.N. (2005) *Comment on Barabasi, Nature 435, 207 (2005)*. pages 7–10.

Stouffer D.B., Malmgren R.D. and Amaral L.a.N. (2006) *Log-normal statistics in e-mail communication patterns*. page 18.

Strausfeld N.J. (1976) *Atlas of an Insect Brain*. Springer-Verlag Berlin Heidelberg Berlin. ISBN 978-3-642-66179-2.

Strauss R. (2002) *The central complex and the genetic dissection of locomotor behaviour*. Current opinion in neurobiology 12(6):633–638.

Strauss R. and Heisenberg M. (1993) *A higher control center of locomotor behavior in the Drosophila brain.* The Journal of neuroscience : the official journal of the Society for Neuroscience 13(5):1852–1861.

Stumpf M.P.H. and Porter M.A. (2012) *Critical Truths About Power Laws*. Science 335 (6069):665–666. doi: 10.1126/science.1216142.

Szymusiak R. and McGinty D. (2008) *Hypothalamic regulation of sleep and arousal.* Annals of the New York Academy of Sciences 1129:275–86. doi: 10.1196/annals.1417.027.

Taheri S., Zeitzer J.M. and Mignot E. (2002) *The role of hypocretins (orexins) in sleep regulation and narcolepsy.* Annual review of neuroscience 25:283–313. doi: 10.1146/annurev.neuro.25.112701.142826.

Tanaka N.K., Tanimoto H. and Ito K. (2008) *Neuronal assemblies of the Drosophila mushroom body*. Journal of Comparative Neurology 508(5):711–755. doi: 10.1002/cne.21692.

Tang S. and Guo A. (2001) *Choice behavior of Drosophila facing contradictory visual cues.* Science (New York, N.Y.) 294(5546):1543–1547. doi: 10.1126/science.1058237.

Tang S. and Juusola M. (2010) *Intrinsic activity in the fly brain gates visual information during behavioral choices.* PloS one 5(12):e14455. doi: 10.1371/journal.pone.

0014455.

The Drosophila Genomics Resource Center W. () *http://dgrc.bio.indiana.edu*. Retrieved on 2015-08-04.

The FlyBase Consortium, Web () *http://flybase.org*. Retrieved on 2015-08-04.

Tobler I. (1995) *Is sleep fundamentally different between mammalian species?* Behavioural brain research 69(1-2):35–41.

Tonsfeldt K.J. and Chappell P.E. (2012) *Clocks on top: the role of the circadian clock in the hypothalamic and pituitary regulation of endocrine physiology.* Molecular and cellular endocrinology 349(1):3–12. doi: 10.1016/j.mce.2011.07.003.

TriKinetics Inc. (2005) *http://www.trikinetics.com*. Retrieved on 2015-08-13.

Tsien R.W. (1974) *Effects of epinephrine on the pacemaker potassium current of cardiac Purkinje fibers*. Journal of General Physiology 64(3):293–319.

Turchin P. (1998) *Quantitative Analysis of Movement: Measuring and Modeling Population Redistribution in Animals and Plants* volume 1 edition. ISBN 978-0878938476.

Van Buskirk C. and Sternberg P.W. (2007) *Epidermal growth factor signaling induces behavioral quiescence in Caenorhabditis elegans.* Nature neuroscience 10(10):1300–7. doi: 10.1038/nn1981.

van der Vaart A.W. (2000) *Asymptotic Statistics*. Cambridge University Press. ISBN 9780521784504.

van Swinderen B. (2011) *Attention in Drosophila*. International Review of Neurobiology 99:51–85. doi: 10.1016/B978-0-12-387003-2.00003-3.

Vázquez A. (2005) *Exact results for the Barabási model of human dynamics*. Physical Review Letters 95(24):248701. doi: 10.1103/PhysRevLett.95.248701.

Vázquez A., Oliveira J.G., Dezsö Z., Goh K.I., Kondor I. and Barabási A.L. (2006) *Modeling bursts and heavy tails in human dynamics*. Physical Review E 73(3):036127. doi: 10.1103/PhysRevE.73.036127.

Virkar Y. and Clauset A. (2012) *Power-law distributions in binned empirical data*. Arxiv preprint arXiv:1208.3524 page 33. doi: 10.1214/13-AOAS710.

Virsik R. and Reichardt W. (1976) *Detection and tracking of moving objects by the fly Musca domestica*. Biological Cybernetics 23(2):83–98.

Viswanathan G.M., Afanasyev V., Buldyrev S.V., Murphy E.J., Prince P.A. and Stanley H.E. (1996) *Lévy flight search patterns of wandering albatrosses*. Nature 381(6581):

413–415. doi: 10.1038/381413a0.

Viswanathan G.M., Buldyrev S.V., Havlin S., da Luz M.G., Raposo E.P. and Stanley H.E. (1999) *Optimizing the success of random searches.* Nature 401(6756):911–914. doi: 10.1038/44831.

Viswanathan G.M., Raposo E.P. and da Luz M.G.E. (2008) *Lévy flights and superdiffusion in the context of biological encounters and random searches*. Physics of Life Reviews 5 (3):133–150. doi: 10.1016/j.plrev.2008.03.002.

Viswanathan G.M., da Luz M.G.E., Raposo E.P. and Stanley H.E. (2011) *The Physics of Foraging: An Introduction to Random Searches and Biological Encounters*. Cambridge University Press. ISBN 1139497553.

Wahl-Schott C., Fenske S. and Biel M. (2014) *HCN channels: New roles in sinoatrial node function*. Current Opinion in Pharmacology 15(1):83–90. doi: 10.1016/j.coph.2013.12.005.

Wang J.W., Sylwester A.W., Reed D., Wu D.A., Soll D.R. and Wu C.F. (1997) *Morphometric description of the wandering behavior in Drosophila larvae: aberrant locomotion in Na+ and K+ channel mutants revealed by computer-assisted motion analysis.* Journal of neurogenetics 11(319):231–254. doi: 10.3109/01677069709115098.

Wang J.W., Soll D.R. and Wu C.F. (2002) *Morphometric description of the wandering behavior in Drosophila larvae: a phenotypic analysis of K+ channel mutants.* Journal of neurogenetics 16(1):45–63.

Webb B. (2004) *Neural mechanisms for prediction: do insects have forward models?* Trends in neurosciences 27(5):278–82. doi: 10.1016/j.tins.2004.03.004.

Wesensten N.J., Balkin T.J. and Belenky G. (1999) *Does sleep fragmentation impact recuperation? A review and reanalysis.* Journal of sleep research 8(4):237–45.

Wicher D. (2015) *Olfactory signaling in insects.* Progress in molecular biology and translational science 130:37–54. doi: 10.1016/bs.pmbts.2014.11.002.

Wiens J.A., Crist T.O., With K.A. and Milne B.T. (1995) *Fractal Patterns of Insect Movement in Microlandscape Mosaics*. Ecology 76(2):663–666. doi: 10.2307/1941226.

Wolf R. and Heisenberg M. (1991) *Basic organization of operant behavior as revealed in Drosophila flight orientation*. J. comp. Physiol. A 169:669–705.

Wolf R., Voss A., Hein S., Heisenberg M. and Sullivan G.D. (1992) *Can a Fly Ride a Bicycle?* Philosophical Transactions of the Royal Society B: Biological Sciences 337 (1281):261–269. doi: 10.1098/rstb.1992.0104.

Xi W., Peng Y., Guo J., Ye Y., Zhang K., Yu F. and Guo A. (2008) *Mushroom bodies modulate salience-based selective fixation behavior in Drosophila.* The European journal of neuroscience 27(6):1441–51. doi: 10.1111/j.1460-9568.2008.06114.x.

Yin Y., Chen N., Zhang S. and Guo A. (2009) *Choice strategies in Drosophila are based on competition between olfactory memories.* The European journal of neuroscience 30 (2):279–88. doi: 10.1111/j.1460-9568.2009.06821.x.

Yokogawa T., Marin W., Faraco J., Pézeron G., Appelbaum L., Zhang J., Rosa F., Mourrain P. and Mignot E. (2007) *Characterization of Sleep in Zebrafish and Insomnia in Hypocretin Receptor Mutants*. PLoS Biology 5(10):e277. doi: 10.1371/journal.pbio.0050277.

Zhang K., Guo J.Z., Peng Y., Xi W. and Guo A. (2007) *Dopamine-mushroom body circuit regulates saliency-based decision-making in Drosophila.* Science (New York, N.Y.) 316 (5833):1901–4. doi: 10.1126/science.1137357.

Zhang S., Yin Y., Lu H. and Guo A. (2008) *Increased dopaminergic signaling impairs aversive olfactory memory retention in Drosophila.* Biochemical and biophysical research communications 370(1):82–6. doi: 10.1016/j.bbrc.2008.03.015.

Zhdanova I.V., Wang S.Y., Leclair O.U. and Danilova N.P. (2001) *Melatonin promotes sleep-like state in zebrafish.* Brain research 903(1-2):263–8.

Zhdanova I.V. (2006) *Sleep in zebrafish.* Zebrafish 3(2):215–26. doi: 10.1089/zeb.2006.3.215.

Zhdanova I., Yu L., Lopez-Patino M., Shang E., Kishi S. and Guelin E. (2008) *Aging of the circadian system in zebrafish and the effects of melatonin on sleep and cognitive performance*. Brain Research Bulletin 75(2-4):433–441. doi: 10.1016/j.brainresbull.2007.10.053.

Zimmerman J.E., Raizen D.M., Maycock M.H., Maislin G. and Pack A.I. (2008) *A video method to study Drosophila sleep.* Sleep 31(11):1587–1598.

Zisapel N. (2007) *Sleep and sleep disturbances: biological basis and clinical implications*. Cellular and Molecular Life Sciences 64(10):1174–1186. doi: 10.1007/s00018-007-6529-9.

Zolles G., Klöcker N., Wenzel D., Weisser-Thomas J., Fleischmann B.K., Roeper J. and Fakler B. (2006) *Pacemaking by HCN Channels Requires Interaction with Phosphoinositides*. Neuron 52(6):1027–1036. doi: 10.1016/j.neuron.2006.12.005.